Fall 2020

# Determining the Trophic Role of Red Snapper (Lutjanus campechanus) in Mississippi State Waters Using Stomach Content and Stable Isotope Analysis

Branden Kohler

# DETERMINING THE TROPHIC ROLE OF RED SNAPPER (LUTJANUS CAMPECHANUS) IN MISSISSIPPI STATE WATERS USING STOMACH CONTENT AND STABLE ISOTOPE ANALYSIS

by

Branden Kohler

A Thesis
Submitted to the Graduate School,
the College of Arts and Sciences
and the School of Ocean Science and Engineering
at The University of Southern Mississippi
in Partial Fulfillment of the Requirements
for the Degree of Master of Science

Approved by:

Dr. Kevin Dillon, Committee Chair
Dr. Zachary Darnell
Dr. Frank Hernandez

December 2020

## ABSTRACT

The goal of this study was to determine the diet composition, trophic position and ecological role of red snapper *(Lutjanus campechanus*) in Mississippi state waters utilizing stable isotopes ($\delta^{13}C$ and $\delta^{15}N$) and stomach content analysis. Stable isotope analysis of fish and their prey can provide information on species-specific basal resource utilization, diet composition and trophic position which can improve food web models and inform fisheries management decisions. Particulate organic matter (POM), the presumed base of the food web, red snapper muscle tissue, and red snapper stomach contents were collected from 25 sites in 2016 and 2017 for stable isotope analysis. POM $\delta^{13}C$ values showed high variability for both years, with 2016 values being lower at deeper strata sites and steadily decreasing in surface and bottom water samples over the 7-month sampling period. POM $\delta^{13}C$ values from both years may have been affected by increased riverine inputs. POM $\delta^{15}N$ values showed unusual isotopic depletion during the summer months of 2016 and 2017. Stomach content analysis indicated shifts in red snapper diet between 2016 and 2017, with stomatopods and gastropods being the most abundant collected prey items in each year, respectively. Stable Isotope Analysis in R (SIAR) mixing models indicated crab and fish prey are the most isotopically significant contributors across depth strata. Red snapper $\delta^{13}C$ values were highly variable and maybe related to riverine inputs, while red snapper $\delta^{15}N$ values indicated that spatial baseline shifts were occurring in the depth strata possibly due to diet shifts.

ACKNOWLEDGMENTS

I would like to thank my funding sources for this project: The National Fish and Wildlife Foundation, Mississippi Department of Marine Resources and the Mississippi Department of Environmental Quality. I would like to thank the USM GCRL Fisheries Team for their significant amounts of time and effort sampling the fish utilized for this project. I would also like to extend a special thank you to Captain Rick Block and the crew of the R/V Jim Franks for their time and effort sampling throughout this project. Additionally, I would like to thank my colleagues and friends in the Dillon Lab: Morgan Frank, Caitlin Slife and Zehra Mohsin for their assistance in working on this project as well as their feedback. Finally, I would like to thank Dr. Kevin Dillon, Dr. Zachary Darnell and Dr. Frank Hernandez for their guidance, expertise and support for this project.

TABLE OF CONTENTS

LIST OF TABLES

LIST OF ILLUSTRATIONS

LIST OF ABBREVIATIONS

| | |
|---|---|
| *EBFM* | Ecosystem-based Fisheries Management |
| *GoM* | Gulf of Mexico |
| *MS-DMR* | Mississippi Department of Marine Resources |
| *GCRL* | Gulf Coast Research Laboratory |
| *POM* | Particulate organic matter |
| *NFWF* | National Fish and Wildlife Foundation |
| *SCA* | Stomach Content Analysis |
| *SIA* | Stable Isotope Analysis |
| *GF/F* | Glass Fiber Filters |
| *TP* | Trophic Position |
| *IRI* | Index of Relative Importance |
| *Chl-a* | Chlorophyll a |
| *SIAR* | Stable Isotope Analysis in R |

# CHAPTER I – VARIABILITY IN THE STABLE ISOTOPE VALUES OF PARTICULATE ORGANIC MATTER IN COASTAL MISSISSIPPI WATERS IN 2016 AND 2017

## 1.1 Introduction

Understanding the dynamics of food web trophic structure is essential to management strategies for recreationally and commercially important fish species. Typically, ecosystems with more complex trophic structures are more tolerant to variations in population size or habitat condition than ecosystems with more simplified trophic structures. An ecosystem with few species present and only one or two organisms occupying specific trophic levels is more likely to collapse due to population shifts and/or environmental disturbances, while trophically complex systems are more resilient to change and can often persist for extended periods of time even in communities with finite resources (Bell, 2007).

Stable isotope analysis (SIA) can improve food web models for ecosystem-based fisheries management (EBFM) and is commonly used to investigate food web structure in a wide variety of ecosystems. Stable isotopes are an integrated natural tracer that can provide information on longer-term dietary patterns depending on the turnover rate of the analyzed tissue (Fry, 2006). Stable isotopes values are reported in per mil (‰) notation using the following formula:

$$\delta^{H}X\ (‰) = [(R_{sample}/R_{standard} - 1) * 1000$$

where $R_{sample}$ is the ratio of heavy to light stable isotope in the sample and $R_{standard}$ is the ratio of heavy to light isotope in an internationally agreed upon standard (Fry, 2006). Stable isotope values are dependent upon isotope fractionation during biochemical

reactions and mixing of multiple sources with different stable isotope values. Isotope fractionation is mass dependent, with heavier isotopes having a higher discrimination effect and longer reaction times which results in isotopically light biochemical reaction products (Peterson & Fry, 1987). The primary stable isotopes used in food web studies are $^{13}C$ and $^{15}N$. Carbon stable isotopes experience minimal fractionation which results in low trophic enrichment (< 1‰) of consumer tissues, resulting in $\delta^{13}C$ values that reflect the primary producers supporting the base of a food web (Fry, 1983; Peterson, 1999). Plants which utilize the C3 photosynthetic pathway have more depleted $\delta^{13}C$ (-26 to -30 ‰; Fry & Wainright, 1991) than C4 plants (-10.4 to -16.6 ‰; Basu et al., 2015) due to differences in isotopic fractionation between the atmospheric $CO_2$ utilized during photosynthesis. Submerged marine primary producers, on the other hand, utilize bicarbonate from seawater, which may or may not be in in equilibrium with atmospheric $CO_2$, as a carbon source for photosynthesis. Isotopic fraction of marine primary producers can also be influenced by physical factors such as turbidly, temperature and salinity which may all impact photosynthetic rates (Fry & Peterson, 1987). Most marine primary producers have $\delta^{13}C$ values that are between C3 and C4 plants: benthic microalgae (-18.4 to -25.6; Dillon et al., 2015), marine phytoplankton (-19.5 to -22.5 ‰, Daigle et al., 2013), and marine particulate organic matter (-20.5 to -26.7 ‰, Dorado et al., 2012) which is often used as a proxy for marine phytoplankton. If different basal carbon sources are well described and isotopically distinct, contributions from multiple sources can be accurately estimated for consumers, often providing valuable insight into ecological linkages within food webs. Lipids in all organisms are more depleted in $^{13}C$, which can affect the $\delta^{13}C$ of prey items and predators, necessitating either solvent lipid extraction

the lipids prior to analysis or utilizing mathematic lipid corrections to correct for lipid-depleted $^{13}C$ values (Post et al., 2007).

Unlike $^{13}C$, $^{15}N$ undergoes significant trophic fractionation such that consumers are more enriched in $\delta^{15}N$ relative to their prey by 2.2 to 3.4 ‰ due to metabolic processes which favor isotopically light nitrogenous waste and the retention of isotopically heavy nitrogen in body tissues (Fry, 2006). $\delta^{15}N$ values of basal primary producers can also vary temporally and spatially due to differences in nitrogen sources between environments or across time scales, resulting in a isotope baseline shifts of basal resources which are often lead to spatial differences in the isotope values of primary producers which can propagate thru the food web, leading to well defined 'isoscapes' for basal resources and some consumers (McMahon et al., 2013; Radabaugh et al., 2013). Temporal changes in $\delta^{15}N$ can be due to variable nutrient delivery which, in coastal ecosystems is often due to seasonal and annual changes in freshwater inputs (Cai et al., 2012). Using $^{15}N$ in conjunction with other stable isotopes such as $^{13}C$ can illustrate trophic linkages and lead to the development of ecosystem-based food web models that can inform management strategies (Peterson, 1999).

Stable isotopes have been used to study Gulf of Mexico (GoM) food webs in a variety of habitats. For example, Wells et al. (2017) compared food webs in mesoscale oceanographic features such as warm-core, anticyclonic eddies and cold-core, cyclonic eddies. More complicated trophic structures were present in the cyclonic eddy systems when compared to the anticyclonic eddy systems and cyclonic eddies were more enriched in $\delta^{15}N$ (Wells et al., 2017). This research also indicated there were two basal carbon

sources in these mesoscale oceanographic features: POM and *Sargassum* (Wells et al., 2017).

The National Fish and Wildlife Foundation (NFWF) Reef Fisheries Assessment was a multidisciplinary project conducted in Mississippi state waters from 2016 to 2020 with three main objectives: 1) map reef habitats to delineate benthic habitat types for stratified reef fish sampling, 2) utilize standardized NOAA SEAMAP (Southeast Area Monitoring and Assessment Program) sampling methodologies to assess age, growth, reproduction and feeding ecology of red snapper and other reef fish species, and 3) define site-specific relationships between fisheries abundance and environmental conditions. The purpose of this chapter of the research presented herein relates to the third objective and more specifically, using SIA to describe the basal resources and POM variability of Mississippi's artificial reef habitats. This includes determining the isotopic variation of POM in the NGoM as POM is commonly utilized as an isotopic proxy for phytoplankton as the base of reef food webs. To complete this goal, POM samples were collected from multiple sites in Mississippi state waters during 2016 and 2017 for SIA. These POM stable isotope values were then used to inform on basal resource utilization and trophic position calculation of red snapper and its prey items sampled at the same sites.

## 1.2 - Methods

### 1.2.1 - Sampling Area and Timeframe

Samples from 23 randomly selected sites in Mississippi state waters were collected monthly from April through October in 2016 and 2017 for a total of 322 stations (Figure 1.1). The sample sites were randomly selected from a predefined geographic area based upon the type of structure present (1.Artificial reefs including

Rigs-to-Reefs locations, 2.Active petroleum and natural gas platforms, and 3.Bare-bottom control sites) across three depth strata (shallow, 0-20 m; mid, 21-50 m or deep, >50 m). The monthly sampling was conducted by two collection teams: Mississippi Department of Marine Resources (MS-DMR) primarily sampled inshore 'fish haven' sites while GCRL largely sampled offshore sites, composed mostly of oil rigs and Rigs-to-Reef sites. The two teams attempted to sample within one week of each other if weather and other logistical factors allowed but some sampling was more temporally disconnected (Table 1.1).

### 1.2.2 – POM Sample Collection and Processing

Water for POM samples was collected from the surface and near bottom depths at all sampling sites. Additional water samples were collected in 2017 at the chlorophyll maximum depth to characterize stable isotope values of POM at this depth to determine isotopic variability of phytoplankton within the water column. MS-DMR water samples were collected using a weighted WildCo 2.2L clear acrylic horizontal beta sampler, and then transferred to clean, acid-washed 1-2 L bottles which were kept on ice until transported to the laboratory. Water was collected by GCRL with two types of niskin bottles: a WildCo 2.2L clear acrylic horizontal beta sampler was used to collect surface water and a General Oceanics Niskin Sampling Bottle (Model 1010-10L) collected a larger volume water from bottom and chlorophyll maximum depths to minimize sampling time. Triplicate POM filters for surface and bottom water samples were collected by vacuum filtering known volumes of water through 25 mm muffled (500° C for 2 hours) glass filters (Whatman GF/F, 0.7 μm nominal pore size) using 250ml filtration towers (Pall) and a 3-place stainless steel vacuum manifold (Millipore). GCRL

samples were filtered immediately after water collection while MS-DMR water samples were filtered at the end of the sampling day at GCRL. After collection, sample volumes were recorded and filters were placed in labeled petri dishes then frozen. Filters were dried at 65°C for 12-24 h, then each filter was examined for the presence of any large zooplankton, which, if present, were carefully removed from the filter with forceps. Next, the filters were fumed in a concentrated hydrochloric vapor bath for 24 h to remove inorganic carbon and then air dried in a fume hood for one hour. Petri dishes were recapped and stored in a desiccator until the filters were packed whole into tin capsules for stable isotope analysis. δ13C and δ15N values as well as C and N concentrations were measured on a Costech 4010 elemental analyzer coupled to a Thermo Delta V Advantage stable isotope ration mass spectrometer (IRMS) via a Thermo Conflo IV Interface. Two of the three filters for each station and depth were analyzed while the third was archived unless excessive variation (defined as difference of >3‰ between duplicates or unusually depleted δ15N values) between the first two filters was found, in which case the third filter was analyzed. The averaged stable isotope values from the filters were utilized for the analysis.

POM results were split by sampling depth in the water column (surface and bottom) as well as by depth strata (shallow, mid, deep) to examine cross-shelf trends. Water quality data such as salinity, temperature and dissolved oxygen at each station was collected utilizing a CTD instrument deployed at each station throughout the water column. Statistically significant relationships between isotope values and collection month, year, salinity, temperature, dissolved oxygen concentrations, depth strata, and structure type at the time of collection were analyzed using a single-variate ANOVA test.

Spearman rank correlation analysis was done to determine the type and strength of correlations present in the statistically significant results. A Mantel test was used to determine if isotope values varied significantly as a function of geographic location in which samples were collected. The null hypothesis for the POM is that there will be no significant difference in isotopic values (δ13C, δ15N) of the POM regardless of sample location, date of sampling effort, depth strata, salinity, temperature and structure type. The alternative hypothesis is that there will be differences in the isotopic values due to sample location, date of sampling effort, depth strata, salinity, temperature and structure type.

## 1.3 - Results

### 1.3.1 – POM and Basal Resource Utilization

We analyzed 675 GF/F filter replicates for 2016 (n = 312) and 2017 (n = 355). All errors presented are standard deviations. POM collected in 2016 had a broad range of $\delta^{13}C$ and $\delta^{15}N$ (Figure 1.2, 1.3) but the annual average surface and bottom water $\delta^{13}C$ were similar (-23.4‰ ± 2.3 and -24.6‰ ± 3.0, respectively; Appendix A1). Surface water POM $\delta^{13}C$ for all depth strata showed no pattern from April to August then $\delta^{13}C$ declined at all depth strata during September to October (Figure 1.4). POM $\delta^{13}C$ in bottom waters declined throughout the sampling year and there was a monthly trend of $\delta^{13}C$ become more depleted moving from the shallow strata sites to the deep strata sites (Figure 1.5). $\delta^{13}C$ wasn't significantly impacted by temperature, dissolved oxygen, depth strata sampled or salinity. The average 2016 $\delta^{15}N$ for surface water samples across all depth strata was 4.7 ± 5.1‰ with most values being consistent throughout the year with a small dip in values measured during June. Bottom water had a lower average value (0.9‰ ±

9.6) with a larger range due to some unusually low $\delta^{15}N$ (< -10 ‰) measured in all depth strata during the summer near the southern end of the Chandeleur Islands (Figure 1.6) however the phenomenon was most pronounced in June (Appendix A2; Figures 1.7, 1.8). Aside from these low values, surface and bottom water POM $\delta^{15}N$ were similar during the spring and fall sampling months. The unusually low POM $\delta^{15}N$ were primarily found in bottom water samples and were not significantly affected by any measured water parameter (salinity, pH, dissolved oxygen) but they did occur at a narrow range of water temperatures (20 to 24°C) although many samples collected in this temperature range did not show such depletion (Figure 1.9) and the one low $^{15}N$ value measured in surface waters was collected at a higher temperature (27°C). $\delta^{13}C$ and $\delta^{15}N$ of POM collected in bottom water were significantly related to C:N ratios: $\delta^{13}C$ becomes more depleted as the C:N ratio increases (Figure 1.10) while $\delta^{15}N$ generally becomes more depleted as C:N decreases below 6.0 (Figure 1.11). Chlorophyll-a (Chl-a) concentrations were on average higher in the surface waters than bottom water samples, with several high Chl-a outliers in 2017 that skewed the results (Figure 1.12). Chl-a was generally highest when $\delta^{13}C$ was between -25‰ and -20‰ (Figure 1.13)

The POM $\delta^{15}N$ of 116 samples across both years weren't available because of low particulate nitrogen concentrations which prevented accurate isotope analysis. Surface water samples from 2017 had an annual average $\delta^{13}C$ that was similar to that in 2016 (-23.8‰ ± 2.1) while bottom water had a lower average $\delta^{13}C$ (-26.9‰ ± 2.9) (Appendix A3). Like what was measured from April to August 2016, the 2017 surface water $\delta^{13}C$ showed no clear temporal pattern however the shallow strata often had more variable $\delta^{13}C$ (Figure 1.14). Bottom water POM samples from 2017 were more consistent and $^{13}C$

depleted, on average, than those collected in 2016 (Figure 1.15). Moving from the shallow to deep depth strata, bottom water $\delta^{13}C$ generally become more depleted except during July through September. The average 2017 $\delta^{15}N$ for surface and bottom water POM samples across all depth strata were 4.0‰ ± 4.8 and -3.1‰ ± 10.5, respectively (Appendix A4). Surface water POM $\delta^{15}N$ from 2017 were similar to those from 2016 (Figure 1.16). Like in 2016, a decrease in surface water $\delta^{15}N$ were measured across all depth strata (Figure 1.17) during June and July. Bottom water (Figure 1.18) $\delta^{15}N$ were slightly more variable in 2017 than in 2016, with highly depleted $\delta^{15}N$ in June, July and September, at stations in both the northern and southern regions of our sampling area (Figure 1.19). Like the 2016 results, there was no correlation of these unusually low values to any measured water parameter, including temperature. The northern depleted $\delta^{15}N$ in bottom waters were from shallow strata sites near Horn Island while the southern depleted $\delta^{15}N$ were from deep strata sites near the southern Chandelier Islands, as was observed in 2016. The deep strata $\delta^{15}N$ depleted sites had lower temperatures (17 to 21°C) than the shallow strata $\delta^{15}N$ depleted sites (~27°C; Figure 1.20). C:N showed no correlation with 2017 bottom water $\delta^{13}C$ although a weak correlation between C:N and $\delta^{15}N$ was found (Figure 1.21 & 1.22), similar to results from 2016.

Single-variate ANOVA analysis showed that only the sampling month, sampling year, depth strata and dissolved oxygen significantly affected POM $\delta^{13}C$ (Table 1.2). Spearman rank correlation analysis indicated POM $\delta^{13}C$ was positively correlated with dissolved oxygen (Rho = 0.15, p = > 0.01) and negatively correlated with sampling month (Rho = - 0.22, p = > 0.01), year (Rho = - 0.10, p = 0.025) and depth strata (Rho = - 0.07, p = 0.019). The Mantel test indicated there was no relationship between POM $\delta^{13}C$

and sampling location (Mantel R = 0.00769, p = 0.224). The single-variate ANOVA analysis of the POM $\delta^{15}N$ indicated that POM $\delta^{15}N$ was significantly influenced by sampling month, dissolved oxygen and temperature (Table 1.3). Dissolved oxygen was higher in the surface water (Figure 1.23) than in the bottom water (Figure 1.24) for both years. $^{15}N$ in 2016 bottom water samples were highly depleted between 3.5 and 5 mg/L DO, which correlates with lower water temperatures (Figure 11, Figure 1.24). The bottom water depleted $\delta^{15}N$ POM occurred over a large range of DO concentrations in 2017. Water temperature didn't significantly impact POM $\delta^{15}N$ for either year. Spearman rank correlation analysis indicated POM $\delta^{15}N$ didn't correlate with sampling month (Rho = 0.06, p = 0.21) and positively correlated with dissolved oxygen (Rho = 0.21, p = > 0.01). The mantel test indicated that sampling location affected the $\delta^{15}N$ of the POM samples (Mantel R = 0.000197, p = 0.04805).

**1.4 - Discussion**

POM water samples collected in surface waters were more enriched on average in $\delta^{13}C$ in 2016 than in 2017 while POM $\delta^{15}N$ values were consistently similar across depth strata, sampling months and between years. POM bottom water samples in 2016 showed a general trend of depletion over the course of 2016 while POM $\delta^{13}C$ collected in 2017 were generally more depleted throughout the year by comparison. During the summer months of both 2016 and 2017, unusually depleted POM $\delta^{15}N$ samples were collected in bottom water at several sites.

POM is regularly used as a proxy for phytoplankton because phytoplankton are a significant component of marine POM and difficult to separate (Dorado et al., 2012). As discussed in the introduction, marine phytoplankton $\delta^{13}C$ values have been shown to

range from -19.5 to -22.5 ‰ (Daigle et al., 2013) with marine POM occupying a larger, more depleted range (-21 to -25 ‰; Fry & Wainright, 1991). Riverine POM, on the other hand, is more complex mixture of phytoplankton and terrestrial organic matter (Kendall et al., 2001) and previous research has shown that POM $\delta^{13}C$ values of the lower Mississippi River ranges from -28.2‰ to -24.6‰ with an average of -26.3‰ ± 1.1 (Cai et al., 2015), which is similar to our lower POM $\delta^{13}C$ values. Negative shifts in $\delta^{13}C$ of POM sampled from Bay of St Louis, Mississippi have been attributed to riverine DIC being utilized by marine phytoplankton (Cai et al., 2012). The POM samples collected in 2016 and 2017 had high isotopic variability. $\delta^{13}C$ varied by depth strata, sampling month, and sampling year with higher variability occurring earlier in the year for both 2016 and 2017, likely due to differences in freshwater flow regimes during the sampling periods.

There are several local rivers that influence coastal Mississippi waters including the Mississippi River, Pascagoula River, Wolf River and Pearl River. The Mississippi River had a maximum flow of just over 1,100,000 $ft^3$/sec (31,149 $m^3$/sec) in April 2016 before decreasing steadily over the course of the year (Figure 1.25). The peak flow during 2017 was later in the year (May - June) with a peak of about 1,200,000 $ft^3$/sec (33,980 $m^3$/sec) (Figure 1.25). While the Mississippi River had significantly higher discharge rates, the other three rivers had similar freshwater discharge trends in 2016 and 2016 (Figure 1.26 – Figure 1.28). While extensive POM isotope studies have not been conducted in our study area, a 2011 Mississippi River flooding event that occurred during the summer was analyzed using the Aquarius satellite and the SMOS (Soil Moisture and Ocean Salinity) project. The analysis indicated that salinity, Chl-a and temperature shifts were still distinguishable one to three months after peak river discharge in the GoM from

Louisiana to Florida coastal waters out to the continental slope (Gierach et al., 2013). The nature of the numerous freshwater sources and the variability of currents across the sampling area makes it difficult to quantify which sources most significantly contributed to the POM $\delta^{13}C$ values at this time. A combination of marine phytoplankton utilizing riverine DIC to produce biomass as well as riverine POM remaining in coastal waters could explain our depleted $\delta^{13}C$ values. The POM $\delta^{13}C$ values from the 2017 surface water were lower on average than those from 2016 likely due to the increased discharge of the Mississippi River in 2017. The 2017 POM $\delta^{13}C$ values were generally higher in the nearshore waters than the deep-strata sites as a result of riverine waters being pushed further offshore by the peak river flow. Residence times in local estuaries are highly dependent on the rate of freshwater input and wind action (Camacho & Martin, 2013). As the riverine discharge water is pushed further offshore, shifts in salinity and available DIC as a result of the moving river plume may result in the shifts of POM $\delta^{13}C$.

The bottom water POM $\delta^{13}C$ values in both years were variable and more depleted on average than published values for marine phytoplankton or marine POM. In particular, 2016 showed a steady decrease in monthly POM $\delta^{13}C$ by depth strata over the course of the sampling year with the deep-strata sites being the most depleted on average. This suggests that riverine inputs had an effect on bottom water POM $\delta^{13}C$ values likely due the settling of $^{13}C$ depleted POM and phytoplankton from the surface to deeper waters. Aggregates of diatoms and other materials have variable settling rates ranging from 10 to 85 m/day (Average = 33.8 m/day) depending on the aggregates' size (Diercks & Asper, 1997). This settling rate would allow riverine POM or marine phytoplankton that utilized riverine DIC to reach the deep-strata station bottoms in a matter of days,

depending on the size of the aggregates and the rate of aggregate formation. One of the earliest studies of the earliest examining $\delta^{13}C$ of POM from 79 semitropical (GOM, Caribbean, and Atlantic) and polar stations (South Indian Ocean) showed that deep water (>330m) POM $\delta^{13}C$ was generally more negative than surface water POM, except in well mixed polar areas (Eadie & Jeffery, 1973).

The 2017 bottom water POM $\delta^{13}C$ didn't show the same year-long trend observed in 2016 which indicates that changes in river discharge and local water residence times may affect the settling rates of POM. With the peak discharge of the Mississippi River later in the year in 2017, the increased flow rate would increase the accumulation of riverine DIC in marine phytoplankton. When the POM aggregated and settled to the bottom, it had accumulated riverine DIC and was more depleted compared with the 2016 bottom water POM $\delta^{13}C$.Previous work has shown that phytoplankton and POM settling is affected by currents and wind conditions (Kaldy et al., 2005). Additionally, Tropical Storm Cindy moved through our sampling region during June 2017. Hurricanes and large storms have been shown to homogenize the water column, reducing the variability of POM $\delta^{13}C$ (Pre-Hurricane: -21 to -25‰; Post-Hurricane: -23 to -24‰) (Fogel et al., 1999) similarly to what was observed in our sampling locations.

Phytoplankton primarily utilize dissolved inorganic nitrogen (DIN) in the form of nitrate, nitrite or ammonium for photosynthesis (Zehr & Ward, 2002). DIN are brought into coastal marine waters primarily by riverine inputs, nitrogen fixation, and can be brought up from depth to surface waters via water column homogenization (Dorado et al., 2012; Sigman et al., 2009; Bode et al., 2003). Mississippi River nitrate sampled near Belle Chasse, Louisiana had $\delta^{15}N$ values that ranged from 3.5‰ to 6.0‰ (Chang et al.,

2003) although higher and more variable values have also been documented in the lower Mississippi River (4.4‰ to 9.44 ‰) (Cai et al., 2015). Phytoplankton samples collected in coastal Mississippi surface waters using a 53-micron plankton net showed $\delta^{15}N$ ranged from -1.4‰ to 10‰ with a clear isoscape pattern of high values near the coast and low values offshore (Fleming, 2018). The POM we sampled in 2016 and 2017 had similar average $\delta^{15}N$ to other studies, although the range of $\delta^{15}N$ was much greater due to the highly depleted samples. Marine phytoplankton $\delta^{15}N$ have been shown to vary seasonally in the region (Daigle et al., 2013) and the results presented here could suggest a seasonal effect may be driving the highly depleted POM $^{15}N$ since these values were measured during summer months.

The Redfield ratio is the C:N:P (106:16:1) of phytoplankton measured in the Sargasso Sea and is often used as an average elemental ratio of phytoplankton across the world's oceans. The Redfield ratio can also crudely inform whether POM is heterotrophic or autotrophic because heterotrophs tend to accumulate more nitrogen than carbon and thus typically have lower C:N. The POM $\delta^{13}C$ values negatively correlated with C:N in 2016 but not in 2017. The broad range of C:N values indicated the POM is a mix of autotrophic and heterotrophic material. Chlorophyll-a concentrations were higher in surface water than in bottom water, as one would expect, but Chl-a concentrations were generally higher in POM samples with $\delta^{13}C$ between -25 and -20‰.

Several species of cyanobacteria have the ability to fix atmospheric $N_2$ which typically results in phytoplankton $\delta^{15}N$ values near 0 per mil however slightly depleted $\delta^{15}N$ have been measured in the GoM and Mediterranean Sea during cyanobacterial blooms (Dorado et al., 2012; Holl et al., 2007; Kerherve et al., 2001). The cyanobacteria

*Trichodesmium*, common in the northern GoM, has been shown to have $\delta^{15}N$ values near -4‰ (Holl et al., 2007), and C:N ratios slightly lower than the Redfield ratio (5.9 and 6.3; Letelier and Karl, 1998). *Trichodesmium* populations in coastal Mississippi waters are most abundant during the summer in regions of low nitrate and nitrite concentrations (Charkraborty and Lohrenz, 2015; Zhao and Quigg, 2014). Nitrogen fixation often occurs near the surface because of the high energy demand required for the process, which for cyanobacteria, is provided by sunlight used to fuel photosynthesis. Nitrogen fixation may account for part of the unusually depleted $^{15}N$ values observed in 2017 POM sampled from the shallow strata near the barrier islands. However, the majority of the unusually low $^{15}N$ values were much less than -4 ‰ and were from bottom waters which suggests N-fixation could not be the primary driver of these low values. The bottom water $^{15}N$ depletions are odd since deep water nitrate is usually enriched in $^{15}N$ relative to surface waters (Leichter et al., 2007). Partial nitrification in bottom water can theoretically explain these low $\delta^{15}N$ values. Nitrifying microbes are estimated to make up about 40% of all marine prokaryotes (Karner et al., 2001). The first step in nitrification is oxidation of ammonium ($NH_4^+$) to nitrite ($NO_2^-$) by ammonia oxidizing bacteria and archaea (Lehtovirta-Morley, 2018). Cultures of marine ammonia oxidizing archaea have been shown to initially produce $NO_2$ with very low $\delta^{15}N$ (-10‰ to -25‰) under high $NH_4^+$ conditions ( > 5μM), although the remainder of the $NO_2$ produced does become progressively enriched in $^{15}N$ over time as the fraction of nitrified ammonium increased (Casciotti et al., 2010; Santoro and Casciotti, 2011). These extremely low $\delta^{15}N$ are similar to those measured in the shallow and deep strata bottom POM. Lower oxygen concentrations observed in bottom waters (< 5mg/L) may limit the extent of the

nitrification reactions, resulting in isotopically depleted nitrite, which would then available for utilization by autotrophs and microbes. The unusually $^{15}N$-depleted POM samples in bottom waters also had C:N values well below the Redfield Ratio, indicating $^{15}N$ depleted POM consisted of a high proportion of heterotrophic material. The results of the stable isotope analysis of POM supports my alternative hypothesis that the isotope values will be different based upon sampling location, water quality, or date of sampling effort.

# CHAPTER II – DETERMINING RED SNAPPER PREY UTILIZATION, DIET, AND THE TROPHIC ROLES OF RED SNAPPER AND ITS PREY IN COASTAL MISSISSIPPI WATERS.

## 2.1 Introduction

Understanding the trophic interactions of commercially important fish enables fishery managers to assess the effects of overfishing and ecosystem alterations on fish stocks. For example, research efforts to quantifying overfishing of specific communities in the North Sea have shown that there is a progressive decline in the trophic level of targeted demersal species such as haddock and cod, which coincides with progressively smaller catch sizes and individual specimen sizes within those catches (Jennings et al., 2002). This research also demonstrated declines in trophic level among the targeted pelagic fish species such as herring and mackerel, which suggested that pelagic trophic structure was more complicated than previously understood (Jennings et al., 2002).

Shifting from region-specific and single-species assessments to broader ecosystem-based fisheries management (EBFM) requires additional understanding of environmental factors as well as trophic relationships between predators and prey (Longo et al., 2015). Stomach content analysis (SCA) is a relatively simple and widely used method to define trophic relationships. There are several metrics commonly used in SCA: frequency of occurrence (%F, Proportion of individuals containing a certain prey type), numerical (%N, number of items of a prey type proportional to total types of prey), prey by weight (%W, weight of each prey item), or index of relative importance (%IRI, composite metric combining %N, %W and %F) (Baker et al., 2014). An example of SCA effectiveness was with Lingcod *(Ophiodon elongatus*) on nearshore reefs in Oregon

waters. Dive survey data indicated they primarily feed on highly abundant rockfishes; however, SCA showed that rockfish were the least consumed prey, making up less than 5% of Lingcod prey items (Tinus, 2012). While SCA can inform EBFM, it does have limitations, such as providing limited prey information based on a single snapshot in time which may not be reflective of a consumer's complete diet. The condition of prey items due to the degree of digestion within the stomach can also affect visual identification and quantification of prey types being consumed (Buckland et al., 2017). The most recently consumed prey and prey with hard body parts (exoskeletons and bones) are typically more easily observed and identified while softer prey items such as jellyfish and fish eggs are poorly preserved in the stomach. Since partially digested prey condition can result in undercounting of items in a predator diet, combinations of metrics are utilized to determine if particular prey is present and if possible, the proportion of that prey item relative to the total predator diet (Buckland et al., 2017). DNA barcoding can aid in the identification of partially digested prey items that cannot be visually identified; however, a species DNA barcode must be available for comparison from massive online databases. Many diet studies combine traditional SCA with other validated dietary tracers such as stable isotopes or lipids. Due to the ease of sample processing and relatively low analysis costs, stable carbon and nitrogen isotopes have become common tracers in many food web studies.

Stable isotope analysis (SIA) of bulk muscle tissue, in conjunction with stomach content analysis, can improve food web models for EBFM and are commonly used to investigate food web structure in a wide variety of ecosystems. As described in Chapter 1, stable isotopes are an integrated natural tracer that can provide information on longer-

term dietary patterns depending on the turnover rate of the analyzed tissue (Fry, 2006). The primary stable isotopes used in food web studies are $^{13}C$ and $^{15}N$. As previously stated, $\delta^{13}C$ values reflect the primary producers supporting the base of a food web (Fry, 1983; Peterson, 1999) while $^{15}N$ undergoes significant trophic fractionation such that consumers are more enriched in $\delta^{15}N$ relative to their prey and can determine a target species' diet (Fry, 2006). A $^{15}N$ trophic enrichment factor (TEF) of 2.2‰ has been shown for invertebrates (Post, 2002), while vertebrates typically show a slightly higher TEF near 3.4‰ (Minigawa and Wada, 1984; Post, 2002).

A previous study combining stomach content analysis with SIA on mesopelagic fish from 31 species revealed a three-tiered food web where secondary consumers were primarily feeding on copepods, salps and other soft-bodied species that are not easily identifiable via stomach content analysis (McClain-Counts et al., 2017). Trophic dynamics can be affected by environmental perturbations and disasters such as oil spills. After the Deepwater Horizon oil spill, red snapper stomach content analysis indicated a dietary shift from primarily invertebrates to a more fish-based diet, a result that was also supported by elevated red snapper $\delta^{15}N$ indicating these fish were feeding at a higher trophic position following the oil spill (Tarnecki & Patterson, 2015).

Red snapper *(Lutjanus campechanus*) is a structure-associated fish species in the taxonomic order Perciformes (Family Lutjanidae) which has high economic and recreational value within its habitat range in the western Atlantic from the Amazon River delta to Cape Hatteras, NC, including the Gulf of Mexico (Wilson & Nieland, 2001). It's an economically important species with 354,645 red snapper landings recorded by recreational anglers in 2016 alone (GMFMC, 2019). Population surveys throughout the

northern GoM have indicated that red snapper have a lifespan of up to 52 years (based on otolith annuli analysis) and can reach a maximum length of approximately 1039 mm and a maximum weight of 22.79 kg (Wilson and Nieland, 2001; Gallaway et al., 2009). Red snapper spawn pelagically over broad areas and a wide range of depths from April to September peaking from June to August (Wells & Rooker, 2009; Gallaway et al., 2009). Eggs and larvae are transported by currents, then once larvae reach between 15-25 mm in length, they settle on sandy, shell, or muddy bottoms along the continental shelf (Lindeman et al., 2005). Juvenile red snapper between 70-100 mm begin moving to reef or structured habitat, which provides shelter from predation and have a high abundance of prey items (Szedlmeyer and Lee, 2004). Juvenile red snapper can change structures after settlement in order to find a more ideal habitat or prey base and to avoid competition (Patterson, 2007). Red snapper sampled in coastal Alabama waters have shown an increase in average total length moving from sand, to low-relief shell, to high-relief rig habitat (Wells et al., 2008). Once settled, red snapper show high site fidelity, typically staying within half a kilometer of their initial capture sites over a period of several months (Gallaway et al., 2009). Juveniles steadily shift to larger structured habitats and undergo an ontogenetic diet shift from zooplankton and mysid shrimp to larger crustaceans based upon prey availability (Simonsen et al., 2014; Wells et al., 2008, Gallaway et al., 2009). As the fish grow and approach maturity (age 2+ years), they attempt to find more complex structures in deeper offshore waters (Gallaway et al., 2009; Wilson & Nieland, 2001), however mature individuals can remain nearshore if they find suitable habitat with ample prey (Wells et al., 2008). As with juveniles, mature red snapper show high site fidelity, favoring increasingly larger and structured habitats such

as oil rigs, shipwrecks and natural reef formations (Patterson et al., 2001). As they continue to grow, adults progressively feed at higher trophic levels, consuming higher quantities of fish and larger crustaceans such as crabs and stomatopods (Simonsen et al., 2014). Red snapper have been shown to stray from their 'home' structure to feed on benthic or pelagic prey items (McCawley and Cowan, 2003). Previous research in the north-western GOM showed that red snapper do not appear to have a preference between artificial and natural reefs, however stomach content analysis and stable isotope values indicate individuals feeding near artificial reefs consume less diverse prey than their natural reef counterparts (Schwartkopf et al., 2017). Mississippi state waters have few natural reefs so the majority of red snapper populations are supported by artificial reefs (a.k.a. fish havens) and oil platforms. The unique ecology of this species in conjunction with its regional significance lead to the red snapper being selected as the primary study species for this project.

As part of the broader NFWF Reef Fisheries Assessment's second objective, the purpose of the research presented in this chapter relates to using SCA and SIA were utilized to describe the food web structure of Mississippi's artificial reef communities, with an emphasis on the diet and ecological role of red snapper. Developing a better ecological understanding of this species is essential to properly managing Mississippi red snapper stocks. This includes determining what prey items red snapper predominately consume and their trophic positions using POM stable isotope values described in Chapter 1. To complete these goals, reef fish samples were collected from multiple sites in Mississippi state waters during 2016 and 2017 for SCA and SIA. Identified prey items obtained from SCA were utilized for SIA. A limited number of biofilm samples were also

obtained by divers from hard reef substrates in 2017 for SIA and inclusion in isotope mixing models to determine the potential of biofilms as a food source for red snapper.

## 2.2 - Methods

### 2.2.1 – Sampling Area and Timeframe

The sampling area and timeframe are described in Chapter 1.

### 2.2.2 – Red Snapper Collection and Processing

Red snapper were collected using three motorized bandit reels deployed at each station for five-minutes. Each reel had 10 hooks spaced 24 inches apart for a total of 30 hooks of different sizes (8/0, 11/0, 15/0) to target a broad size range. The lines were deployed to within five feet of the seafloor or above any structure at the site (i.e., artificial reef, near base of an active platform). Once caught, each fish was tagged with a unique sample number and biometric parameters (total length, standard length, fork length, weight, sex) were recorded. A small amount of dorsal muscle tissue (~1 $in^3$) was collected from each fish then placed in labeled Whirl-Pak bags and stored in a -20°C freezer. Muscle tissue samples were freeze dried for 48 hours, ground to a fine powder with a mortar and pestle and then stored in labeled 20 ml scintillation vials in a desiccator cabinet. Replicate tissue samples (0.3-0.7 mg) were packed into tin capsules then analyzed for $\delta^{13}C$ and $\delta^{15}N$ values as described for POM analysis.

The trophic position (TP) of biofilm, prey items, and each red snapper were calculated using the formula:

$$TP = (\delta^{15}N_{Consumer} - \delta^{15}N_{Base}) / \Delta n + \lambda$$

where $\delta^{15}N_{Consumer}$ is that of Red Snapper, $\delta^{15}N_{Base}$ is the $\delta^{15}N$ of the primary producer that serves as the base of the food web (i.e. phytoplankton), $\Delta n$ is the isotopic

trophic enrichment factor (3.0‰) previously used for red snapper (Wells et al., 2008) and λ is the trophic position of the basal resource (λ = 1 for primary producers). Two different $\delta^{15}N$ baselines were used for TP calculations to compare different methods commonly found in the literature. The first $\delta^{15}N$ baseline calculation was using the two-year average bottom water POM (λ = 1) $\delta^{15}N$ value (5.71‰ ± 2.57) which excluded highly depleted $\delta^{15}N$ values measured during some summer months to prevent unrealistically skewed results. This average POM $\delta^{15}N$ value is very similar to the phytoplankton value used previously to estimate red snapper TP in coastal Alabama waters (5.82‰ ± 0.13 SE; Tarnecki and Patterson, 2015). The second TP calculation involved using the $\delta^{15}N$ of a consumer with a 'known' TP as a baseline proxy. White shrimp (*Litopenaeus setiferus),* a common prey species that was collected across the sampling area, has been determined to have a TP of 2.14 in a Texas estuary (Akin and Winemiller, 2008). This estuarine white shrimp λ was utilized along with the average $\delta^{15}N$ of white shrimp sampled during this study (10.44‰ ± 0.8) for this calculation. Stable isotope values of red snapper were analyzed using a single-variate ANOVA test to determine if each isotope was statistically affected by collection month, year, salinity, temperature, depth strata, structure type, sex, length or fish weight. A Mantel test was used to determine if isotope values varied with the sampling locations. Source contributions of prey items from stomach contents (see below) to red snapper diets were examined using Stable Isotopes Analysis in R (SIAR). The null hypothesis is that there will be no significant difference in isotopic values for the red snapper regardless of sample location, date of sampling effort, depth strata, salinity, temperature and structure type. The alternative hypothesis is that $\delta^{13}C$ and $\delta^{15}N$ will show

spatial and temporal variability based on sampling date, depth strata being sampled, or water quality factors.

### 2.2.3 – Red Snapper Prey Item Collection and Processing

Prey items found in the red snapper's mouth or stomach were collected and visually identified to the lowest possible taxonomic level before identification with DNA barcoding by collaborators at GCRL. Samples were stored at -20°C until being freeze dried for 48 hours. To remove any inorganic carbon associated with the carapace, dried crustacean prey items were acid-washed with 10% HCl and then centrifuged at 500 RPM for five minutes before being rinsed with deionized water and centrifuged an additional three times to remove residual acid and then re-dried. Prey samples were ground to a fine powder using a mortar and pestle and then stored in 20 ml scintillation vials in a desiccator cabinet until being packed in tin capsules and analyzed for $\delta^{13}C$ and $\delta^{15}N$ as described previously. Prey items collected were quantified by GCRL collaborators using several metrics: 1) numerical (%N) is the number of a particular type of prey as a proportion to all prey collected (Buckland et al., 2017); 2) the weight (%W) of the prey items of each type (Buckland et al., 2017); 3) the frequency of occurrence (%F) of red snapper that had consumed a particular prey type (Tinus, 2012); and 4) the index of relative importance (IRI):

$$IRI = (\%N + \%W) * \%F$$

All SCA data presented is in %N. The TP of each prey item was calculated with the two methods described for red snapper using POM and white shrimp as baselines. A $\delta^{15}N$ TEF of 3.4‰ was utilized for all vertebrate prey (Minigawa and Wada, 1984; Post, 2002) while a TEF of 2.2‰ was used for invertebrate prey (Post, 2002). To correct for

the low $\delta^{13}C$ of lipids within tissues, a lipid correction was applied to the fish, shrimp and crab prey items with carbon to nitrogen ratios (C:N) greater than 3.5 (Logan et al., 2008) following the equation from Fry (2003):

$$\delta^{13}C_{Corrected} = (\delta^{13}C_{Untreated} * C{:}N_{Sample}) + (6 * (C{:}N_{Sample} - 3.5))) / C{:}N_{Sample}$$

Lipid corrected $\delta^{13}C$ for prey with C:N > 3.5 were used for all analysis. The $\delta^{13}C$ and $\delta^{15}N$ of the prey items were analyzed using a single-variate ANOVA test to determine the significance of the stable isotope values calculated in relation to the month, year, salinity, temperature, depth strata and structure type at the time of collection. Like the red snapper, the relationship of sampling location and stable isotope values was assessed using a Mantel test. Mixing models using the R package SIAR were used for the red snapper prey based upon the depth strata collected and the sampling year. Errors (i.e. standard deviations) were propagated in the models for both isotopes for predators and prey, and TEFs of 3.4 and 2.2 were utilized for fish and invertebrates as described for TP calculation. All prey types with $n < 5$ were excluded from the mixing model to avoid any false extrapolations based on small sample size.

Opportunistic biofilm samples obtained by Gulf Fishing Banks divers during the spring of 2017 from several artificial reef sites in the northern portion of the study area were also analyzed for stable isotopes to examine if this attached biofilm could be an important yet overlooked basal resource for reef food webs. The biofilm samples were placed in labeled zip lock bags and stored one ice in the field then rinsed with DI water before being frozen and then freeze dried for 48 hours. Dried biofilm material was ground using a mortar and pestle and packed in tin capsules for $\delta^{13}C$ and $\delta^{15}N$ analysis.

## 2.3 – Results

### 2.3.1 – Red Snapper Prey Utilization and Diet Composition

Stomach content analysis utilizing visual identification and DNA barcoding techniques successfully identified most of the collected red snapper prey items. While some prey items were successfully identified down to species level, most identification was to taxonomic class or family so all prey type categories presented herein were grouped near those taxonomic levels for consistency. Unfortunately, the DNA barcoding technique utilized most of the prey item samples so only a limited number of prey had enough material remaining to be analyzed for stable isotope values.

Stomach content analysis identified 1497 red snapper prey items in 2016 (Table 2.1). The %N SCA results indicated that stomatopods were the most commonly identified prey group (737, 49.9%), followed by Gastropoda (233, 15.8%), then Brachyura, Amphipoda, Actinopterygii, Salpidae, Dendrobranchiata, Bivalvia and Cephalopoda by frequency of occurrence (Figure 2.1). Stomach content analysis was able to identify 1609 prey items from 2017 (Table 2.2) with Gastropoda being the most common prey (736, 41.9%) followed by Dendrobranchiata (20.3%), Stomatopoda (257, 14.7%), Actinopterygii, Brachyura, Amphipoda, Tunicata and Cephalopoda by %N (Figure 2.2). Only 220 prey items from 2016 and 162 prey items from 2017 had sufficient tissue remaining after genetic identification to be analyzed for stable isotopes. The prey items occupy a broad range of δ13C and δ15N values however most δ15N fell below that of red snapper in isotope space (Figure 2.3).

Brachyura (crabs) were the largest prey item group that was analyzed for stable isotopes (n = 75 and 53 from 2016 and 2017, respectively). The identified crab taxonomic groups are the Aethroidea (Superfamily: calico crabs), Albunidae (Family: mole crabs), Calappidae (Family: box crabs), Callinectes (Genus: blue crabs), Hippoidea (Superfamily: sand crabs), Menippidae (Family: stone crabs), Parthenopidae (Family: elbow crabs), Portunidae (Family: swimming crabs), and Xanthidae (mud crabs). The crab prey items had a broad range of stable isotope values (Figure 2.4) across both 2016 and 2017. Aethroidea had the lowest average δ13C while the Parthenopidae had the highest (Appendix A5). Low numbers of crab prey analyzed across both years and depth strata prevented any meaningful statistical analysis for certain crab groups. The frequency of crab prey sampled from predatory red snapper increased as red snapper matured (Table 2.3)

Taxonomic diversity within the crab prey group in 2016 was higher across depth strata with a broader isotopic range (Figure 2.5) than in 2017 (Figure 2.6). Portunidae and Xanthidae were the only crab groups collected across all depth strata in 2016 with the Portunidae having a larger range of δ13C and being more depleted on average (Figure 2.7). Portunidae prey collected in 2017 had similar δ13C in the shallow and mid-depth strata (Figure 2.8). Callinectes prey collected in 2016 had a broader range of δ13C and were more enriched on average than 2017. Salinity, dissolved oxygen, temperature and C:N did not significantly affect crab δ13C. Single-variate ANOVA analysis showed that only sampling month and sampling year significantly affected the δ13C of the crab prey (Table 2.4). The Mantel test indicated sampling location did not significantly impact crab prey δ13C (Mantel R = 0.02084, p = 0.22328).

δ15N of the crab prey are highly variable within taxonomic groups and depth strata (Figure 2.9). Calappidae crabs had the most depleted 15N on average while the Aethroidea prey were on average the highest (Appendix A6). The Calappidae prey became more 15N depleted shifting from the mid strata to the deep strata while the Callinectes prey showed no difference in δ15N shifting from the shallow to the mid depth strata (Figure 2.9).With the exception of the single Aethroidea processed in 2016, no crab prey item had δ15N greater than 12.5‰ in either 2016 (Figure 2.9) or 2017 (Figure 2.10). Callinectes and Portunidae prey showed high δ15N variability in 2017. As with δ13C, crab prey δ15N wasn't significantly affected by salinity, dissolved oxygen and temperature on the sampling timescales of this study. In both 2016 and 2017, the δ15N of the crab prey was inversely related to C:N (Figures 2.11 & 2.12). The results of the single-variate ANOVA indicate that the taxonomic group of the crab, the month and the year of sampling are statistically impacted crab δ15N values (Table 2.5). The Mantel test indicated the crab prey δ15N values were not significantly influenced by sampling location (Mantel $R = 0.04734$, $p = 0.05794$).

The prey groups Stomatopoda and the Dendrobranchiata (shrimp and prawns) showed less 13C variation than crabs but had a similarly wide range of δ15N (Figure 2.13). The few Stomatopoda identified beyond that order were primarily members of the genus Squilla. The Dendrobranchiata group broke down into: Acetes (Genus: "krill-like" shrimps), Litopenaeus (Genus: white shrimp), Penaeoidea (Family: brown shrimp) and Sicyoniidae (Family: prawns). Four of the Penaeoidea were identified down to the genus Farfantepenaeus, but ten of the other specimens could not be identified beyond family. The frequency of Dendrobranchiata prey sampled from predatory red snapper was

highest in the < 1-year age class red snapper (Table 2.3), although this may be a byproduct of few < 2-year red snapper being sampled with identifiable stomach contents. Stomatapoda prey became a more frequent prey item as red snapper matured (Table 2.3)

The stomatopods and other shrimp prey δ13C ranged from -23.5‰ to -14.7‰ across the two sampling years (Appendix A7). Three of the four Dendrobranchiata groups along with the Stomatopoda were analyzed from at least one depth in both 2016 and 2017. There weren't any Acetes prey identified from 2016 and no Sicyoniidae prey were identified in 2017. The range of δ13C of stomatopods was similar between 2016 (Figure 2.14) and 2017 (Figure 2.15), with minor shifts between each depth strata for both years. Not enough Penaeid shrimp were analyzed in 2016 to make ecological distinctions (Figure 2.14) but the Penaeid shrimp from 2017 had similar shallow and mid strata δ13C averages and ranges (Figure 2.15) while the deep strata shrimp had a slightly higher average value. Low numbers of analyzed Sicyoniidae and Litopenaeus prey items limited statistical analysis. Stomatopoda and Dendrobranchiata δ 13C in 2016 were positively correlated with the C:N ratios in 2016 and 2017 (Figure 2.16) although the correlation isn't very strong. Single-variate ANOVA analysis indicates sampling date, structure type, depth strata, temperature, dissolved oxygen or prey group significantly affected shrimp δ13C (Table 2.6). The sampling location of the shrimp prey items does influence the δ13C values (Mantel R = 0.04558, P = 0.025597).

Stomatopoda had the broadest range of δ15N among all prey types, ranging from 1.6‰ to 14.0‰ (Appendix A8). The members of the Dendrobranchiata grouping all occupied a narrower range of δ15N that overlapped (Figure 2.13). Like with 13C, Sicyoniidae and Litopenaeus δ15N analysis was limited by the low number of prey items

analyzed. While the number of prey items analyzed limits the results, the mid strata Penaeoidea prey had similar δ15N ranges in 2016 (Figure 2.17) and 2017 (Figure 2.18). Stomatopod δ15N was highly variable during both 2016 (Figure 2.17) and 2017 (Figure 2.18) with significant overlap of values in both years and no statistical differences between the depth strata. Similar to the crab prey item results, Dendrobranchiata and the Stomatopoda in both 2016 and 2017 had δ15N that were negatively related to the C:N ratio (Figures 2.19 and 2.20) with r2 values of 0.61 and 0.74 respectively. Single-variate ANOVA analysis indicates a difference in δ15N between prey items collected at platforms sites and those collected at artificial reef sites (Table 2.7). This variation in δ15N based on structure type at a site doesn't appear to be a byproduct of sampling location (Mantel R = -0.01611, 0.7632).

The Actinopterygii (ray-finned fish) prey items had the highest taxonomic diversity among any of different prey categories (Figures 2.21, 2.22) with greater diversity in 2016 than in 2017. The fish classifications were: Anguilliformes (Order: eels), Clupeidae (Family: herrings & shad), Cynoglossidae (Family: tonguefishes), Dussumieriidae (Family: round herrings), Bremacerotidae (Family: codlets), Gobiidae (Family: gobies), Antennariidae (Family: frogfish), Lutjanus (Genus: snapper), Ophichthidae (Family: snake eels), Ophidiidae (Family: cusk eels), Perciformes (Order: "perch-like"), Phycidae (Family: hakes), Pomatomidae (Family, bluefish), Sciaenidae (Family: drums & croaker), Triglidae (Family: sea robins), Serranidae (Family: groupers). The frequency of Actinopterygii prey sampled from predatory red snapper didn't correlate with the age of the red snapper (Table 2.3). DNA barcoding analysis showed that all of the Lutjanus prey items analyzed for stable isotopes during this project

were indeed red snapper. Laboratory tests previously done by GCRL Fisheries staff have shown minor contamination issues.

The fish prey δ13C ranged from -26.9‰ to -9.0‰ (Appendix A9). Shifts in δ13C were observed among several of the classifications moving from the shallow to deep depth strata sites in 2016 (Figure 2.23). Limited analysis could be done on most of the fish classes across year and depth strata due to low prey sample numbers. Clupeidae from deep strata were more 13C-depleted in 2016 (Figure 2.23) than 2017 (Figure 2.24). The Lutjanus prey had overlapping δ13C values across all depth-strata in 2016 (Figure 2.23), as did the Ophichthidae prey in 2017 (Figure 2.24). Fish prey items were primarily found in the stomach contents of red snapper feeding in water with dissolved oxygen above 3.0 mg/L in both 2016 and 2017 (Figure 2.25). The δ13C of the fish prey items didn't correlate with C:N (Figure 2.26). δ13C of all the fish prey items only significantly affected by sampling month (Table 2.8). Sampling location does not appear to be a factor in the fish prey δ13C values (Mantel R = 0.03869, P = 0.13179).

δ15N among all prey fish ranged from 5.1‰ to 14.9‰ across both sampling years (Appendix A10). The range of δ15N for the 2016 (Figure 2.27) Clupeidae prey was larger than in 2017 (Figure 2.28), with comparable average δ15N. Lutjanus prey items from Red Snapper stomachs had a broad range of δ15N that overlapped across all depth strata in 2016 (Figure 2.27) with mid-strata being slightly more enriched on average. Shallow strata Ophichthidae were more enriched on average than the mid or deep strata samples, which were similar (Figure 2.28). Single-variate ANOVA analysis confirms that sampling month, year and depth strata significantly affectedδ15N of the fish prey

(Table 2.9). Sampling location didn't impact the fish prey δ15N (Mantel R = -0.0003187, P = 5.0085).

Biofilm samples from eight sites were collected for analysis in 2017 (Table 2.10). Biofilm δ13C and δ15N ranged from -16.8‰ to -21.5‰ and 7.9‰ to 10.1‰, respectively (Figure 2.29). The C:N ratios (Range = 4.3 – 5.7) were inversely correlated with δ15N (Figure 2.30) but no correlation was found between C:N and δ13C.

**2.3.2 – Red Snapper Isotope Results and Trophic Level Estimations**

Of the 955 predatory fish sampled in 2016 and 2017, 847 were red snapper: 426 were collected in 2016 (Figure 2.31) and 421 in 2017 (Figure 2.32). The average red snapper δ13C in 2016 was -16.7‰ ± 0.4 while the 2017 red snapper δ13C were more variable with an average δ13C of -17.5‰ ± 1.2 (Appendix A11). The lower δ13C in 2017 are primarily from red snapper collected in the shallow and mid-strata sites in the summer and early fall (Figure 2.33) near the Chandeleur Islands and the Mississippi River Delta (Figure 2.34). Some of the red snapper with depleted 13C were also juveniles (Cohorts 1-3 years, < 2kg, 200-400 mm TL) with 13C values shifting from a partial contributions of terrestrially derived organic matter to purely marine phytoplankton based organic matter (Figure 2.35). In 2016, δ13C by month and depth strata are extremely consistent (Figure 2.36) whereas in 2017 δ13C shows more variability by month and depth strata (Figure 2.37) with increasing variability through the sampling period. In 2016, δ13C had the lowest variability at high water temperatures (Figure 2.38). During 2017, δ13C variability was greatest among high water temperatures (Figure 2.38). Sampling location did affect red snapper δ13C (Mantel R = 0.00421, P = 9.99 ×10-5). Water temperature, salinity, depth strata and dissolved oxygen content didn't significantly affect red snapper δ13C

(Table 2.13). Spearman rank correlation analysis indicated sampling year negatively correlated with red snapper δ13C (Rho = -0.50, p = >0.01) while depth strata and month didn't significantly correlate with red snapper δ13C. While some fish were collected at the control sites (n = 2), the number was too low to be utilized for this or any analysis. Red snapper collected at the platform sites had a greater range in δ13C than those collected at the artificial reef sites (Figure 2.39). The gender of the red snapper had no correlation with either δ13C or δ15N.

The average red snapper δ15N in 2016 and 2017 were similar (14.3‰ ± 0.4 and 14.2‰ ± 0.6, respectively; Appendix A12). Unlike δ13C, the δ15N of the red snapper had similar ranges regardless of sampling date (Figure 2.40). Red snapper collected in 2016 showed consistent δ15N across all months and depth strata with significant overlap (Figure 2.41). The 2017 snapper showed more variability between month and depth strata, but no significant differences (Figure 2.42). Temperature, salinity, dissolved oxygen, total length and total weight were not significantly affected by δ15N of the predatory red snapper (Table 2.14). Spearman rank correlation analysis indicated sampling month positively correlated with red snapper δ15N (Rho = 0.08, p = 0.025) while structure type (Rho = -0.39, p = > 0.01) negatively correlated with red snapper δ15N. The Mantel test indicates that the different sampling locations significantly affect the δ15N of the red snapper (Mantel R statistic = 0.169, P = 9.99 ×10-5).

Trophic position estimates were highly variable and often unrealistic when monthly averaged POM δ15N values were used. Estimated trophic positions for red snapper in 2016 ranged from: 4.78-5.47 (April), 4.58 -5.27 (May), 11.58-11.77 (June), 3.62 – 4.35 (July), 5.78 – 6.31 (August), 3.28 - 3.68 (September) and 3.23 – 4.04

(October) while those from 2017 were: 3.24 – 4.23 (April), 4.42 – 5.70 (May), 8.50 - 9.13 (June), 10.01 – 10.75 (July), 4.73 – 5.03 (August), 9.73 – 10.17 (September) and 1.98 – 3.36 (October). Using the two-year average POM δ15N with highly depleted 15N (< -10 per mil) removed as the baseline resulted in a calculated average red snapper trophic position of 3.89 ± 0.18 with a range from 2.8 to 4.4. Using Litopenaeus setiferus as a baseline proxy resulted in slightly lower TP estimates of 3.41 ± 0.18, ranging from 2.32 to 3.93.

### 2.3.3 – Trophic Position of Red Snapper Prey

Trophic positions for the prey classifications were calculated using the two methods described previously (Table 2.11). The Aethroidea crab TP was highest among all of the prey items collected in each calculation method; however, only one sample was analyzed. With the exception of the Gobiidae, the fish prey groups had the most consistent trophic positions (Two-Year POM Range = 1.50 to 3.30, *Litopenaeus* Range = 1.25 to 3.05; Table 2.11). The calculated TP's of identified prey items were compared with literature values for their species (Table 2.12). Calculated TPs for Tunicate were below 1 with both methods with high standard deviations. Other prey with a standard deviation one-half of the calculated TP include: Amphipoda, Ceriantharia, Portunidae, Xanthidae, Sicyoniidae, Bremacerotidae, and Stomatopoda. The ranges and average TP for both methods were consistent across most of the prey types.

### 2.3.4 – Mixing Model Using SIAR

Eight prey types were utilized across the depth strata in 2016, with seven being utilized in 2017 (Table 2.15). The 2016 SIAR shallow model indicated the Sciaenidae prey followed by the Portunidae prey were the largest proportions of red snapper diet

based on isotope values while the 2017 shallow model indicated *Callinectes* and Ophichthidae were the largest contributors to red snapper diet (Figure 2.43). When incorporated in the 2017 shallow model, the biofilm samples were the lowest isotopic contributor to red snapper diet. The mid strata 2016 model indicated the *Lutjanus* and the Xanthidae prey were the largest diet contributors while the 2017 mid strata model indicated *Callinectes* and *Acetes* were the largest proportion of red snapper diet by isotopes, although there was substantial overlap (Figure 2.44). When the *Lujanus* prey items are removed from the 2016 mid strata SIAR model, stomatopods make up the largest proportion of predatory red snapper diet followed by Xanthidae and *Callinectes* (Figure 2.44). Only two prey types were utilized for the deep strata 2016 model (Figure 2.45), with Clupeidae making up the majority over the next highest contributor, Stomatopoda prey. The 2017 deep strata model only had Ophichthidae prey with $n \geq 5$ so no dietary proportions could be calculated.

**2.4 - Discussion**

SCA showed large shifts in red snapper diet between 2016 and 2017. While SIA of prey items was limited due to the numbers of prey available, there is evidence of possible ontogenetic diet shifts in the crustacean prey items based upon trend in stable isotope values, C:N, and high TP variability. Portunidae crabs, particularly *Callinectes* species, have been shown to be the preferred crab prey for mature red snapper and can make up a large proportion of their identified diet (Crab %IRI = 25.02% Age 3+ Fish; Wells et al., 2008). In our study, Brachyura and Stomatopoda prey were the only prey groups that became a larger proportion of the diet as red snapper matured. *Callinectes* crabs have been shown to feed on phytoplankton and POM early in life, but begin to prey

upon other crustaceans and detritus as they mature (Dittel et al., 2006). The $\delta^{15}N$ of the Portunidae and the few Xanthidae prey indicate that these crab taxa consume prey across multiple trophic positions, resulting in similar average TP estimates with large standard deviations. Similar to the crab prey, mantis shrimp $\delta^{15}N$ indicate that they are also feeding at multiple trophic levels, which has been shown to be due to the mantis shrimp's growth and offshore movement as they mature (Fry & Arnold, 1982). Crabs and stomatopod $\delta^{15}N$ both correlated negatively with C:N, indicating that these organisms undergo an ontogenetic diet shift, feeding on larger and trophically higher prey items as they grow.

Ophichthidae (eel) prey from 2017 in the shallow strata had higher $\delta^{15}N$ than those from the mid or deep strata, which indicates a spatial isotope baseline shift moving from nearshore to offshore. Similar isotopic shifts have been shown to occur in POM as well as consumers utilizing POM (Dorado et al., 2012). *Lutjanus* prey items were more $^{15}N$ enriched on average in the shallow and deep strata than in the mid strata. This could be the result of nearshore red snappers recently moving offshore, as the *Lutjanus* prey items TP didn't vary with depth strata. Nearshore fish that recently migrated to offshore reefs would be expected have elevated $\delta^{15}N$ values after feeding on nearshore phytoplankton that incorporated $^{15}N$-enriched riverine nitrogen during photosynthesis (Kerherve et al., 2001; Peterson and Fry, 1987; Wissel & Fry, 2005). The *Lutjanus* prey items, which were genetically confirmed to be red snapper, were slightly depleted in both $^{13}C$ and $^{15}N$ compared to predatory red snapper, with an average TPs about one trophic level below that of predatory red snapper. Research on red snapper cannibalism has shown mixed results. Cannibalism by larger fish of juveniles has been observed in

aquaculture settings (Leu et al., 2003) but there is also evidence that larger red snapper will avoid cannibalizing in aquaculture if other prey are available (Bailey et al., 2001). A field study in coastal Alabama waters observed that red snapper showed no interest in cannibalism beyond aggressively defending structured habitat by chasing away smaller red snapper (Piko and Szedlmayer, 2007).

Predatory red snapper $\delta^{13}C$ in 2016 closely followed the trend in POM $\delta^{13}C$ discussed earlier and is similar to the Mississippi River outflow patterns. Like the POM and prey items, the predatory red snapper $\delta^{13}C$ and $\delta^{15}N$ appear to be influenced by riverine inputs. The similarity in the trends of POM, prey items and predatory red snapper $\delta^{13}C$ indicates that phytoplankton sampled and analyzed as POM are the primary basal resource supporting coastal reef food webs. The 2017 red snapper samples collected from August through October were $^{13}C$-enriched in the deep strata, indicating proximity to shore being a factor. This also indicates that the shallow and mid strata sites are exposed to depleted $\delta^{13}C$ values from riverine input. In 2017, some juvenile red snapper collected near the Chandeleur Islands indicated they were isotopically more similar to terrestrial basal resources. Stable carbon isotope values of the predatory red snapper became more enriched with fish size in both years which supports the belief that red snapper move further offshore as they grow and mature in search of prey and structured habitat (Gallaway et al., 2009). Changes in fish $\delta^{13}C$ values have been shown to be correlated with riverine inputs (Soares et al., 2014).

Red snapper average TP estimates for both methods across both years were nearly identical, indicating that red snapper's calculated TP is rather consistent despite their highly variable diet. While the *Litopenaeus*-based TP estimates were lower than the

POM-based estimates, both average values were within one standard deviation of the TP estimates from FishBase TP (3.90 ± 0.72) and the POM estimates were similar to the previous estimates of Tarnecki and Patterson (3.85 ± 0.13 SE); Tarnecki, 2015). As shown herein, POM isotope values in the northern GoM are highly variable so limited temporal and spatial sampling of POM may not be sufficient to estimate TP in systems that are highly influenced by variable freshwater inputs. When red snapper TP was calculated with monthly averaged $\delta^{15}N$ POM values extremely high TP variability was calculated. The unusually large $^{15}N$ depletion in bottom water POM during some summer months resulted in unrealistically high TP estimates during several months over both years. These results show that monthly or seasonal variation in POM $\delta^{15}N$ can substantially affect TP calculations and researchers should characterize POM throughout the year to obtain long-term average POM $\delta^{15}N$ values to better estimate TP. If such long-term sampling isn't a viable option, using a prey item with a known trophic position, such *Litopenaeus setiferus*, as a baseline proxy provides reasonable TP estimates. The *Litopenaeus setiferus* sampled during Akin and Winemiller's estuarine study may not have been mature shrimp and as a result, the lambda (TP) derived from their study may have been lower than the lambda of mature *Litopenaeus setiferus*. The *Litopenaeus setiferus* from the Akin and Winemiller study (2008) had a mean length of 59.1 ± 20.5 mm, while previous research has shown mature *Litopenaeus setiferus* reaching a maximum length of between 160-200 mm (Holthuis, 1980). If the lambda of *Litopenaeus setiferus* was increased from 2.14 to 2.7, the TP estimates of the prey items calculated using the shrimp proxy become significantly similar to the POM TP estimates.

Species such as spot, Atlantic croaker, bay whiff, sand trout, and scaled sardine had TP estimates that were within one standard deviation of previous literature estimates. Our shrimp-based method resulted in invertebrate TP estimates that were much lower than those from our POM based method or literature values. *Callinectes similis, Ovalipes floridanus (*both Portunidae) and *Squilla empusa* had POM-calculated TPs that were similar (within one standard deviation) to literature estimates. While the Brachyura as a broad group showed large variability, most of the narrower taxonomic groupings had small $\delta^{15}N$ ranges. The stomatopods were unique among the narrower taxonomic groupings by having a large range of $\delta^{15}N$ across all months and depth strata. Red snapper of various size and age classes were likely consuming stomatopods and crabs of varying sizes, which would affect the isotope values of the predator as well as their calculated trophic positions. A laboratory or field prey study analyzing stomatopods and crabs to determine the effect development and size has on isotope values and trophic position would be a useful future study.

The SIAR model indicated predatory red snapper diet was variable by depth strata as well as sampling year. The 2016 shallow-strata SIAR model indicated Sciaenidae prey accounting for about 70% of red snapper diet followed by Portunidae and *Callinectes*. The high proportion of *Lutjanus* prey in the 2016 mid strata SIAR model may be due the isotopic similarity between the *Lutjanus* prey items and the predatory red snapper themselves. This similarity must be skewing the mixing model results, indicating these fish are primarily cannibalistic predators while SCA indicates a broad diet. When *Lutjanus* prey were excluded, the red snapper diet from the mid strata in 2016 were primarily stomatopod, Xanthidae and *Callinectes* based and more similar to the SCA

results. The 2017 mid-strata SIAR model indicated *Acetes*, *Callinectes* and other Portunidae crabs were the largest isotopic contributors to red snapper diet, a shift away from the primarily fish-based results of 2016. Mixing models for the deep strata red snapper were limited by the number of prey analyzed for isotopes from both years. Stomach content examinations showed that a large percentage of red snapper collected from the deep strata had prey in their stomachs, but genetic barcoding analysis utilized most of the sample tissue which prevented SIA from being conducted. Stomatopoda prey items was one of the largest components of identified stomach contents in both years but never accounted for more than 20% of the predatory red snapper diet in the mixing model results. These conflicting results suggests that the highly variable $\delta^{15}N$ values of stomatopods affected the diet proportion analysis. Other modeling programs such as the Bayesian-based SIMMR are being explored by our lab to improve the accuracy of our analysis. Expanding these mixing models with additional sampling data from 2018 - 2020 will also make them more effective.

Applying the modified Fry (et al., 2003) lipid correction to prey items with C:N > 3.5 significantly affected the mixing model results. The non-lipid corrected models used for the shallow strata indicated that *Lutjanus* were the most significant component of red snapper diet instead of Sciaenidae, which is probably due to the isotopic similarities between fish of the same species. The 2016 mid-strata mixing model indicated Xanthidae crabs were a larger component than the lipid-corrected version indicated, while the 2017 non-lipid corrected mid-strata model indicated *Acetes* was the largest component of diet followed by *Callinectes*. The lipid-corrected model indicated that *Callinectes* was a larger component than *Acetes*. Several methods of lipid correction were reviewed besides the

modified Fry (et al., 2003) that was used. One of the more prominent was developed by Post (et al., 2007) based on analysis of numerous aquatic organisms. The equation is shown below:

$$\delta^{13}C_{Corrected} = \delta^{13}C_{Untreated} - 3.22 + 0.99 * C{:}N_{Sample}$$

Post's equation has been shown to be effectively used to determine the lipid corrected $\delta^{13}C$ of fish (Skinner et al., 2016). However, the Post equation is a linear correction, which has been shown to be less effective at high C:N (>10) (Logan et al., 2008; Boecklen et al., 2011), resulting in unrealistically large isotope corrections. When comparing both mathematic corrections to our results, the range of Post lipid corrected $\delta^{13}C$ were always more enriched than the Fry lipid corrected $\delta^{13}C$ across all prey types and as expected, the greatest difference in the lipid isotope corrections were for samples with high C:N ratios (i.e. Calappidae, Xanthidae, Gobiidae and *Lutjanus*)

Consistent with previous studies, red snapper diet in this study appeared to vary spatially and temporally. Regional variability in red snapper diet across the NGoM has been shown previously, with crabs being a primary dietary component in Louisiana waters, while red snapper in Texas coastal waters primarily consumed gastropods (Dance et al., 2018). Structure type and prey availability have also been shown to be the primary factors in determining red snapper diet in Louisiana waters (Simonsen et al., 2014). These regional differences were attributed to differences in sampling locations, however red snapper diet has also been shown to vary seasonally. Stomach content analysis of red snapper collected off the Alabama coast indicated crabs were the largest component of red snapper diet in summer (43% by IRI) however mantis shrimp dominated the diet in the fall (42% by IRI) while fish prey accounted for 28% – 30% IRI regardless of season

(McCawley et al., 2003). Red snapper collected pre and post Deep-Water Horizon from the same habitats have shown significant changes in diet (Tarnecki & Patterson, 2015). While these studies are effective, our sampling design of sampling monthly over two years across Mississippi state waters incorporating multiple depth strata and structure types allows us to see how red snapper's diet is shifting across space and time to develop a better understanding of red snapper ecology and reef food webs.

# CHAPTER III - SUMMARY OF CHAPTERS I AND II

The goal of this study was to better understand the trophic relationships between red snapper, it's prey items and basal resource utilization in coastal Mississippi waters. Stable isotope analysis of POM as a proxy for phytoplankton indicated significant monthly and yearly variability for $\delta^{13}C$ and $\delta^{15}N$. This variability is the result of riverine inputs affecting the isotopes available for phytoplankton utilization. These shifts have been shown to subsequently affect the isotope values of red snapper prey items and predatory red snapper in our sampling area. Long term POM average values are ideal for trophic position calculation, but diet studies can also use prey items with known TP as a proxy for the calculations if POM $\delta^{15}N$ is highly variable. Mature red snapper showed little isotopic variation, because they are integrating the wide range of isotope values from their prey items across all sites. This results in the predatory red snapper having a narrow range of isotope values despite the dynamic taxonomic and isotopic diet. The results of this study expands our knowledge of trophic dynamics of red snapper and their prey in coastal Mississippi, and may contribute to more effective population and habitat management for red snapper.

# APPENDIX A - ADDITIONAL DATA

*Table A.1 2016 POM $\delta^{13}C$ showing the range and average $\delta^{13}C$ values for each month, depth strata, and collection point in the water column*

| **$\delta^{13}C$** | | | | | |
|---|---|---|---|---|---|
| | **n** | **Min** | **Max** | **Avg** | **Stdev** |
| **April Bot Water** | 18 | -24.1 | -19.1 | -22.5 | 1.10 |
| Shallow Strata | 4 | -22.6 | -19.1 | -21.2 | 1.46 |
| Mid Strata | 9 | -24.1 | -21.6 | -22.7 | 0.78 |
| Deep Strata | 5 | -23.6 | -22.9 | -23.1 | 0.29 |
| **April Surf Water** | 16 | -25.2 | -18.2 | -22.4 | 2.03 |
| Shallow Strata | 4 | -25.2 | -19.4 | -22.0 | 2.94 |
| Mid Strata | 9 | -24.9 | -18.2 | -22.2 | 1.92 |
| Deep Strata | 3 | -24.1 | -23.0 | -23.6 | 0.56 |
| **May Bot Water** | 23 | -24.5 | -19.8 | -22.6 | 1.27 |
| Shallow Strata | 8 | -24.4 | -20.6 | -22.7 | 1.35 |
| Mid Strata | 8 | -24.5 | -22.7 | -23.4 | 0.62 |
| Deep Strata | 7 | -23.8 | -19.8 | -21.7 | 1.20 |
| **May Surf Water** | 23 | -25.7 | -19.2 | -22.7 | 1.68 |
| Shallow Strata | 8 | -25.7 | -21.8 | -23.6 | 1.43 |
| Mid Strata | 8 | -24.4 | -22.9 | -23.5 | 0.56 |
| Deep Strata | 7 | -22.1 | -19.2 | -20.7 | 1.00 |
| **June Bot Water** | 23 | -26.3 | -19.0 | -23.2 | 2.09 |
| Shallow Strata | 9 | -26.3 | -21.1 | -23.6 | 1.96 |
| Mid Strata | 7 | -26.0 | -23.8 | -24.7 | 0.97 |
| Deep Strata | 7 | -24.8 | -19.0 | -21.7 | 1.98 |
| **June Surf Water** | 23 | -28.3 | -20.0 | -22.7 | 2.07 |
| Shallow Strata | 9 | -28.3 | -20.0 | -22.8 | 2.92 |
| Mid Strata | 7 | -23.6 | -21.3 | -22.6 | 1.09 |
| Deep Strata | 7 | -24.7 | -21.0 | -22.6 | 1.26 |
| **July Bot Water** | 23 | -28.6 | -21.1 | -23.8 | 1.97 |
| Shallow Strata | 7 | -28.6 | -21.2 | -24.6 | 2.86 |
| Mid Strata | 10 | -23.4 | -21.1 | -22.7 | 0.76 |
| Deep Strata | 6 | -25.6 | -23.3 | -24.5 | 0.97 |
| **July Surf Water** | 23 | -26.5 | -18.3 | -22.9 | 2.24 |
| Shallow Strata | 7 | -26.5 | -19.8 | -24.6 | 2.33 |
| Mid Strata | 10 | -23.3 | -18.3 | -21.5 | 1.57 |
| Deep Strata | 6 | -25.8 | -22.2 | -23.1 | 1.52 |
| **August Bot Water** | 23 | -30.0 | -19.7 | -24.2 | 2.98 |

| | | | | | |
|---|---|---|---|---|---|
| Shallow Strata | 8 | -26.0 | -20.6 | -22.4 | 1.74 |
| Mid Strata | 8 | -26.8 | -19.7 | -23.7 | 2.76 |
| Deep Strata | 7 | -30.0 | -22.0 | -26.7 | 2.87 |
| **August Surf Water** | 23 | -24.7 | -19.4 | -22.0 | 1.29 |
| Shallow Strata | 8 | -23.1 | -20.5 | -21.4 | 0.81 |
| Mid Strata | 8 | -24.7 | -20.5 | -22.2 | 1.31 |
| Deep Strata | 7 | -24.1 | -19.4 | -22.4 | 1.63 |
| **September Bot Water** | 23 | -32.8 | -23.0 | -27.2 | 2.96 |
| Shallow Strata | 8 | -25.2 | -23.0 | -23.9 | 0.92 |
| Mid Strata | 8 | -32.8 | -25.7 | -27.9 | 2.46 |
| Deep Strata | 7 | -31.6 | -27.7 | -29.7 | 1.35 |
| **September Surf Water** | 23 | -27.7 | -21.0 | -24.8 | 1.80 |
| Shallow Strata | 8 | -24.2 | -21.0 | -22.7 | 1.35 |
| Mid Strata | 8 | -27.7 | -25.6 | -26.3 | 0.72 |
| Deep Strata | 7 | -26.1 | -23.8 | -25.2 | 0.70 |
| **October Bot Water** | 23 | -31.7 | -24.2 | -28.2 | 1.76 |
| Shallow Strata | 7 | -28.4 | -24.2 | -26.9 | 1.49 |
| Mid Strata | 8 | -28.9 | -26.5 | -27.6 | 0.84 |
| Deep Strata | 8 | -31.7 | -28.5 | -30.1 | 1.03 |
| **October Surf Water** | 23 | -29.0 | -23.8 | -26.2 | 1.32 |
| Shallow Strata | 7 | -29.0 | -24.6 | -27.0 | 1.47 |
| Mid Strata | 8 | -28.0 | -25.1 | -26.5 | 0.88 |
| Deep Strata | 8 | -25.9 | -23.8 | -25.1 | 0.81 |
| **Surface 2016** | 154 | -29.0 | -18.2 | -23.4 | 2.3 |
| Shallow | 51 | -29.0 | -19.4 | -23.5 | 2.6 |
| Mid | 58 | -28.0 | -18.2 | -23.5 | 2.3 |
| Deep | 45 | -26.1 | -19.2 | -23.3 | 1.9 |
| **Bottom 2016** | 156 | -32.8 | -19.0 | -24.6 | 3.0 |
| Shallow | 51 | -28.6 | -19.1 | -23.7 | 2.3 |
| Mid | 58 | -32.8 | -19.7 | -24.6 | 2.6 |
| Deep | 47 | -31.7 | -19.0 | -25.6 | 3.8 |

*Table A.2 2016 POM $\delta^{15}N$ showing the range and average $\delta^{15}N$ values for each month, depth strata, and collection point in the water column*

| **$\delta^{15}N$** | | | | | |
|---|---|---|---|---|---|
| | **n** | **Min** | **Max** | **Avg** | **Stdev** |
| **April Bot Water** | 18 | -1.7 | 5.4 | 2.3 | 2.34 |
| Shallow Strata | 4 | -1.7 | 5.4 | 4.0 | 2.27 |
| Mid Strata | 9 | -1.4 | 4.2 | 2.7 | 1.96 |
| Deep Strata | 5 | 3.4 | 4.1 | 3.6 | 0.31 |
| **April Surf Water** | 16 | -3.1 | 23.4 | 4.7 | 5.81 |
| Shallow Strata | 4 | -3.1 | 7.3 | 2.9 | 4.48 |
| Mid Strata | 9 | -2.0 | 23.4 | 5.8 | 7.12 |
| Deep Strata | 3 | 0.9 | 6.2 | 3.8 | 2.70 |
| **May Bot Water** | 23 | -3.8 | 8.1 | 3.0 | 3.12 |
| Shallow Strata | 8 | -2.3 | 8.1 | 3.2 | 3.66 |
| Mid Strata | 8 | -3.8 | 7.3 | 2.2 | 3.61 |
| Deep Strata | 7 | 1.3 | 6.6 | 3.6 | 1.89 |
| **May Surf Water** | 23 | -5.4 | 7.8 | 4.1 | 3.27 |
| Shallow Strata | 8 | 0.9 | 5.7 | 3.8 | 1.60 |
| Mid Strata | 8 | -5.4 | 7.8 | 2.4 | 4.75 |
| Deep Strata | 7 | 5.6 | 7.8 | 6.2 | 0.73 |
| **June Bot Water** | 23 | -36.7 | -0.9 | -17.8 | 10.95 |
| Shallow Strata | 9 | -33.3 | -3.4 | -14.4 | 10.20 |
| Mid Strata | 7 | -22.7 | -12.4 | -16.8 | 4.32 |
| Deep Strata | 7 | -36.7 | -0.9 | -22.6 | 13.67 |
| **June Surf Water** | 23 | -25.7 | 6.3 | -2.7 | 6.40 |
| Shallow Strata | 9 | -25.7 | 6.3 | -4.9 | 9.07 |
| Mid Strata | 7 | -5.7 | -0.5 | -2.2 | 2.36 |
| Deep Strata | 7 | -2.7 | 0.9 | -0.1 | 1.22 |
| **July Bot Water** | 23 | -19.0 | 11.2 | 5.1 | 6.87 |
| Shallow Strata | 7 | 6.2 | 9.3 | 7.4 | 1.00 |
| Mid Strata | 10 | 3.1 | 11.2 | 8.0 | 2.80 |
| Deep Strata | 6 | -19.0 | 5.8 | -2.7 | 10.30 |
| **July Surf Water** | 23 | 4.7 | 27.3 | 8.0 | 4.41 |
| Shallow Strata | 7 | 6.1 | 7.9 | 7.3 | 0.58 |
| Mid Strata | 10 | 4.7 | 8.9 | 7.2 | 1.22 |
| Deep Strata | 6 | 5.8 | 27.3 | 10.5 | 9.36 |
| **August Bot Water** | 23 | -14.4 | 9.0 | -0.8 | 6.81 |
| Shallow Strata | 8 | -8.1 | 6.9 | 3.2 | 4.69 |
| Mid Strata | 8 | -7.8 | 9.0 | 0.7 | 7.19 |

| | | | | | |
|---|---|---|---|---|---|
| Deep Strata | 7 | -14.4 | -2.6 | -6.9 | 4.02 |
| **August Surf Water** | 23 | -3.4 | 8.2 | 4.7 | 2.82 |
| Shallow Strata | 8 | 3.3 | 8.2 | 5.7 | 1.99 |
| Mid Strata | 8 | -3.4 | 7.9 | 3.2 | 3.96 |
| Deep Strata | 7 | 3.9 | 7.0 | 5.4 | 1.15 |
| **September Bot Water** | 23 | 1.3 | 10.4 | 6.6 | 2.20 |
| Shallow Strata | 8 | 5.8 | 9.5 | 7.7 | 1.20 |
| Mid Strata | 8 | 4.9 | 10.4 | 6.8 | 1.75 |
| Deep Strata | 7 | 1.3 | 9.6 | 5.3 | 2.91 |
| **September Surf Water** | 23 | 3.4 | 9.8 | 6.9 | 1.66 |
| Shallow Strata | 8 | 6.2 | 9.8 | 7.8 | 1.27 |
| Mid Strata | 8 | 3.4 | 8.3 | 5.6 | 1.72 |
| Deep Strata | 7 | 5.9 | 8.8 | 7.4 | 1.13 |
| **October Bot Water** | 23 | 0.5 | 10.8 | 6.3 | 1.94 |
| Shallow Strata | 7 | 5.5 | 7.1 | 6.2 | 0.56 |
| Mid Strata | 8 | 4.6 | 8.2 | 6.0 | 1.38 |
| Deep Strata | 8 | 0.5 | 10.8 | 6.8 | 3.05 |
| **October Surf Water** | 23 | 4.4 | 12.0 | 6.8 | 1.82 |
| Shallow Strata | 7 | 4.5 | 7.7 | 5.6 | 1.11 |
| Mid Strata | 8 | 4.4 | 12.0 | 7.0 | 2.47 |
| Deep Strata | 8 | 6.5 | 9.5 | 7.7 | 0.88 |
| **Surface All** | 154 | -25.7 | 27.3 | 4.7 | 5.1 |
| Shallow | 51 | -25.7 | 9.8 | 3.8 | 5.9 |
| Mid | 58 | -5.7 | 23.4 | 4.7 | 4.6 |
| Deep | 45 | -2.7 | 27.3 | 5.9 | 4.3 |
| **Bottom All** | 156 | -36.7 | 11.2 | 0.9 | 9.6 |
| Shallow | 51 | -33.3 | 9.5 | 1.6 | 9.2 |
| Mid | 58 | -22.7 | 11.2 | 2.6 | 7.1 |
| Deep | 47 | -36.7 | 10.8 | -1.9 | 11.8 |

*Table A.3 2017 POM δ13C showing the range and average δ13C values for each month, depth strata, and collection point in the water column*

| **$\delta^{13}C$** | | | | | |
|---|---|---|---|---|---|
| | **n** | **Min** | **Max** | **Avg** | **Stdev** |
| **April Bot Water** | 23 | -37.0 | -24.0 | -27.6 | 2.71 |
| Shallow Strata | 9 | -31.1 | -24.0 | -26.9 | 2.05 |
| Mid Strata | 7 | -29.0 | -25.5 | -27.0 | 1.45 |
| Deep Strata | 7 | -37.0 | -26.7 | -29.9 | 4.13 |
| **April Surf Water** | 23 | -32.3 | -20.6 | -25.1 | 2.77 |
| Shallow Strata | 9 | -28.1 | -21.9 | -24.7 | 1.91 |
| Mid Strata | 7 | -32.3 | -23.0 | -27.3 | 3.16 |
| Deep Strata | 7 | -25.4 | -20.6 | -23.2 | 1.90 |
| **May Bot Water** | 23 | -42.6 | -23.3 | -27.9 | 4.34 |
| Shallow Strata | 8 | -28.3 | -23.3 | -25.8 | 1.70 |
| Mid Strata | 8 | -31.9 | -25.8 | -28.0 | 2.33 |
| Deep Strata | 7 | -42.6 | -27.9 | -33.3 | 8.09 |
| **May Mid Water** | 5 | -22.4 | -20.1 | -21.2 | 0.89 |
| Shallow Strata | 2 | -22.4 | -20.6 | -21.5 | 1.26 |
| Mid Strata | 1 | -20.1 | -20.1 | -20.1 | |
| Deep Strata | 2 | -21.6 | -21.4 | -21.5 | 0.20 |
| **May Surf Water** | 23 | -27.1 | -19.9 | -21.9 | 1.63 |
| Shallow Strata | 8 | -23.9 | -21.5 | -22.6 | 0.89 |
| Mid Strata | 8 | -27.1 | -20.1 | -22.5 | 2.08 |
| Deep Strata | 7 | -21.4 | -19.9 | -20.5 | 0.54 |
| **June Bot Water** | 23 | -32.7 | -25.1 | -28.2 | 2.38 |
| Shallow Strata | 7 | -27.0 | -25.1 | -26.0 | 0.79 |
| Mid Strata | 8 | -31.9 | -26.8 | -28.5 | 2.11 |
| Deep Strata | 8 | -32.7 | -28.7 | -30.6 | 1.43 |
| **June Mid Water** | 9 | -24.6 | -22.1 | -23.1 | 0.86 |
| Mid Strata | 2 | -23.3 | -23.1 | -23.2 | 0.16 |
| Deep Strata | 7 | -24.6 | -22.1 | -23.1 | 0.99 |
| **June Surf Water** | 23 | -31.2 | -19.5 | -23.7 | 2.75 |
| Shallow Strata | 7 | -31.2 | -20.5 | -24.6 | 4.01 |
| Mid Strata | 8 | -29.2 | -23.2 | -24.6 | 1.94 |
| Deep Strata | 8 | -23.7 | -19.5 | -22.1 | 1.24 |
| **July Bot Water** | 23 | -30.0 | -22.3 | -26.5 | 3.17 |
| Shallow Strata | 8 | -26.7 | -22.3 | -24.5 | 3.11 |
| Mid Strata | 8 | -30.0 | -30.0 | -30.0 | |
| Deep Strata | 7 | -26.8 | -26.8 | -26.8 | |

| | | | | | |
|---|---|---|---|---|---|
| **July Surf Water** | 23 | -26.3 | -22.5 | -24.6 | 1.10 |
| Shallow Strata | 8 | -26.3 | -22.5 | -24.4 | 1.25 |
| Mid Strata | 8 | -26.3 | -23.2 | -25.3 | 0.95 |
| Deep Strata | 7 | -24.8 | -23.1 | -23.9 | 0.64 |
| **August Bot Water** | 23 | -30.5 | -22.1 | -25.8 | 2.93 |
| Shallow Strata | 8 | -27.0 | -22.1 | -23.7 | 1.69 |
| Mid Strata | 8 | -30.5 | -22.9 | -27.9 | 2.80 |
| Deep Strata | 7 | -26.9 | -24.9 | -25.9 | 1.39 |
| **August Mid Water** | 2 | -22.1 | -21.4 | -21.7 | 0.50 |
| Shallow Strata | 2 | -22.1 | -21.4 | -21.7 | 0.50 |
| **August Surf Water** | 23 | -25.1 | -20.5 | -23.0 | 1.34 |
| Shallow Strata | 8 | -24.3 | -20.5 | -22.4 | 1.50 |
| Mid Strata | 8 | -25.1 | -21.7 | -23.9 | 1.15 |
| Deep Strata | 7 | -23.8 | -21.9 | -22.6 | 0.67 |
| **September Bot Water** | 23 | -28.6 | -23.4 | -25.8 | 1.32 |
| Shallow Strata | 8 | -28.6 | -23.4 | -25.2 | 1.78 |
| Mid Strata | 8 | -27.7 | -24.7 | -26.2 | 1.13 |
| Deep Strata | 7 | -27.2 | -25.1 | -25.9 | 0.72 |
| **September Mid Water** | 10 | -28.2 | -21.4 | -23.8 | 1.85 |
| Mid Strata | 3 | -28.2 | -21.4 | -24.5 | 3.45 |
| Deep Strata | 7 | -24.8 | -22.4 | -23.5 | 0.90 |
| **September Surf Water** | 23 | -26.6 | -21.9 | -23.4 | 1.32 |
| Shallow Strata | 8 | -25.5 | -21.9 | -23.7 | 1.44 |
| Mid Strata | 8 | -26.6 | -22.1 | -23.9 | 1.39 |
| Deep Strata | 7 | -23.3 | -22.0 | -22.4 | 0.45 |
| **October Bot Water** | 23 | -30.7 | -22.2 | -25.9 | 2.31 |
| Shallow Strata | 8 | -27.1 | -22.9 | -24.4 | 1.29 |
| Mid Strata | 8 | -28.4 | -22.2 | -25.8 | 2.02 |
| Deep Strata | 7 | -30.7 | -25.0 | -27.8 | 2.36 |
| **October Mid Water** | 3 | -27.4 | -25.5 | -26.2 | 1.06 |
| Deep Strata | 3 | -27.4 | -25.5 | -26.2 | 1.06 |
| **October Surf Water** | 23 | -27.4 | -23.3 | -25.0 | 0.89 |
| Shallow Strata | 8 | -27.4 | -24.0 | -25.3 | 1.01 |
| Mid Strata | 8 | -26.4 | -24.4 | -25.3 | 0.64 |
| Deep Strata | 7 | -25.5 | -23.3 | -24.4 | 0.80 |
| **Surface All** | 161 | -32.3 | -19.5 | -23.8 | 2.1 |
| Shallow | 56 | -31.2 | -20.5 | -24.0 | 2.1 |
| Mid | 55 | -32.3 | -20.1 | -24.6 | 2.2 |
| Deep | 50 | -25.5 | -19.5 | -22.7 | 1.5 |
| **Bottom All** | 161 | -42.6 | -22.1 | -26.9 | 2.9 |

| | | | | | |
|---|---|---|---|---|---|
| Shallow | 56 | -31.1 | -22.1 | -25.4 | 1.9 |
| Mid | 55 | -31.9 | -22.2 | -27.3 | 2.2 |
| Deep | 50 | -42.6 | -24.9 | -28.6 | 3.7 |

*Table A.4 2017 POM $\delta^{15}N$ showing the range and average $\delta^{15}N$ values for each month, depth strata, and collection point in the water column*

| **$\delta^{15}N$** | | | | | |
|---|---|---|---|---|---|
| | **n** | **Min** | **Max** | **Avg** | **Stdev** |
| **April Bot Water** | 23 | -1.5 | 7.4 | 5.5 | 2.34 |
| Shallow Strata | 9 | 4.5 | 7.4 | 6.1 | 1.10 |
| Mid Strata | 7 | -1.5 | 7.0 | 6.0 | 1.22 |
| Deep Strata | 7 | 0.0 | 0.0 | | |
| **April Surf Water** | 23 | 4.5 | 7.8 | 6.5 | 1.04 |
| Shallow Strata | 9 | 5.5 | 7.8 | 6.7 | 0.85 |
| Mid Strata | 7 | 6.5 | 7.6 | 7.2 | 0.43 |
| Deep Strata | 7 | 4.5 | 7.3 | 5.6 | 1.06 |
| **May Bot Water** | 23 | -11.2 | 12.7 | 1.4 | 7.34 |
| Shallow Strata | 8 | -3.9 | 10.1 | 4.0 | 5.99 |
| Mid Strata | 8 | 0.3 | 12.7 | 4.8 | 6.90 |
| Deep Strata | 7 | -11.2 | -3.1 | -7.0 | 4.06 |
| **May Mid Water** | 5 | -3.1 | 7.0 | 3.1 | 4.15 |
| Shallow Strata | 2 | 1.0 | 4.4 | 2.7 | 2.38 |
| Mid Strata | 1 | 6.2 | 6.2 | 6.2 | |
| Deep Strata | 2 | -3.1 | 7.0 | 2.0 | 7.11 |
| **May Surf Water** | 23 | -1.4 | 9.7 | 4.3 | 2.39 |
| Shallow Strata | 8 | 3.4 | 9.7 | 5.7 | 2.16 |
| Mid Strata | 8 | -1.4 | 4.1 | 2.4 | 1.82 |
| Deep Strata | 7 | 3.8 | 9.2 | 4.9 | 1.92 |
| **June Bot Water** | 23 | -16.2 | -1.5 | -9.1 | 4.89 |
| Shallow Strata | 7 | -16.2 | -2.4 | -10.6 | 4.66 |
| Mid Strata | 8 | -12.3 | -1.6 | -9.4 | 4.48 |
| Deep Strata | 8 | -4.0 | -1.5 | -2.7 | 1.74 |
| **June Mid Water** | 9 | -6.0 | 13.2 | 3.9 | 6.30 |
| Mid Strata | 2 | 2.6 | 8.8 | 5.7 | 4.42 |
| Deep Strata | 7 | -6.0 | 13.2 | 3.4 | 6.96 |
| **June Surf Water** | 23 | -10.4 | 18.0 | 1.2 | 6.77 |
| Shallow Strata | 7 | -8.1 | 18.0 | 0.5 | 9.01 |
| Mid Strata | 8 | -10.4 | 11.1 | -0.4 | 7.56 |
| Deep Strata | 8 | 0.3 | 7.2 | 3.4 | 2.87 |
| **July Bot Water** | 23 | -26.4 | 2.2 | -14.1 | 9.95 |
| Shallow Strata | 8 | -26.4 | 2.2 | -14.5 | 11.37 |
| Mid Strata | 8 | -17.5 | -8.2 | -12.9 | 6.58 |
| Deep Strata | 7 | 0.0 | 0.0 | | |

| | | | | | |
|---|---|---|---|---|---|
| **July Surf Water** | 23 | -7.9 | 4.9 | -0.1 | 3.09 |
| Shallow Strata | 8 | -6.9 | 4.9 | 0.5 | 3.77 |
| Mid Strata | 8 | -7.9 | 2.8 | -0.6 | 3.63 |
| Deep Strata | 7 | -2.0 | 2.7 | -0.1 | 1.47 |
| **August Bot Water** | 23 | -3.8 | 11.2 | 2.8 | 5.44 |
| Shallow Strata | 8 | -3.8 | 11.2 | 3.6 | 5.41 |
| Mid Strata | 8 | -2.5 | -2.5 | -2.5 | |
| Deep Strata | 7 | 0.0 | 0.0 | | |
| **August Mid Water** | 2 | -3.9 | 2.4 | -0.8 | 4.41 |
| Shallow Strata | 2 | -3.9 | 2.4 | -0.8 | 4.41 |
| **August Surf Water** | 23 | 2.2 | 15.4 | 7.0 | 3.27 |
| Shallow Strata | 8 | 2.8 | 15.4 | 6.8 | 4.13 |
| Mid Strata | 8 | 2.2 | 12.9 | 7.2 | 3.91 |
| Deep Strata | 7 | 5.4 | 8.6 | 7.1 | 1.14 |
| **September Bot Water** | 23 | -27.3 | 5.7 | -12.2 | 11.30 |
| Shallow Strata | 8 | -7.3 | 5.7 | 0.0 | 6.66 |
| Mid Strata | 8 | -15.4 | 4.6 | -9.3 | 9.34 |
| Deep Strata | 7 | -27.3 | -15.7 | -21.9 | 5.15 |
| **September Surf Water** | 10 | -5.5 | 8.5 | 1.6 | 5.23 |
| Mid Strata | 3 | -3.8 | 8.1 | 1.5 | 6.02 |
| Deep Strata | 7 | -5.5 | 8.5 | 1.7 | 5.41 |
| **September Surf Water** | 23 | -6.4 | 16.1 | 4.1 | 4.67 |
| Shallow Strata | 8 | 0.8 | 8.2 | 3.1 | 2.62 |
| Mid Strata | 8 | -6.4 | 16.1 | 3.8 | 7.73 |
| Deep Strata | 7 | 1.3 | 9.6 | 5.3 | 3.07 |
| **October Bot Water** | 23 | 6.2 | 10.6 | 8.0 | 1.51 |
| Shallow Strata | 8 | 6.2 | 10.6 | 8.1 | 1.94 |
| Mid Strata | 8 | 8.1 | 8.1 | 8.1 | |
| Deep Strata | 7 | 7.7 | 7.7 | 7.7 | |
| **October Surf Water** | 3 | 18.5 | 18.5 | 18.5 | |
| Deep Strata | 3 | 18.5 | 18.5 | 18.5 | |
| **October Surf Water** | 23 | -7.5 | 16.7 | 6.2 | 5.36 |
| Shallow Strata | 8 | -7.5 | 6.2 | 6.1 | 7.88 |
| Mid Strata | 8 | 2.6 | 10.1 | 7.0 | 3.48 |
| Deep Strata | 7 | 1.2 | 16.7 | 7.8 | 4.60 |
| **Surface All** | 161 | -10.4 | 18.0 | 4.0 | 4.8 |
| Shallow | 56 | -8.1 | 18.0 | 3.8 | 5.1 |
| Mid | 55 | -10.4 | 16.1 | 3.3 | 5.6 |
| Deep | 50 | -2.0 | 16.7 | 4.8 | 3.5 |
| **Bottom All** | 161 | -27.3 | 12.7 | -3.1 | 10.5 |

| | | | | | |
|---|---|---|---|---|---|
| Shallow | 56 | -26.4 | 11.2 | -0.7 | 10.0 |
| Mid | 55 | -17.5 | 12.7 | -3.2 | 9.2 |
| Deep | 50 | -27.3 | 7.7 | -11.6 | 11.2 |

*Table A.5 $\delta^{13}C$ Brachyura (crab) prey item analysis, showing number of samples, isotopic minimum and maximum, average $\delta^{13}C$ value and standard deviation for each Brachyura prey item, as well as at each depth strata. Values are lipid corrected when C:N is greater than 3.5*

| **$\delta^{13}C$** | | | | | |
|---|---|---|---|---|---|
| | **n** | **Min** | **Max** | **Avg** | **Stdev** |
| **Shallow** | 62.0 | -19.0 | -11.6 | -16.5 | 1.6 |
| **Mid** | 53.0 | -19.7 | -9.8 | -16.0 | 2.1 |
| **Deep** | 13.0 | -18.3 | -7.0 | -15.6 | 2.9 |
| | | | | | |
| **Platform** | 83.0 | -19.7 | -7.0 | -16.3 | 2.1 |
| **Artificial Reef** | 45.0 | -19.4 | -11.6 | -16.1 | 1.7 |
| | | | | | |
| **Aethroidea** | 1 | -18.9 | -18.9 | -18.9 | |
| **Albunidae** | 6 | -16.1 | -14.2 | -15.0 | 0.68 |
| Shallow 2016 | 4 | -15.2 | -14.2 | -14.6 | 0.4 |
| Shallow 2017 | 2 | -16.1 | -15.2 | -15.6 | 0.7 |
| **Calappidae** | 3 | -18.2 | -17.1 | -17.6 | 0.54 |
| Mid 2016 | 2 | -18.2 | -17.4 | -17.8 | 0.54 |
| Deep 2016 | 1 | -17.1 | -17.1 | -17.1 | |
| **Callinectes** | 50 | -19.7 | -9.8 | -16.7 | 1.81 |
| Shallow 2016 | 10 | -17.8 | -12.6 | -15.5 | 1.84 |
| Shallow 2017 | 17 | -18.7 | -16.2 | -17.5 | 0.74 |
| Mid 2016 | 15 | -19.4 | -9.8 | -15.9 | 2.21 |
| Mid 2017 | 8 | -19.7 | -17.2 | -18.0 | 0.77 |
| **Hippoidea** | 2 | -16.6 | -14.3 | -15.4 | 1.61 |
| **Menippidae** | 3 | -18.3 | -7.0 | -13.9 | 6.06 |
| Deep 2016 | 2 | -16.4 | -7.0 | -11.7 | 6.66 |
| Deep 2017 | 1 | -18.3 | -18.3 | -18.3 | |
| **Parthenopidae** | 3 | -15.4 | -10.5 | -13.7 | 2.79 |
| Mid 2016 | 2 | -15.4 | -10.5 | -12.9 | 3.48 |
| Deep 2016 | 1 | -15.2 | -15.2 | -15.2 | |
| **Portunidae** | 49 | -19.0 | -13.7 | -16.6 | 1.20 |
| Shallow 2016 | 11 | -17.8 | -13.8 | -15.9 | 1.33 |
| Shallow 2017 | 16 | -19.0 | -16.1 | -17.3 | 0.68 |
| Mid 2016 | 11 | -17.7 | -13.7 | -15.6 | 1.12 |
| Mid 2017 | 6 | -18.4 | -16.7 | -17.4 | 0.62 |

| | | | | | |
|---|---|---|---|---|---|
| Deep 2016 | 4 | -17.5 | -15.8 | -16.6 | 0.73 |
| Deep 2017 | 1 | -17.5 | -17.5 | -17.5 | |
| **Xanthidae** | 11 | -17.3 | -11.6 | -13.9 | 1.51 |
| Shallow 2016 | 1 | -11.6 | -11.6 | -11.6 | |
| Shallow 2017 | 1 | -17.3 | -17.3 | -17.3 | |
| Mid 2016 | 7 | -15.2 | -12.1 | -13.8 | 0.98 |
| Mid 2017 | 1 | -13.4 | -13.4 | -13.4 | |
| Deep 2016 | 1 | -13.9 | -13.9 | -13.9 | |

*Table A.6 $\delta^{15}N$ Brachyura (crab) prey item analysis, showing number of samples, isotopic minimum and maximum, average $\delta^{15}N$ value and standard deviation. Also indicates difference in $\delta^{15}N$ value based upon year and depth strata.*

| **$\delta^{15}N$** | | | | | |
|---|---|---|---|---|---|
| | **n** | **Min** | **Max** | **Avg** | **Stdev** |
| **Shallow** | 62 | 2.9 | 12.6 | 9.9 | 2.3 |
| **Mid** | 54 | 3.1 | 13.9 | 9.3 | 2.1 |
| **Deep** | 14 | 5.0 | 12.5 | 10.1 | 2.6 |
| | | | | | |
| **Platform** | 84 | 2.9 | 13.9 | 10.0 | 2.3 |
| **Artificial Reef** | 46 | 4.4 | 12.5 | 9.0 | 2.0 |
| **Aethroidea** | 1 | 13.9 | 13.9 | 13.9 | |
| **Albunidae** | 6 | 7.5 | 11.4 | 10.3 | 1.50 |
| Shallow 2016 | 4 | 7.5 | 11.1 | 9.8 | 1.7 |
| Shallow 2017 | 2 | 11.0 | 11.4 | 11.2 | 0.3 |
| **Calappidae** | 3 | 5.0 | 7.8 | 6.5 | 1.44 |
| Mid 2016 | 2 | 6.9 | 7.8 | 7.3 | 0.58 |
| Deep 2016 | 1 | 5.0 | 5.0 | 5.0 | |
| **Callinectes** | 50 | 4.2 | 12.1 | 9.7 | 1.81 |
| Shallow 2016 | 10 | 4.2 | 11.3 | 8.8 | 2.67 |
| Shallow 2017 | 17 | 6.8 | 12.0 | 10.5 | 1.21 |
| Mid 2016 | 15 | 5.2 | 10.8 | 9.4 | 1.63 |
| Mid 2017 | 8 | 7.7 | 12.1 | 10.0 | 1.50 |
| **Hippoidea** | 2 | 11.0 | 12.3 | 11.7 | 0.91 |
| **Menippidae** | 3 | 7.9 | 12.0 | 10.3 | 2.15 |
| Deep 2016 | 2 | 7.9 | 11.0 | 9.4 | 2.20 |
| Deep 2017 | 1 | 12.0 | 12.0 | 12.0 | |
| **Parthenopidae** | 3 | 9.5 | 10.7 | 10.0 | 0.65 |
| Mid 2016 | 2 | 9.5 | 9.9 | 9.7 | 0.26 |
| Deep 2016 | 1 | 10.7 | 10.7 | 10.7 | |
| **Portunidae** | 49 | 2.9 | 12.6 | 9.5 | 2.70 |
| Shallow 2016 | 11 | 2.9 | 12.4 | 7.9 | 3.09 |
| Shallow 2017 | 16 | 10.0 | 12.6 | 11.3 | 0.65 |
| Mid 2016 | 11 | 3.1 | 11.4 | 8.4 | 2.81 |
| Mid 2017 | 6 | 5.5 | 12.0 | 9.6 | 2.76 |
| Deep 2016 | 4 | 5.7 | 12.5 | 9.4 | 3.04 |
| Deep 2017 | 1 | 12.4 | 12.4 | 12.4 | |
| **Xanthidae** | 11 | 6.0 | 11.6 | 9.2 | 2.00 |

| | | | | | |
|---|---|---|---|---|---|
| Shallow 2016 | 1 | 6.0 | 6.0 | 6.0 | |
| Shallow 2017 | 1 | 8.5 | 8.5 | 8.5 | |
| Mid 2016 | 7 | 6.6 | 11.0 | 9.8 | 1.47 |
| Mid 2017 | 1 | 6.4 | 6.4 | 6.4 | |
| Deep 2016 | 1 | 11.6 | 11.6 | 11.6 | |

*Table A.7 Dendrobranchiata and Stomatopoda $\delta^{13}C$ prey item analysis, showing number of samples, isotopic minimum and maximum, average $\delta^{13}C$ value and standard deviation for each depth strata and year. Values are lipid corrected when C:N is greater than 3.5.*

| **$\delta^{13}C$** | **n** | **Min** | **Max** | **Avg** | **Stdev** |
|---|---|---|---|---|---|
| **2016** | 74 | -20.3 | -14.7 | -17.5 | 1.1 |
| **2017** | 49 | -23.5 | -15.7 | -18.1 | 1.5 |
| **2016+2017** | 123 | -23.5 | -14.7 | -17.8 | 1.3 |
| | | | | | |
| **Shallow** | 28 | -23.5 | -17.2 | -18.8 | 1.3 |
| **Mid** | 75 | -21.1 | -16.4 | -18.9 | 1.0 |
| **Deep** | 21 | -21.5 | -16.7 | -19.1 | 1.4 |
| | | | | | |
| **Platform** | 47 | -23.5 | -16.4 | -18.9 | 1.2 |
| **Artificial Reef** | 71 | -21.5 | -16.9 | -18.9 | 1.1 |
| | | | | | |
| **Acetes** Mid 2017 **Only** | 7 | -18.5 | -18.1 | -18.3 | 0.1 |
| **Litopenaeus** | 6 | -19.6 | -16.5 | -17.8 | 1.2 |
| Shallow 2016 | 3 | -19.6 | -16.5 | -17.9 | 1.6 |
| Mid 2016 | 2 | -17.2 | -16.9 | -17.1 | 0.2 |
| Deep 2017 | 1 | -18.8 | -18.8 | -18.8 | |
| **Penaeoidea** | 14 | -23.5 | -17.0 | -19.0 | 1.8 |
| Shallow 2016 | 1 | -19.3 | -19.3 | -19.3 | |
| Shallow 2017 | 2 | -23.5 | -17.5 | -20.5 | 4.2 |
| Mid 2016 | 3 | -19.2 | -17.8 | -18.5 | 0.7 |
| Mid 2017 | 5 | -21.1 | -18.1 | -19.7 | 1.4 |
| Deep 2016 | 1 | -17.2 | -17.2 | -17.2 | |
| Deep 2017 | 2 | -17.7 | -17.0 | -17.3 | 0.5 |
| **Sicyoniidae** | 2 | -18.6 | -17.9 | -18.2 | 0.5 |
| Shallow 2016 | 1 | -18.6 | -18.6 | -18.6 | |
| Mid 2016 | 1 | -17.9 | -17.9 | -17.9 | |
| **Stomatopoda** | 94 | -20.3 | -14.7 | -17.5 | 1.2 |
| Shallow 2016 | 11 | -18.7 | -15.8 | -17.4 | 1.0 |
| Shallow 2017 | 9 | -20.3 | -15.7 | -17.5 | 1.3 |
| Mid 2016 | 37 | -20.3 | -14.7 | -17.4 | 1.2 |
| Mid 2017 | 20 | -20.2 | -16.4 | -17.8 | 1.3 |
| Deep 2016 | 14 | -19.3 | -16.1 | -17.6 | 1.0 |
| Deep 2017 | 3 | -18.2 | -16.7 | -17.6 | 0.8 |

*Table A.8 Dendrobranchiata and Stomatopoda $\delta^{15}N$ prey item analysis, showing number of samples, isotopic minimum and maximum, average $\delta^{15}N$ value and standard deviation across each year and depth strata*

| **$\delta^{15}N$** | | | | | |
|---|---|---|---|---|---|
| | **n** | **Min** | **Max** | **Avg** | **Stdev** |
| **2016** | 74 | 1.6 | 14.0 | 9.2 | 3.2 |
| **2017** | 50 | 3.0 | 12.8 | 9.2 | 2.4 |
| **2016+2017** | 124 | 1.6 | 14.0 | 9.2 | 2.9 |
| | | | | | |
| **Shallow** | 28 | 2.4 | 12.3 | 9.3 | 2.7 |
| **Mid** | 75 | 2.4 | 14.0 | 9.5 | 2.8 |
| **Deep** | 21 | 1.6 | 13.7 | 8.2 | 3.4 |
| | | | | | |
| **Platform** | 47 | 4.1 | 13.7 | 10.1 | 2.2 |
| **Artificial Reef** | 71 | 1.6 | 14.0 | 8.7 | 3.1 |
| | | | | | |
| **Acetes** Mid 2017 | 7 | 9.8 | 10.3 | 10.1 | 0.2 |
| **Litopenaeus** | 6 | 9.3 | 12.6 | 10.8 | 1.1 |
| Shallow 2016 | 3 | 9.3 | 11.1 | 10.2 | 0.9 |
| Mid 2016 | 2 | 11.3 | 12.6 | 12.0 | 0.9 |
| Deep 2017 | 1 | 10.4 | 10.4 | 10.4 | |
| **Penaeoidea** | 14 | 6.3 | 12.7 | 10.6 | 1.6 |
| Shallow 2016 | 1 | 11.8 | 11.8 | 11.8 | |
| Shallow 2017 | 2 | 9.1 | 10.8 | 10.0 | 1.2 |
| Mid 2016 | 3 | 9.0 | 11.7 | 10.7 | 1.5 |
| Mid 2017 | 5 | 6.3 | 12.7 | 10.5 | 2.5 |
| Deep 2016 | 1 | 11.2 | 11.2 | 11.2 | |
| Deep 2017 | 2 | 10.0 | 10.8 | 10.4 | 0.6 |
| **Sicyoniidae** | 2 | 9.3 | 12.6 | 11.0 | 2.3 |
| Shallow 2016 | 1 | 9.3 | 9.3 | 9.3 | |
| Mid 2016 | 1 | 12.6 | 12.6 | 12.6 | |
| **Stomatopoda** | 95 | 1.6 | 14.0 | 8.8 | 3.1 |
| Shallow 2016 | 11 | 2.4 | 12.3 | 8.8 | 3.5 |
| Shallow 2017 | 10 | 4.4 | 12.2 | 9.3 | 2.4 |
| Mid 2016 | 37 | 2.4 | 14.0 | 9.7 | 3.1 |

| | | | | | |
|---|---|---|---|---|---|
| Mid 2017 | 20 | 3.0 | 11.9 | 8.0 | 2.5 |
| Deep 2016 | 14 | 1.6 | 13.7 | 6.7 | 3.1 |
| Deep 2017 | 3 | 11.4 | 12.8 | 12.1 | 0.7 |

*Table A.9 $\delta^{13}C$ values of Actinopterygii prey items, showing number of samples, isotopic minimum and maximum, average $\delta^{13}C$ value and standard deviation by year and depth strata collected. Values are lipid corrected when C:N is greater than 3.5.*

| $\delta^{13}C$ | | | | | |
|---|---|---|---|---|---|
| | **n** | **Min** | **Max** | **Avg** | **Stdev** |
| **Shallow** | 24 | -24.4 | -9.0 | -18.2 | 2.9 |
| **Mid** | 17 | -26.9 | -16.7 | -18.7 | 2.3 |
| **Deep** | 31 | -22.6 | -11.6 | -17.8 | 1.9 |
| | | | | | |
| **Platform** | 50 | -26.9 | -9.0 | -18.2 | 2.7 |
| **Artificial Reef** | 24 | -23.1 | -16.5 | -17.9 | 1.5 |
| | | | | | |
| **Anguilliformes (Shallow 2016)** | 2 | 0.0 | -16.7 | -16.9 | 0.2 |
| **Clupeidae** | 11 | -26.9 | -16.5 | -18.8 | 3.0 |
| Shallow 2017 | 1 | -21.7 | -21.7 | -21.7 | |
| Mid 2017 | 1 | -26.9 | -26.9 | -26.9 | |
| Deep 2016 | 4 | -17.8 | -16.5 | -17.2 | 0.5 |
| Deep 2017 | 5 | -18.9 | -17.2 | -18.0 | 0.7 |
| **Cynoglossidae (Mid 2016)** | 1 | -18.0 | -18.0 | -18.0 | |
| **Dussumieriidae** | 2 | -20.5 | -16.9 | -18.7 | 2.5 |
| **Bremacerotidae (Deep 2016)** | 4 | -17.4 | -16.5 | -16.9 | 0.4 |
| **Gobiidae (Deep 2016)** | 4 | -19.1 | -16.9 | -17.6 | 1.1 |
| **Antenariidae (Shallow 2016)** | 1 | -16.4 | -16.4 | -16.4 | |
| **Lutjanus** | 19 | -19.1 | -9.0 | -17.1 | 2.6 |
| Shallow 2016 | 8 | -18.6 | -9.0 | -16.5 | 3.2 |
| Mid 2016 | 8 | -19.1 | -17.9 | -18.3 | 0.5 |
| Deep 2017 | 3 | -17.9 | -11.6 | -15.6 | 3.5 |
| **Ophichthidae** | 13 | -24.4 | -16.5 | -19.5 | 2.4 |
| Shallow 2017 | 5 | -24.4 | -16.5 | -19.5 | 3.2 |
| Mid 2017 | 2 | -17.7 | -17.2 | -17.4 | 0.3 |
| Deep 2017 | 6 | -22.6 | -17.1 | -20.2 | 2.0 |
| **Ophidiidae (Shallow 2016)** | 2 | -19.4 | -16.9 | -18.2 | 1.8 |
| **Perciformes (Deep 2016)** | 1 | -16.4 | -16.4 | -16.4 | |
| **Phycidae (Mid 2016)** | 1 | -17.2 | -17.2 | -17.2 | |
| **Pomatomus (2017 Shallow)** | 1 | -17.8 | -17.8 | -17.8 | |
| **Sciaenidae** | 9 | -23.1 | -16.8 | -18.7 | 2.0 |
| Shallow 2016 | 5 | -23.1 | -17.1 | -18.9 | 2.4 |
| Mid 2016 | 1 | -19.5 | -19.5 | -19.5 | |

| | | | | | |
|---|---|---|---|---|---|
| Mid 2017 | 1 | -20.1 | -20.1 | -20.1 | |
| Deep 2017 | 2 | -17.1 | -16.8 | -16.9 | 0.3 |
| **Triglidae (Deep 2016)** | 2 | -17.6 | -16.0 | -16.8 | 1.1 |
| **Serranidae (Shallow 2016)** | 1 | -19.0 | -19.0 | -19.0 | |

*Table A.10 $\delta^{15}N$ values of Actinopterygii prey items, showing number of samples, isotopic minimum and maximum, average $\delta^{15}N$ value and standard deviation across year and depth strata*

| **$\delta^{15}N$** | | | | | |
|---|---|---|---|---|---|
| | **n** | **Min** | **Max** | **Avg** | **Stdev** |
| **Shallow** | 26 | 5.8 | 14.2 | 12.1 | 2.1 |
| **Mid** | 17 | 8.6 | 14.5 | 12.5 | 1.4 |
| **Deep** | 32 | 5.1 | 14.8 | 11.3 | 2.5 |
| | | | | | |
| **Platform** | 50 | 5.1 | 14.8 | 11.6 | 2.4 |
| **Artificial Reef** | 24 | 6.2 | 14.4 | 12.5 | 1.7 |
| | | | | | |
| **Anguilliformes (Shallow 2016)** | 2 | 12.4 | 13.2 | 12.8 | 0.5 |
| **Clupeidae** | 11 | 10.0 | 13.9 | 12.8 | 1.4 |
| Shallow 2017 | 1 | 13.8 | 13.8 | 13.8 | |
| Mid 2017 | 1 | 13.0 | 13.0 | 13.0 | |
| Deep 2016 | 5 | 10.0 | 13.4 | 11.9 | 1.58 |
| Deep 2017 | 4 | 13.4 | 13.9 | 13.7 | 0.30 |
| **Cynoglossidae (Mid 2016)** | 1 | 12.1 | 12.1 | 12.1 | |
| **Dussumieriidae** | 2 | 12.4 | 13.9 | 13.1 | 1.1 |
| **Bremacerotidae (Deep 2016)** | 4 | 5.1 | 11.6 | 9.7 | 3.1 |
| **Gobiidae (Deep 2016)** | 4 | 5.4 | 10.8 | 7.4 | 2.4 |
| **Antenariidae (Shallow 2016)** | 1 | 11.9 | 11.9 | 11.9 | |
| **Lutjanus** | 19 | 5.8 | 14.1 | 11.0 | 2.4 |
| Shallow 2016 | 8 | 5.8 | 12.9 | 10.2 | 2.70 |
| Mid 2016 | 8 | 8.6 | 14.1 | 12.1 | 1.82 |
| Deep 2017 | 7 | 5.4 | 12.0 | 8.7 | 2.69 |
| **Ophichthidae** | 13 | 10.1 | 13.9 | 12.6 | 1.01 |
| Shallow 2017 | 5 | 11.9 | 13.9 | 13.1 | 0.78 |
| Mid 2017 | 2 | 12.1 | 12.9 | 12.5 | 0.57 |
| Deep 2017 | 6 | 10.1 | 13.3 | 12.1 | 1.14 |
| **Ophidiidae (Shallow 2016)** | 2 | 13.1 | 13.5 | 13.3 | 0.3 |
| **Perciformes (Deep 2016)** | 1 | 11.8 | 11.8 | 11.8 | |
| **Phycidae (Mid 2016)** | 1 | 12.9 | 12.9 | 12.9 | |
| **Pomatomus (2017 Shallow)** | 1 | 12.6 | 12.6 | 12.6 | |
| **Sciaenidae** | 9 | 10.7 | 14.8 | 13.7 | 1.2 |
| Shallow 2016 | 6 | 10.7 | 14.2 | 12.9 | 1.34 |
| Mid 2016 | 1 | 14.5 | 14.5 | 14.5 | |

| | | | | | |
|---|---|---|---|---|---|
| Mid 2017 | 1 | 14.4 | 14.4 | 14.4 | |
| Deep 2017 | 2 | 13.8 | 14.8 | 14.3 | 0.70 |
| **Triglidae (Deep 2016)** | 2 | 10.8 | 12.1 | 11.5 | 1.0 |
| **Serranidae (Shallow 2016)** | 1 | 12.0 | 12.0 | 12.0 | |

*Table A.11 Predator red snapper $\delta^{13}C$ analysis results. Showing the number of Actinopterygii in each category, the minimum, maximum and average isotope value across each depth strata, month, and year*

| **$\delta^{13}C$** | | | | | |
|---|---|---|---|---|---|
| | **n** | **Min** | **Max** | **Avg** | **Stdev** |
| **2016 Shallow** | 124 | -17.9 | -15.9 | -16.6 | 0.36 |
| **2017 Shallow** | 150 | -21.8 | -16.2 | -17.5 | 0.94 |
| **2016 Mid** | 203 | -18.0 | -15.9 | -16.7 | 0.41 |
| **2017 Mid** | 199 | -24.1 | -16.1 | -17.5 | 1.44 |
| **2016 Deep** | 99 | -17.7 | -16.3 | -16.8 | 0.31 |
| **2017 Deep** | 72 | -22.7 | -16.3 | -17.5 | 0.98 |
| | | | | | |
| **April Shallow 2016** | 34 | -17.1 | -16.3 | -16.6 | 0.19 |
| **April Shallow 2017** | 21 | -18.5 | -16.2 | -16.8 | 0.71 |
| | | | | | |
| **April Mid 2016** | 31 | -16.9 | -16.0 | -16.5 | 0.19 |
| **April Mid 2017** | 12 | -17.3 | -16.3 | -16.7 | 0.31 |
| | | | | | |
| **April Deep 2016** | 3 | -17.5 | -16.7 | -17.0 | 0.38 |
| **April Deep 2017** | 19 | -19.7 | -16.3 | -17.8 | 0.79 |
| | | | | | |
| **May Shallow 2016** | 23 | -17.6 | -16.5 | -16.9 | 0.37 |
| **May Shallow 2017** | 26 | -21.1 | -16.7 | -17.5 | 0.89 |
| | | | | | |
| **May Mid 2016** | 46 | -17.9 | -16.2 | -16.8 | 0.54 |
| **May Mid 2017** | 44 | -19.9 | -16.1 | -16.9 | 0.59 |
| | | | | | |
| **May Deep 2016** | 33 | -17.7 | -16.3 | -16.9 | 0.42 |
| **May Deep 2017** | 23 | -18.3 | -16.5 | -17.3 | 0.51 |
| | | | | | |
| **June Shallow 2016** | 9 | -17.9 | -16.6 | -16.9 | 0.43 |
| **June Shallow 2017** | 2 | -18.3 | -16.8 | -17.5 | 1.06 |
| | | | | | |
| **June Mid 2016** | 0 | | | | |
| **June Mid 2017** | 39 | -20.6 | -16.1 | -17.3 | 1.20 |
| | | | | | |
| **June Deep 2016** | 1 | -16.7 | -16.7 | -16.7 | #DIV/0! |
| **June Deep 2017** | 7 | -19.9 | -17.2 | -17.8 | 0.99 |

| | | | | | |
|---|---|---|---|---|---|
| **July Shallow 2016** | 8 | -17.6 | -16.6 | -17.0 | 0.38 |
| **July Shallow 2017** | 30 | -20.3 | -16.5 | -17.7 | 0.87 |
| | | | | | |
| **July Mid 2016** | 43 | -18.0 | -16.4 | -17.0 | 0.36 |
| **July Mid 2017** | 23 | -19.1 | -16.4 | -17.1 | 0.65 |
| | | | | | |
| **July Deep 2016** | 5 | -17.2 | -16.8 | -17.0 | 0.14 |
| **July Deep 2017** | 11 | -18.5 | -16.8 | -17.3 | 0.56 |
| | | | | | |
| **August Shallow 2016** | 3 | -16.7 | -16.1 | -16.4 | 0.31 |
| **August Shallow 2017** | 36 | -21.8 | -17.0 | -17.7 | 1.22 |
| | | | | | |
| **August Mid 2016** | 14 | -16.7 | -16.2 | -16.5 | 0.18 |
| **August Mid 2017** | 30 | -22.2 | -16.2 | -17.4 | 1.16 |
| | | | | | |
| **Augsust Deep 2016** | 32 | -17.4 | -16.3 | -16.7 | 0.26 |
| **Augsust Deep 2017** | 1 | -22.7 | -22.7 | -22.7 | #DIV/0! |
| | | | | | |
| **September Shallow 2016** | 11 | -16.5 | -16.1 | -16.3 | 0.13 |
| **September Shallow 2017** | 14 | -18.3 | -16.5 | -17.3 | 0.61 |
| | | | | | |
| **September Mid 2016** | 32 | -16.9 | -16.2 | -16.5 | 0.14 |
| **September Mid 2017** | 29 | -24.1 | -16.5 | -18.9 | 2.34 |
| | | | | | |
| **September Deep 2016** | 17 | -16.9 | -16.3 | -16.7 | 0.15 |
| **September Deep 2017** | 3 | -17.6 | -16.5 | -16.9 | 0.61 |
| | | | | | |
| **October Shallow 2016** | 36 | -16.8 | -15.9 | -16.3 | 0.23 |
| **October Shallow 2017** | 21 | -18.9 | -17.0 | -17.8 | 0.65 |
| | | | | | |
| **October Mid 2016** | 37 | -17.5 | -15.9 | -16.4 | 0.32 |
| **October Mid 2017** | 22 | -22.0 | -16.8 | -18.0 | 1.47 |
| | | | | | |
| **October Deep 2016** | 8 | -16.9 | -16.4 | -16.7 | 0.17 |
| **October Deep 2017** | 8 | -20.2 | -16.6 | -17.2 | 1.21 |
| | | | | | |
| **Platform** | 489 | -24.1 | -15.9 | -17.3 | 1.14 |
| **Artificial Reef** | 358 | -21.0 | -15.9 | -16.8 | 0.62 |

| | | | | | |
|---|---|---|---|---|---|
| **Control** | 2 | -17.4 | -17.3 | -17.3 | 0.09 |
| | | | | | |
| **Female** | 424 | -23.5 | -15.9 | -17.1 | 1.01 |
| **Male** | 423 | -24.1 | -15.9 | -17.0 | 0.96 |

*Table A.12 Predator red snapper $\delta^{15}N$ analysis results. Showing the number of Actinopterygii in each category, the minimum, maximum and average isotope value across each depth strata, month, and year*

| **$\delta^{15}N$** | | | | | |
|---|---|---|---|---|---|
| | **n** | **Min** | **Max** | **Avg** | **Stdev** |
| **2016 Shallow** | 124 | 13.0 | 15.4 | 14.2 | 0.49 |
| **2017 Shallow** | 150 | 11.0 | 15.3 | 14.1 | 0.63 |
| **2016 Mid** | 203 | 13.0 | 15.2 | 14.3 | 0.38 |
| **2017 Mid** | 199 | 13.1 | 15.5 | 14.5 | 0.55 |
| **2016 Bot** | 99 | 13.3 | 15.8 | 14.2 | 0.42 |
| **2017 Bot** | 72 | 11.7 | 15.2 | 13.9 | 0.62 |
| | | | | | |
| **April Shallow 2016** | 34 | 13.4 | 15.4 | 14.1 | 0.45 |
| **April Shallow 2017** | 21 | 13.3 | 14.9 | 13.8 | 0.48 |
| | | | | | |
| **April Mid 2016** | 31 | 13.7 | 15.1 | 14.4 | 0.35 |
| **April Mid 2017** | 12 | 14.7 | 15.3 | 15.0 | 0.22 |
| | | | | | |
| **April Deep 2016** | 3 | 13.7 | 14.2 | 13.9 | 0.25 |
| **April Deep 2017** | 19 | 12.3 | 14.7 | 13.7 | 0.51 |
| | | | | | |
| **May Shallow 2016** | 23 | 13.9 | 15.1 | 14.4 | 0.30 |
| **May Shallow 2017** | 26 | 13.0 | 15.1 | 13.7 | 0.59 |
| | | | | | |
| **May Mid 2016** | 46 | 13.7 | 15.1 | 14.4 | 0.30 |
| **May Mid 2017** | 44 | 13.1 | 15.5 | 14.3 | 0.76 |
| | | | | | |
| **May Deep 2016** | 33 | 13.7 | 15.8 | 14.4 | 0.54 |
| **May Deep 2017** | 23 | 11.7 | 14.3 | 13.5 | 0.51 |
| | | | | | |
| **June Shallow 2016** | 9 | 14.1 | 14.6 | 14.3 | 0.15 |
| **June Shallow 2017** | 2 | 13.9 | 14.0 | 13.9 | 0.02 |
| | | | | | |
| **June Mid 2016** | 0 | | | | |
| **June Mid 2017** | 39 | 13.4 | 15.3 | 14.3 | 0.63 |
| | | | | | |
| **June Deep 2016** | 1 | 14.0 | 14.0 | 14.0 | |
| **June Deep 2017** | 7 | 13.8 | 14.9 | 14.2 | 0.36 |

| | | | | | |
|---|---|---|---|---|---|
| **July Shallow 2016** | 8 | 13.2 | 14.5 | 13.9 | 0.52 |
| **July Shallow 2017** | 30 | 13.0 | 15.2 | 13.7 | 0.46 |
| | | | | | |
| **July Mid 2016** | 43 | 13.0 | 15.2 | 14.3 | 0.40 |
| **July Mid 2017** | 23 | 13.8 | 15.2 | 14.7 | 0.29 |
| | | | | | |
| **July Deep 2016** | 5 | 14.0 | 14.3 | 14.2 | 0.14 |
| **July Deep 2017** | 11 | 13.9 | 14.6 | 14.3 | 0.25 |
| | | | | | |
| **August Shallow 2016** | 3 | 14.0 | 14.4 | 14.2 | 0.22 |
| **August Shallow 2017** | 36 | 14.0 | 14.7 | 14.3 | 0.20 |
| | | | | | |
| **August Mid 2016** | 14 | 13.6 | 14.3 | 14.1 | 0.20 |
| **August Mid 2017** | 30 | 14.1 | 14.9 | 14.5 | 0.26 |
| | | | | | |
| **Augsust Deep 2016** | 32 | 13.7 | 15.2 | 14.2 | 0.34 |
| **Augsust Deep 2017** | 1 | 14.6 | 14.6 | 14.6 | |
| | | | | | |
| **September Shallow 2016** | 11 | 13.5 | 14.2 | 13.9 | 0.24 |
| **September Shallow 2017** | 14 | 14.8 | 15.3 | 15.1 | 0.13 |
| | | | | | |
| **September Mid 2016** | 32 | 13.4 | 14.4 | 14.0 | 0.22 |
| **September Mid 2017** | 29 | 14.0 | 15.3 | 14.7 | 0.32 |
| | | | | | |
| **September Deep 2016** | 17 | 13.7 | 14.6 | 14.1 | 0.22 |
| **September Deep 2017** | 3 | 14.5 | 15.2 | 15.0 | 0.39 |
| | | | | | |
| **October Shallow 2016** | 36 | 13.5 | 15.4 | 14.3 | 0.65 |
| **October Shallow 2017** | 21 | 11.0 | 15.1 | 14.2 | 0.82 |
| | | | | | |
| **October Mid 2016** | 37 | 13.0 | 15.2 | 14.6 | 0.38 |
| **October Mid 2017** | 22 | 13.7 | 14.9 | 14.2 | 0.34 |
| | | | | | |
| **October Deep 2016** | 8 | 13.3 | 14.8 | 13.9 | 0.45 |
| **October Deep 2017** | 8 | 14.3 | 15.1 | 14.7 | 0.24 |
| | | | | | |
| **2016 DMR** | 189 | 13.0 | 15.4 | 14.5 | 0.42 |
| **2017 DMR** | 158 | 13.6 | 15.5 | 14.7 | 0.40 |
| **2016 JF** | 237 | 13.0 | 15.8 | 14.1 | 0.37 |

| | | | | | |
|---|---|---|---|---|---|
| **2017 DMR** | 263 | 11.0 | 15.2 | 13.9 | 0.54 |
| | | | | | |
| **Platform** | 489 | 11.0 | 15.8 | 14.1 | 0.50 |
| **Artificial Reef** | 358 | 13.0 | 15.5 | 14.5 | 0.49 |
| **Control** | 2 | 13.9 | 14.0 | 13.9 | 0.04 |
| | | | | | |
| **Female** | 424 | 11.7 | 15.8 | 14.3 | 0.55 |
| **Male** | 418 | 11.0 | 15.5 | 14.2 | 0.53 |

# APPENDIX B - TABLES

## Table 1.1: *Sampling dates in 2016 and 2017*

2016 and 2017 sampling dates for each month based on which team was doing the sampling. Poor weather in October 2016 lead to large difference in the GCRL sampling dates.

| **Sampling Month** | **Sampling Team** | **2016** | **2017** | **Days Offset** |
|---|---|---|---|---|
| April | GCRL | 4/26-4/27 | 4/20-4/21 | 5 |
| | DMR | 5/3 | 4/25 | 8 |
| May | GCRL | 5/16-5/17 | 5/8-5/9 | 7 |
| | DMR | 5/26 | 5/25 | 1 |
| June | GCRL | 6/15-6/16 | 6/9-6/10 | 5 |
| | DMR | 6/23 | 6/15 | 8 |
| July | GCRL | 7/14-7/15 | 7/14-7/15 | 0 |
| | DMR | 7/21 | 7/19 | 2 |
| August | GCRL | 8/23-8/24 | 8/14-8/15 | 8 |
| | DMR | 8/25 | 8/10 | 15 |
| September | GCRL | 9/19-9/20 | 9/18-9/19 | 1 |
| | DMR | 9/15 | 9/14 | 1 |
| October | GCRL | 10/14, 11/22 | 10/30-10/31 | 16, 22 |
| | DMR | 11/11 | 10/31 | 11 |

Table 1.2: *POM $\delta^{13}C$ single-variate ANOVA results*

Bolded sections indicate statistical significance.

| $\delta^{13}C$ | Df | Sum Sq | Mean Sq | F value | Pr(>F) |
|---|---|---|---|---|---|
| **Month** | 6 | 447.7 | 74.62 | 21.814 | **3.48E-10** |
| **Year** | 2 | 32.8 | 16.41 | 4.797 | **0.01483** |
| **Depth Strata** | **3** | **54.5** | **18.16** | **5.309** | **0.0426** |
| Structure Type | 2 | 4.5 | 2.27 | 0.662 | 0.5224 |
| **Dissolved Oxygen (mg/L)** | **88** | **385.1** | **4.38** | **1.279** | **0.01024** |
| Temperature (°C) | 120 | 546.9 | 4.56 | 1.332 | 0.17185 |
| Salinity (PSU) | 170 | 581.9 | 3.42 | 1.001 | 0.52316 |

Table 1.3*: POM $\delta^{15}N$ single-variate ANOVA results.*

Bolded sections indicate statistical significance

| $\delta^{15}N$ | Df | Sum Sq | Mean Sq | F value | Pr(>F) |
|---|---|---|---|---|---|
| **Month** | 6 | 6945 | 1157.6 | 37.094 | **< 2e-16** |
| Year | 2 | 65 | 32.7 | 1.049 | 0.35329 |
| Depth Strata | 3 | 50 | 16.7 | 0.537 | 0.65807 |
| Structure Type | 2 | 7 | 3.5 | 0.114 | 0.89257 |
| Vessel | 1 | 28 | 27.9 | 0.895 | 0.34593 |
| **Dissolved Oxygen (mg/L)** | 92 | 8443 | 91.8 | 2.941 | **1.50E-08** |
| **Temperature (°C)** | 125 | 5976 | 47.8 | 1.532 | **0.00915** |
| Salinity (PSU) | 174 | 5540 | 31.8 | 1.02 | 0.4561 |

Table 2.1: *Red snapper prey items from 2016*

Identified using stomach content analysis and DNA barcoding

| 2016 | |
|---|---|
| **ID** | **n** |
| Stomatopoda | 737 |
| Gastropoda | 233 |
| Calappidae | 125 |
| Amphipoda | 116 |
| Portunidae | 45 |
| Salpidae | 35 |
| Lutjanus | 31 |
| Callinectes | 23 |
| Bivalvia | 19 |
| Penaeoidea | 19 |
| Cephalopoda | 15 |
| Amphipoda | 14 |
| Xanthidae | 12 |
| Other | 73 |
| Total | 1497 |

Table 2.2: *Red snapper prey items collected in 2017*

Identified using stomach content analysis and DNA barcoding

| 2017 | |
|---|---|
| **ID** | **n** |
| Gastropoda | 736 |
| Stomatopoda | 257 |
| Mysidae | 248 |
| Penaeoidea | 75 |
| Amphipoda | 67 |
| Portunidae | 60 |
| Calinectes | 29 |
| Acetes | 15 |
| Tunicata | 15 |
| Albunidae | 14 |
| Ophicthidae | 14 |
| Solenocera | 14 |
| Other | 65 |
| Total | 1609 |

Table 2.3: *Frequency of occurrence (%F) of identified prey items ran for stable isotope analysis based upon age of the predatory red snapper.*

| | < 1yr | 1yr | 2yr | 3+ |
|---|---|---|---|---|
| Actinopterygii | 8.695652 | 7.142857 | 5.151515 | 9.210526 |
| Amphipoda | | | | 0.263158 |
| Anemone | | | | 0.526316 |
| Brachyura | 8.695652 | 10.90909 | 11.22449 | 15.78947 |
| Cephalapoda | | | 0.30303 | 0.263158 |
| Dendrobranchiata | 4.347826 | 1.020408 | 2.727273 | 2.631579 |
| Gastropoda | | | | 1.052632 |
| Nematoda | | | | 0.263158 |
| Salpidae | | | 0.30303 | |
| Stomatapoda | | 6.363636 | 8.163265 | 13.15789 |
| Trematoda | | 1.020408 | 0.909091 | 1.052632 |
| Tunicata | | | | 1.052632 |

Table 2.4: *Brachyura $\delta^{13}C$ single-variate ANOVA results.*

Bolded sections indicate statistical significance.

| $\delta^{13}C$ | Df | Sum Sq | Mean Sq | F value | Pr(>F) |
|---|---|---|---|---|---|
| **Month** | 6 | 25.96 | 4.327 | 2.494 | **0.0315** |
| **Year** | 1 | 14.23 | 14.226 | 8.198 | **0.00569** |
| Structure Type | 2 | 0 | 0 | 0 | 0.99046 |
| Depth Strata | 2 | 9.47 | 4.735 | 2.729 | 0.07302 |
| Temperature (°C) | 25 | 58.31 | 2.332 | 1.344 | 0.17239 |
| Dissolved Oxygen (mg/L) | 4 | 10.92 | 2.729 | 1.573 | 0.19254 |
| Brachyura Grouping | 4 | 8.97 | 2.243 | 1.293 | 0.28251 |

Table 2.5: *Brachyura $\delta^{15}N$ single-variate ANOVA results.*

Bolded sections indicate statistical significance.

| $\delta^{15}N$ | Df | Sum Sq | Mean Sq | F value | Pr(>F) |
|---|---|---|---|---|---|
| **Month** | 6 | 127.4 | 21.24 | 4.991 | **7.68E-05** |
| **Year** | 1 | 100.9 | 100.91 | 23.718 | **2.02E-06** |
| **StructureType** | 2 | 91.7 | 45.87 | 10.781 | **3.27E-05** |
| DepthStrata | 2 | 2.1 | 1.06 | 0.249 | 0.7797 |
| Temperature | 49 | 554.3 | 11.31 | 2.659 | 0.449 |
| Dissolved.Oxygen | 33 | 458.9 | 13.91 | 3.268 | 0.723 |
| PreyGroup | 34 | 192.4 | 5.66 | 1.33 | 0.1147 |

Table 2.6: *Dendrobranchiata and Stomatopoda $\delta^{13}C$ single-variate ANOVA analysis.*

All significant values are in bold.

| $\delta^{13}C$ | Df | Sum Sq | Mean Sq | F value | Pr(>F) |
|---|---|---|---|---|---|
| Month | 6 | 21.6 | 3.6 | 6.606 | 0.189 |
| Year | 1 | 0.42 | 0.421 | 0.772 | 0.38304 |
| Structure Type | 2 | 2.95 | 1.473 | 2.702 | 0.07481 |
| Depth Strata | 2 | 1.33 | 0.665 | 1.22 | 0.30211 |
| Temperature | 36 | 93.51 | 2.598 | 4.766 | 0.329 |
| Dissolved Oxygen (mg/L) | 8 | 3.25 | 0.406 | 0.745 | 0.652 |
| Prey Grouping | 4 | 1.45 | 0.363 | 0.666 | 0.61828 |

Table 2.7: *Dendrobranchiata and Stomatopoda $\delta^{15}N$ single-variate ANOVA analysis.*

All significant values are in bold.

| $\delta^{15}N$ | Df | Sum Sq | Mean Sq | F value | Pr(>F) |
|---|---|---|---|---|---|
| Month | 6 | 94.1 | 15.68 | 3.365 | 0.6104 |
| Year | 1 | 2.3 | 2.31 | 0.497 | 0.483603 |
| **Structure Type** | 2 | 61 | 30.48 | 6.541 | **0.002624** |
| Depth Strata | 2 | 4.7 | 2.35 | 0.503 | 0.60704 |
| Temperature (°C) | 36 | 436.9 | 12.14 | 2.604 | 0.432 |
| Dissolved.Oxygen (mg/L) | 8 | 44.5 | 5.56 | 1.192 | 0.318001 |
| Prey Group | 4 | 4.4 | 1.11 | 0.238 | 0.915875 |

Table 2.8: *Actinopterygii prey item $\delta^{13}C$ single-variate ANOVA analysis.*

All significant values are in bold

| $\delta^{13}C$ | Df | Sum Sq | Mean Sq | F value | Pr(>F) |
|---|---|---|---|---|---|
| **Month** | 6 | 72.79 | 12.131 | 2.728 | **0.0377** |
| Year | 1 | 11.29 | 11.287 | 2.538 | 0.1248 |
| Structure Type | 1 | 4.78 | 4.779 | 1.075 | 0.3107 |
| Depth Strata | 2 | 2.42 | 1.208 | 0.272 | 0.7646 |
| Temperature (°C) | 21 | 210.18 | 10.008 | 2.25 | 0.306 |
| Dissolved Oxygen (mg/L) | 8 | 29.87 | 3.733 | 0.839 | 0.5782 |
| Prey Group | 10 | 38.35 | 3.835 | 0.862 | 0.5787 |

Table 2.9: *Actinopterygii prey item $\delta^{15}N$ single-variate ANOVA analysis.*

All significant values are in bold.

| $\delta^{15}N$ | Df | Sum Sq | Mean Sq | F value | Pr(>F) |
|---|---|---|---|---|---|
| **Month** | 6 | 77.81 | 12.97 | 6.606 | **0.000367** |
| **Year** | 1 | 34.41 | 34.41 | 17.53 | **0.000353** |
| Structure Type | 1 | 1.56 | 1.56 | 0.797 | 0.381247 |
| **Depth Strata** | 2 | 15.88 | 7.94 | 4.045 | **0.041234** |
| Temperature (°C) | 21 | 120.17 | 5.72 | 2.915 | 0.7176 |
| **Dissolved Oxygen (mg/L)** | 8 | 33.41 | 4.18 | 2.128 | **0.074956** |
| Prey Classification | 10 | 29.5 | 2.95 | 1.503 | 0.201347 |

Table 2.10: *Sampling information and stable isotope values for biofilm samples collected in 2017.*

| **Sample Site** | **Sample Date** | **$\delta^{13}C$** | **$\delta^{15}N$** | **C:N** |
|---|---|---|---|---|
| Cat Island | 5/2/2017 | -17.5735 | 7.865 | 5.729797 |
| FH-1 Ole Faithful | 4/21/2017 | -16.7965 | 9.241 | 4.990185 |
| FH-2 St. Elmo | 4/21/2017 | -20.1305 | 8.205 | 4.489787 |
| FH-3 Chevron Boat | 4/21/2017 | -18.4385 | 9.9625 | 4.293094 |
| FH-5 O.S. Barge | 4/21/2017 | -18.916 | 8.8905 | 5.055841 |
| FH-8 | 5/2/2017 | -17.898 | 8.603 | 5.168718 |
| FH-10 | 5/2/2017 | -20.0325 | 8.2715 | 5.239295 |
| FH-14 | 5/2/2017 | -18.106 | 9.7145 | 4.40528 |

Table 2.11: *Trophic position calculations for prey items and predators*

Utilizing the two-year $\delta^{15}N$ value with depleted $\delta^{15}N$ values removed and utilizing the literature value for the TP of **Litopenaeus vannamei** and the average $\delta^{15}N$ values of the **Litopenaeus setiferus**

| Prey Group | Prey Classification | n | POM TP | stdev | *L. setiferus* TP | stdev |
|---|---|---|---|---|---|---|
| **Amphipod** | Amphipoda | 2 | 1.88 | 0.77 | 0.87 | 0.77 |
| **Anemone** | Ceriantharia | 2 | 2.51 | 1.46 | 1.50 | 1.46 |
| **Cephalopoda** | Loliginidae | 6 | 3.50 | 0.59 | 2.50 | 0.59 |
| **Brachyura** | Aethroidea | 1 | 4.73 | | 3.72 | |
| | Albunea | 6 | 3.07 | 0.68 | 2.06 | 0.68 |
| | Calappidae | 4 | 1.43 | 0.54 | 0.43 | 0.54 |
| | Callinectes | 50 | 2.84 | 0.82 | 1.83 | 0.82 |
| | Hippoidea | 2 | 3.71 | 0.41 | 2.71 | 0.41 |
| | Menippidae | 3 | 3.07 | 0.98 | 2.06 | 0.98 |
| | Parthenopidae | 3 | 2.96 | 0.29 | 1.95 | 0.29 |
| | Portunidae | 49 | 2.74 | 1.23 | 1.74 | 1.23 |
| | Xanthid | 11 | 2.59 | 0.91 | 1.58 | 0.91 |
| **Dendrobranchiata** | Acetes | 7 | 3.01 | 0.10 | 2.00 | 0.10 |
| | Litopenaeus | 6 | 3.31 | 0.52 | 2.31 | 0.52 |
| | Penaeoidea | 14 | 3.21 | 0.73 | 2.20 | 0.73 |
| | Sicyoniidae | 2 | 3.39 | 1.08 | 2.38 | 1.08 |
| **Actinopterygii** | Anguilliformes | 2 | 3.09 | 0.15 | 2.84 | 0.15 |
| | Bremacerotidae | 4 | 2.19 | 0.91 | 1.94 | 0.91 |
| | Clupeidae | 11 | 3.09 | 0.40 | 2.84 | 0.40 |
| | Cynoglossidae | 1 | 2.87 | | 2.62 | |
| | Dussumieriidae | 2 | 3.18 | 0.33 | 2.94 | 0.33 |
| | Gobiidae | 4 | 1.50 | 0.70 | 1.25 | 0.70 |
| | Lutjanus | 19 | 2.76 | 0.79 | 2.33 | 0.79 |
| | Ophichthidae | 13 | 3.02 | 0.30 | 2.77 | 0.30 |
| | Ophidiidae | 2 | 3.23 | 0.09 | 2.98 | 0.09 |
| | Perciformes | 1 | 2.79 | | 2.54 | |
| | Phycidae | 1 | 3.12 | | 2.87 | |
| | Pomatomidae | 1 | 3.02 | | 2.77 | |
| | Sciaenidae | 10 | 3.30 | 0.37 | 3.05 | 0.37 |
| | Triglidae | 1 | 2.49 | | 2.24 | |
| **Gastropod** | Sinum | 1 | 2.72 | | 1.71 | |
| | Thecosomata | 4 | 2.32 | 0.73 | 1.32 | 0.73 |
| **Nematode** | Round worm | 1 | 3.67 | | 2.66 | |
| **Salp** | Salpidae | 1 | 3.55 | | 2.54 | |
| **Stomatopoda** | Mantis Shrimp | 95 | 2.42 | 1.41 | 1.41 | 1.41 |
| **Trematode** | Trematoda | 9 | 4.06 | 1.44 | 3.05 | 1.44 |
| **Tunicate** | Tunicate | 4 | 1.62 | 1.20 | 0.62 | 1.20 |

Table 2.12: *Comparison of the trophic position calculations with literature values for specific red snapper prey and predatory red snapper collected in 2016 and 2017.*

TP1: Two-year average POM $\delta^{15}N$ value with depleted $\delta^{15}N$ values removed, TP2: Trophic position calculations using **Litopenaeus setiferus**

| **ACTINOPTERYGII PREY** | **TP 1** | **Stdev** | **TP 2** | **Stdev** | **Literature TP** | **Stdev** | **Source Name** |
|---|---|---|---|---|---|---|---|
| Shrimp eel (Anguilliformes) | 3.09 | 0.15 | 3.10 | 0.15 | 4.0 | 0.70 | FishBase |
| Common Anchovy (Clupeidae) | 2.26 | | 2.27 | | 3.3 | | Wilson et al., 2009 |
| Scaled Sardine (Clupeidae) | 3.28 | | 3.29 | | 3.4 | | FishBase |
| Offshore Tonguefish (Cynglossidae) | 2.87 | | 2.88 | | 3.3 | 0.40 | FishBase |
| Red-eye round herring (Dussumieriidae) | 2.95 | | 2.96 | | 3.6 | 0.20 | FishBase |
| Bay Whiff (Dussumieriidae) | 3.42 | | 3.43 | | 3.6 | 0.58 | FishBase |
| Striped Codlet (Bremacerotidae) | 2.19 | 0.91 | 2.20 | 0.91 | 3.1 | 0.30 | FishBase |
| Singlespot Frogfish (Antenarriidae) | 2.82 | | 2.83 | | 3.5 | 0.60 | FishBase |
| Red Snapper Prey (Lutjanus) | 2.76 | 0.79 | 2.59 | 0.79 | 3.85 | | Tarnecki & Patterson, 2015 |
| Speckled Worm Eel (Ophichthidae) | 3.29 | | 3.30 | | 2.98 | | Akin and Winemiller, 2008 |
| Bluefish (Pomatomidae) | 3.02 | | 3.03 | | 4.2 | 0.2 | Woodland and Secor, 2011 |
| Sand trout (Sciaenidae) | 3.58 | | 3.59 | | 3.5 | | Wilson et al., 2009 |
| Atlantic Croaker (Sciaenidae) | 3.11 | 0.43 | 3.12 | 0.43 | 3.07 | 0.019 | Akin and Winemiller, 2008 |
| Spot (Sciaenidae) | 3.51 | | 3.52 | | 3.3 | | Wilson et al., 2009 |
| Shortwing searobin (Triglidae) | 2.69 | 0.28 | 2.70 | 0.28 | 3.5 | 0.50 | FishBase |
| Soap Fish (Serranidae) | 2.84 | | 2.85 | | 4.1 | 0.50 | FishBase |

| | | | | | | | |
|---|---|---|---|---|---|---|---|
| Callinectes similis | 2.84 | 0.82 | 2.09 | 0.82 | 3.0 | 0.08 | Carozzo et al, 2014 |
| Ovalipes floridanus (Portunidae | 2.54 | 0.94 | 1.79 | 0.94 | 3.3 | 0.30 | Careddu et al., 2017 |
| Squilla empusa | 3.24 | 0.88 | 2.49 | 0.88 | 3.5 | | Antony et al., 2010 |
| Lutjanus Campechanus (Predator) | 3.89 | 0.18 | 3.67 | 0.18 | 3.85 | | Tarnecki & Patterson, 2015 |

Table 2.13: *Predator red snapper $\delta^{13}C$ single-variate ANOVA results.*

Statistically significant values are in bold.

| $\delta^{13}C$ | Df | Sum Sq | Mean Sq | F value | Pr(>F) |
|---|---|---|---|---|---|
| **Month** | 7 | 40.13 | 5.73 | 15.7 | **3.21E-16** |
| **Year** | 1 | 134.7 | 134.7 | 368.896 | **< 2e-16** |
| **Structure Type** | 2 | 21.2 | 10.6 | 29.033 | **9.63E-12** |
| Depth Strata | 2 | 2.02 | 1.01 | 2.77 | 0.06519 |
| Temperature (°C) | 61 | 128.27 | 2.1 | 5.759 | 0.216 |
| Dissolved Oxygen (mg/L) | 45 | 124.57 | 2.77 | 7.581 | 0.287 |
| Salinity (PSU) | 5 | 1.73 | 0.35 | 0.95 | 0.450 |
| Length (mm) | 326 | 167.44 | 0.51 | 1.407 | 0.474 |
| Weight (kg) | 202 | 105.8 | 0.52 | 1.434 | 0.594 |

Table 2.14: *Predator red snapper $\delta^{15}N$ single-variate ANOVA results.*

Statistically significant values are in bold.

| $\delta^{15}N$ | Df | Sum Sq | Mean Sq | F value | Pr(>F) |
|---|---|---|---|---|---|
| **Month** | 7 | 5.52 | 0.788 | 12.799 | **1.85E-13** |
| Year | 1 | 0.13 | 0.131 | 2.124 | 0.1466 |
| **Structure Type** | 2 | 38.38 | 19.188 | 311.673 | **< 2e-16** |
| **Depth Strata** | 2 | 6.11 | 3.054 | 49.61 | **< 2e-16** |
| Temperature (°C) | 61 | 63.83 | 1.046 | 16.997 | 0.1716 |
| Dissolved Oxygen (mg/L) | 45 | 30.99 | 0.689 | 11.186 | 0.5340 |
| Salinity (PSU) | 5 | 2.23 | 0.446 | 7.241 | 0.2798 |
| Length (mm) | 326 | 50.47 | 0.155 | 2.514 | 0.5311 |
| Weight (kg) | 202 | 12.89 | 0.064 | 1.037 | 0.4007 |

Table 2.15*: List of prey items being used for each SIAR model*.

| **2016** | | | | **2017** | | |
|---|---|---|---|---|---|---|
| **Depth Strata** | **Prey Group** | **n** | | **Depth Strata** | **Prey Group** | **n** |
| **Shallow** | Callinectes | 10 | | **Shallow** | Callinectes | 17 |
| | Lutjanus | 8 | | | Ophicthidae | 5 |
| | Portunidae | 11 | | | Portunidae | 16 |
| | Sciaenidae | 5 | | | Stomatopoda | 10 |
| | Stomatopoda | 11 | | | | |
| **Mid** | Callinectes | 15 | | **Mid** | Acetes | 7 |
| | Lutjanus | 8 | | | Callinectes | 8 |
| | Portunidae | 11 | | | Penaeoidea | 5 |
| | Stomatopoda | 36 | | | Portunidae | 6 |
| | Xanthidae | 7 | | | Stomatapoda | 20 |
| **Deep** | Clupeidae | 5 | | **Deep** | Ophicthidae | 6 |
| | Stomatopoda | 14 | | | | |

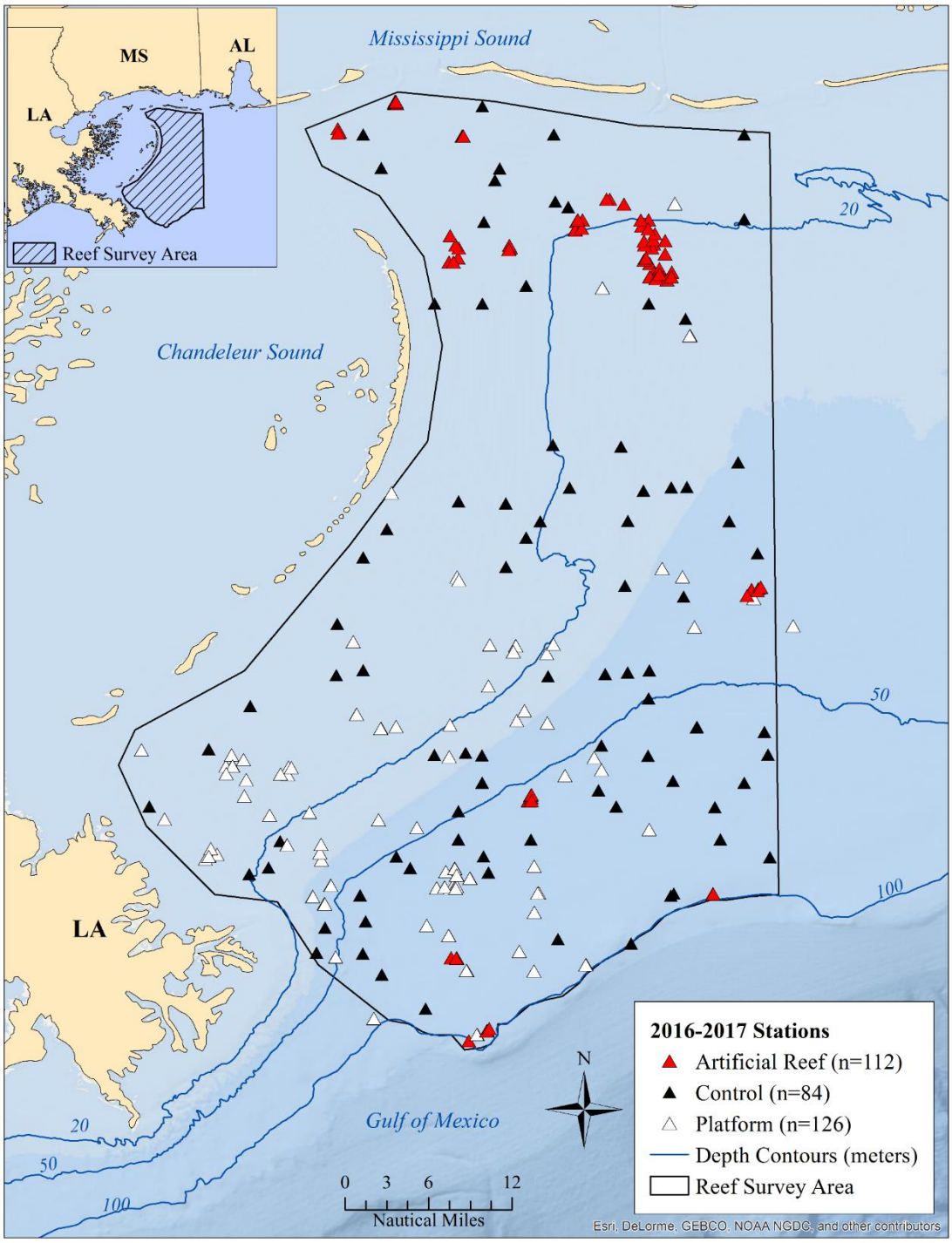


Figure 1.1*: Map showing the sampling effort in both 2016 and 2017*

Locations based upon structure type, as well as depth contours relevant to the reef survey area.

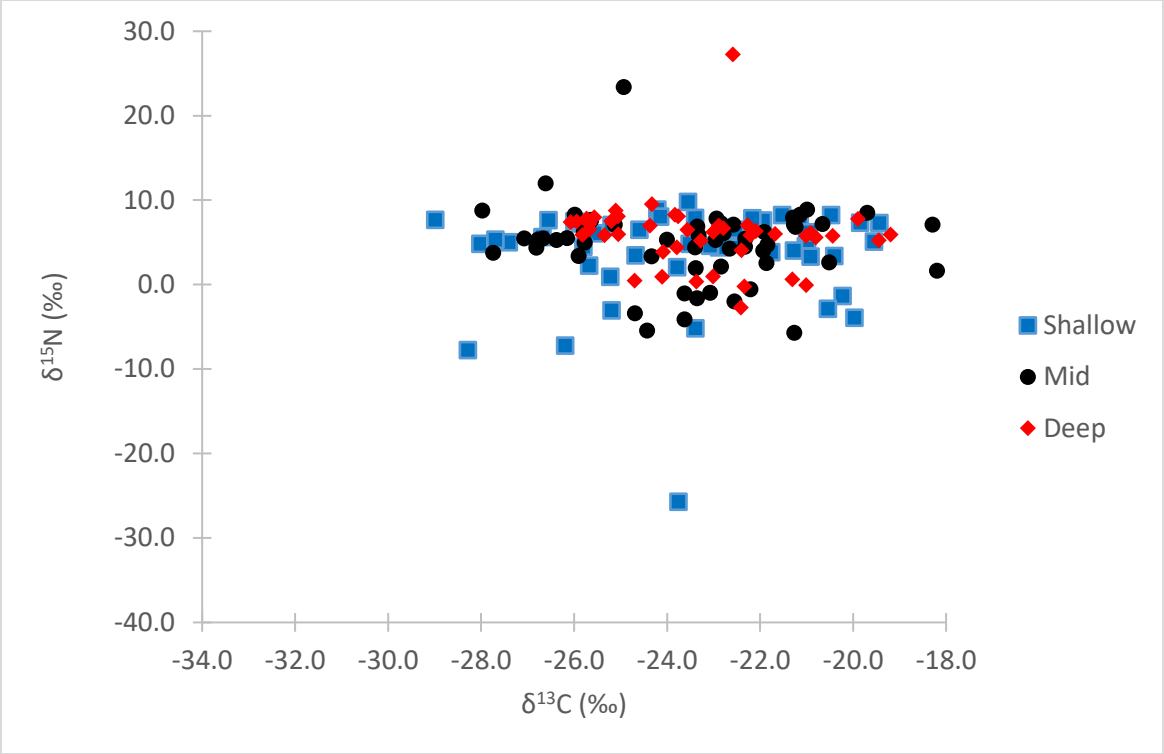

Figure 1.2*: POM stable isotope values sampled from surface water in 2016*

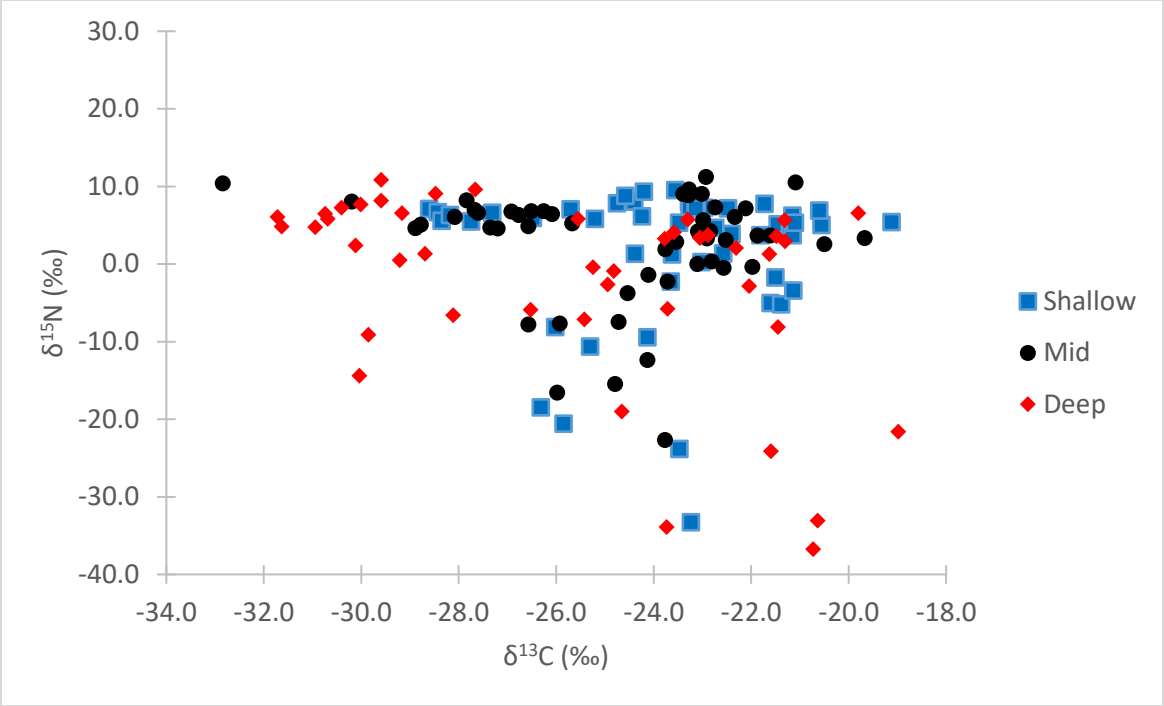

Figure 1.3*: POM stable isotope values sampled from bottom water in 2016.*

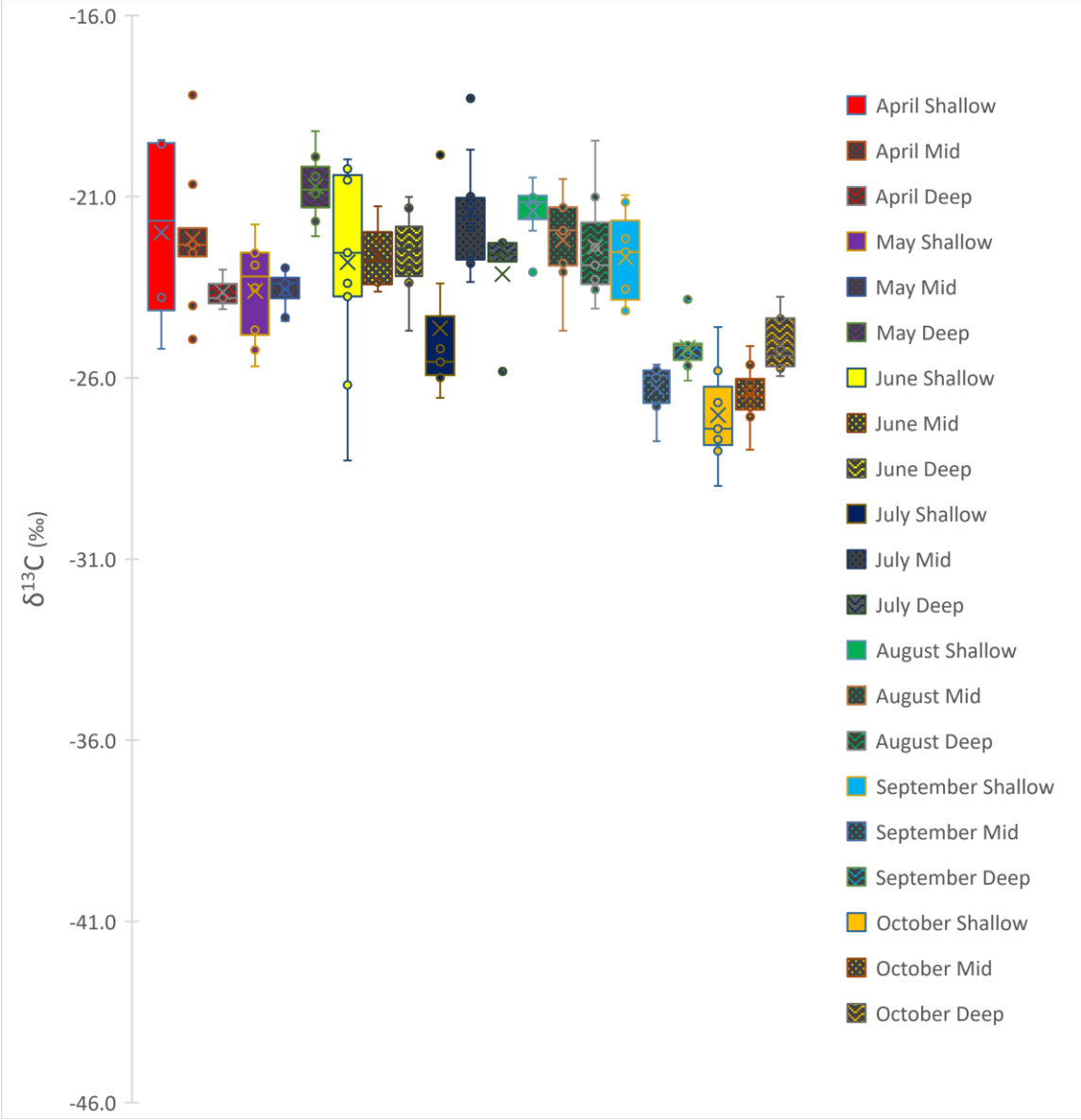


Figure 1.4: *Plot showing the $\delta^{13}C$ values of the POM collected from the surface water in 2016.*

Each color indicates the sampling month while each shading indicates each depth strata. Error bars are in standard deviation.

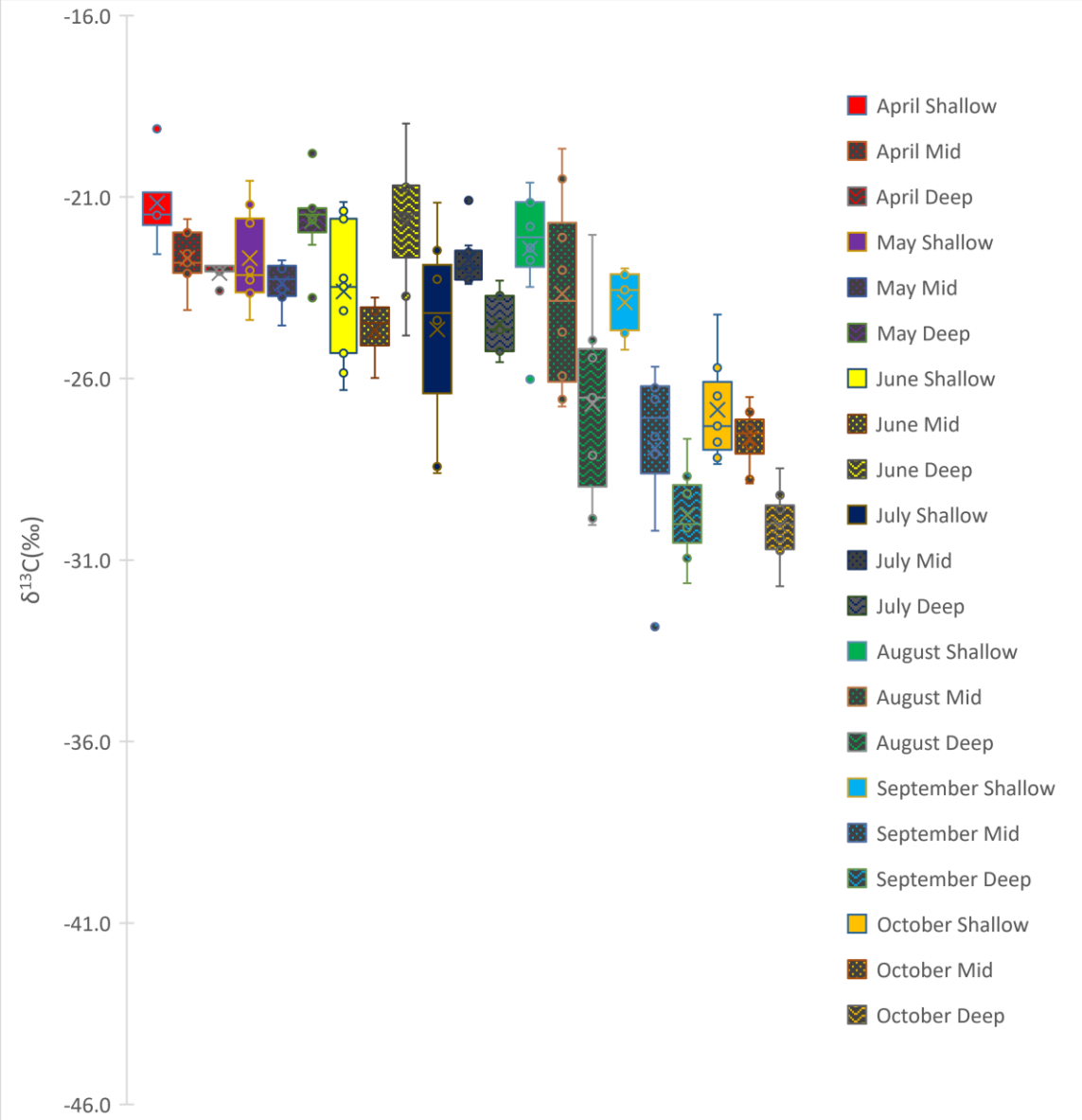


Figure 1.5: *Plot showing the $\delta^{13}C$ values of the POM collected from the bottom water during 2017.*

Each color indicates the sampling month while each shading indicates each depth strata. Error bars are in standard deviation.

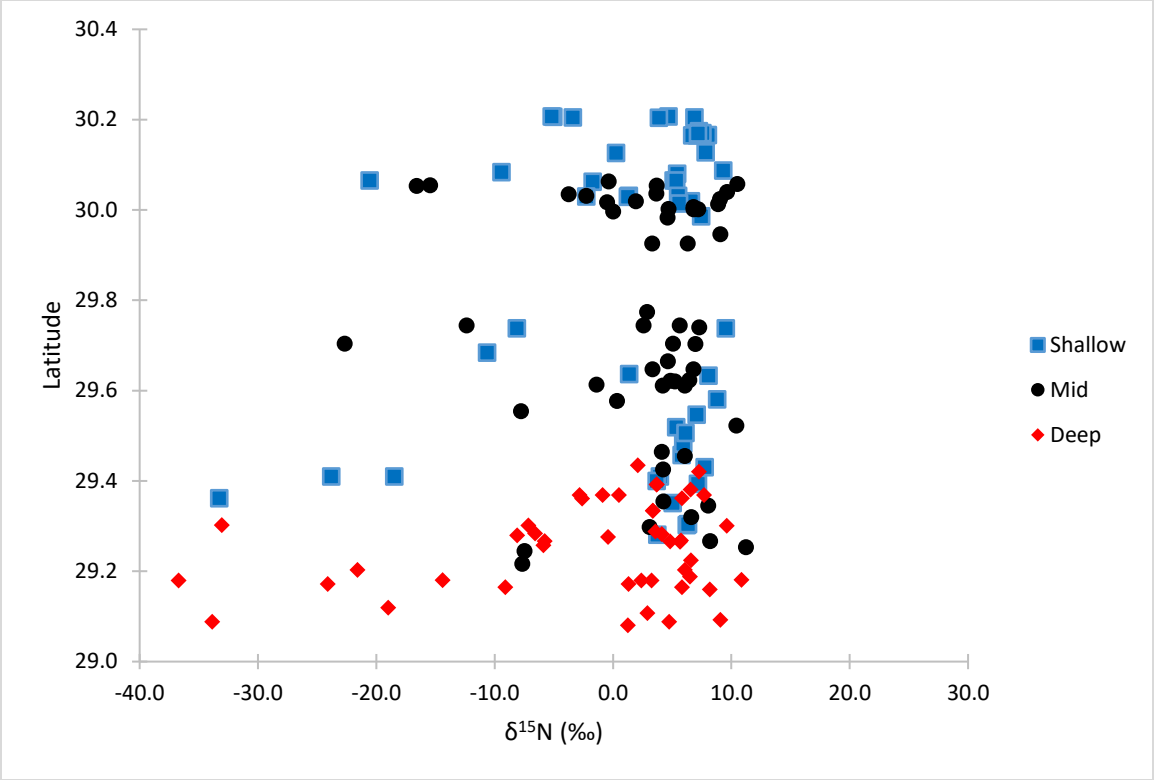


Figure 1.6: *Plot showing the $\delta^{15}N$ values of the POM collected from the bottom water at each depth strata during 2016 by sampling latitude.*

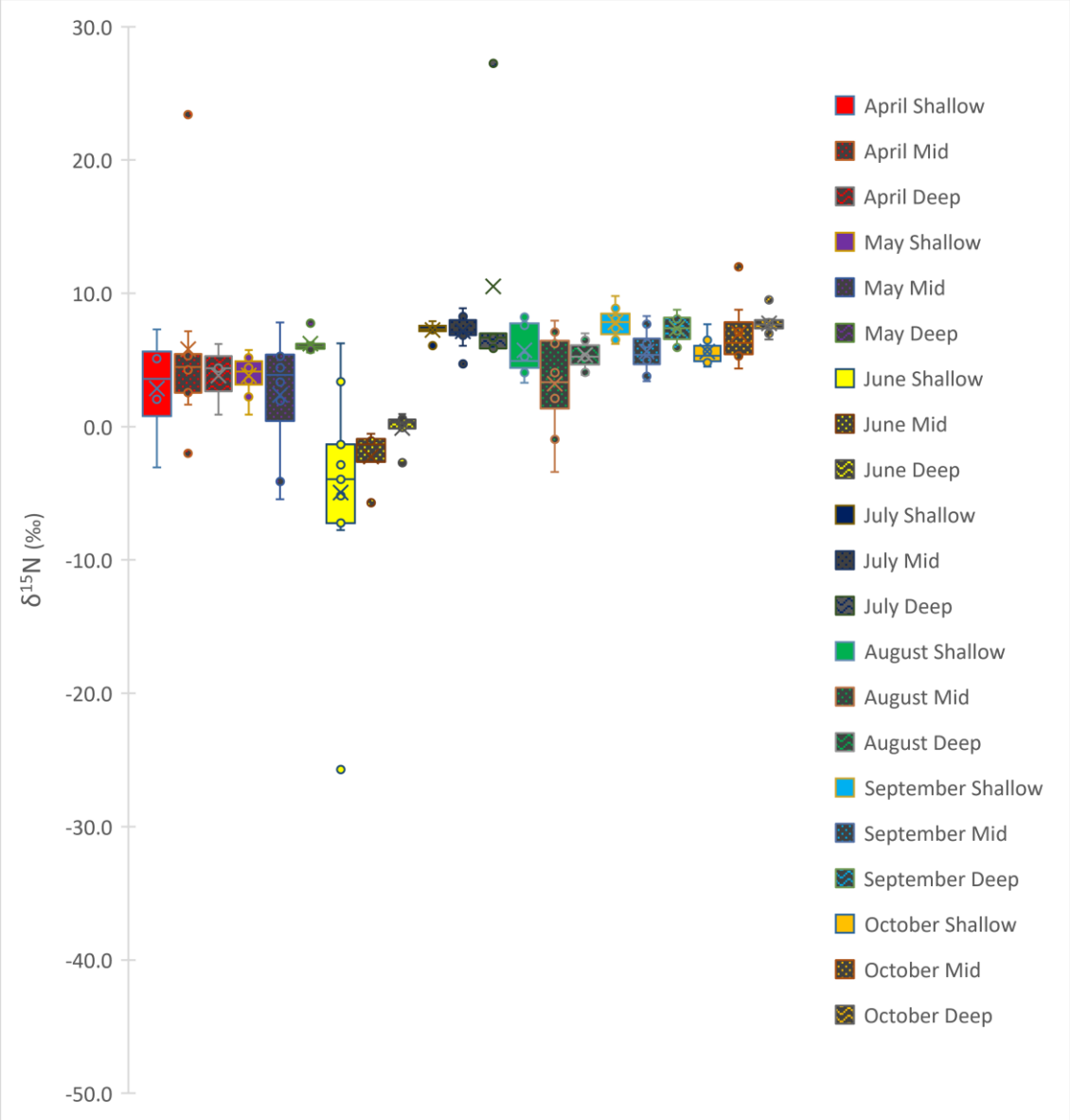


Figure 1.7: *Plot showing the $\delta^{15}N$ values of the POM collected from the surface water during 2016.*

Each color indicates the sampling month while each shading indicates each depth strata. Error bars are in standard deviation.

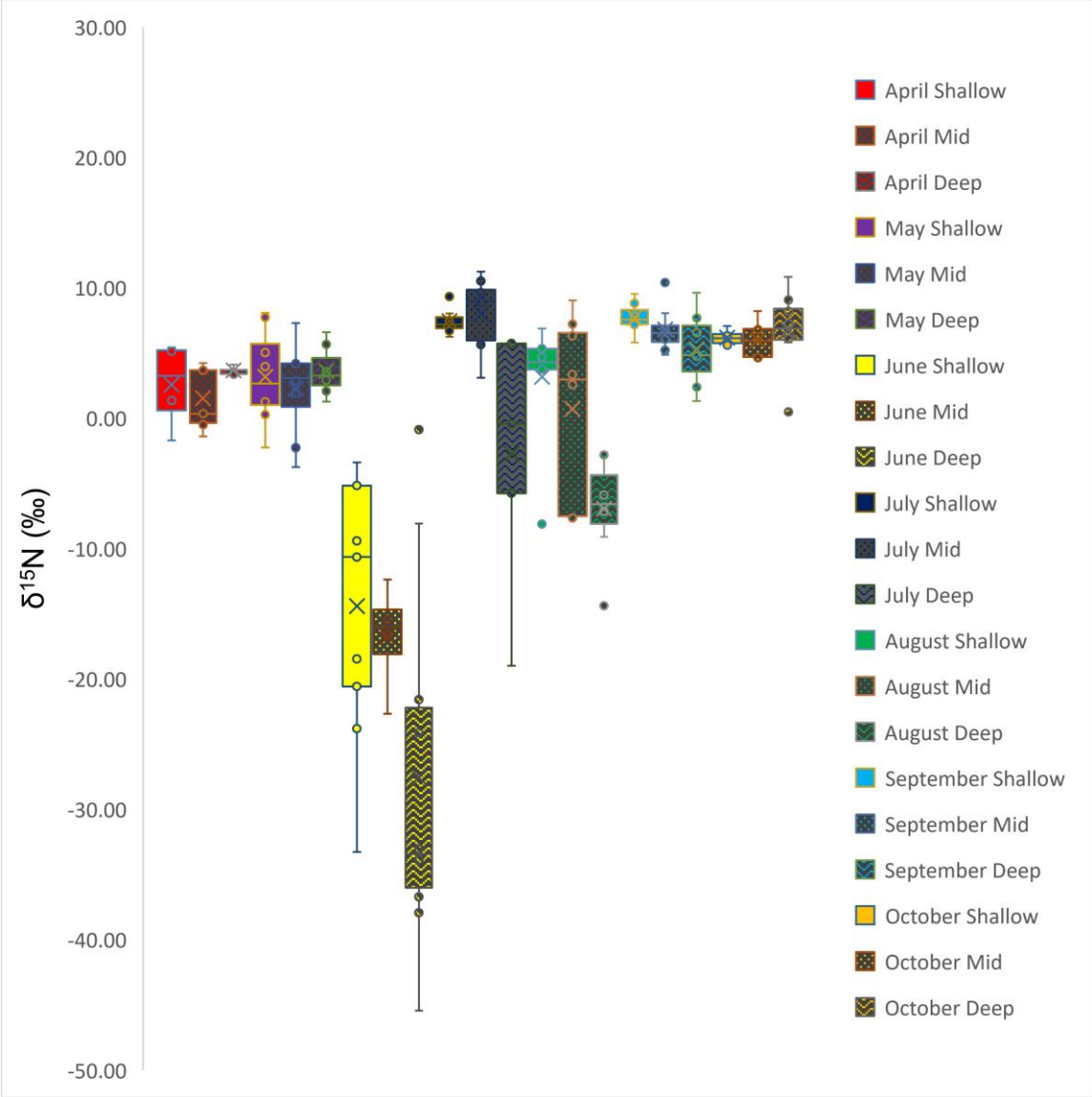


Figure 1.8: *Plot showing the $\delta^{15}N$ values of the POM collected from the bottom water during 2017.*

Each color indicates the sampling month while each shading indicates each depth strata. Error bars are in standard deviation.

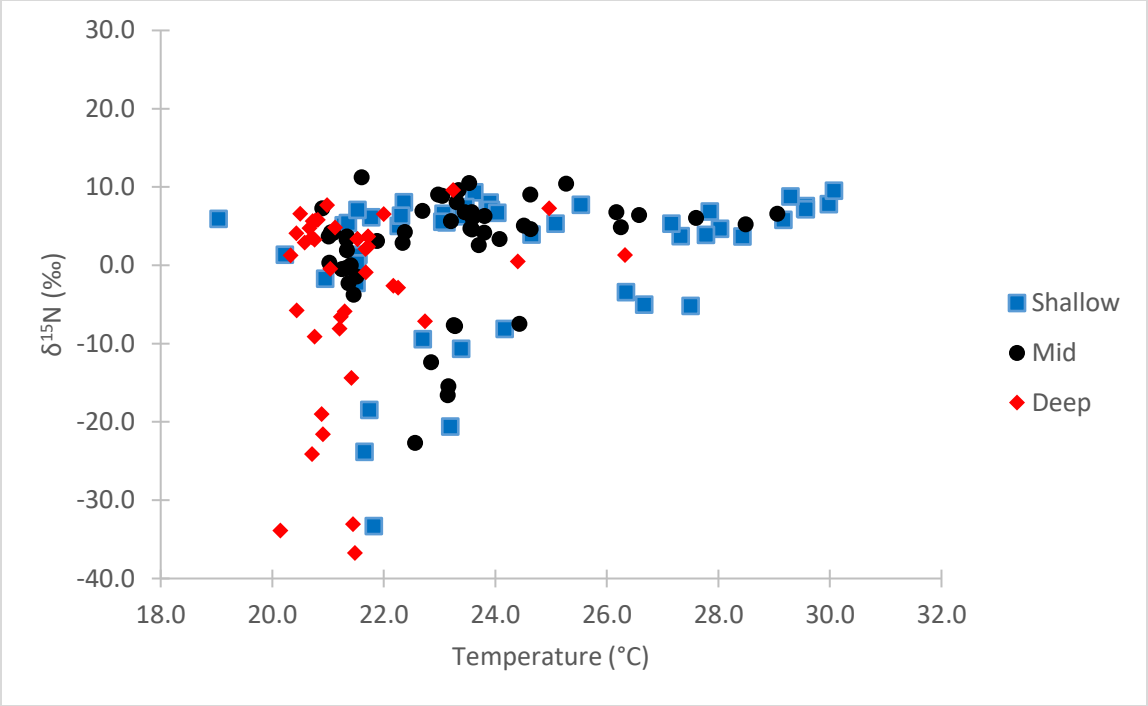


Figure 1.9: *$\delta^{15}N$ values of POM collected from 2016 bottom water versus water temperature at depth.*

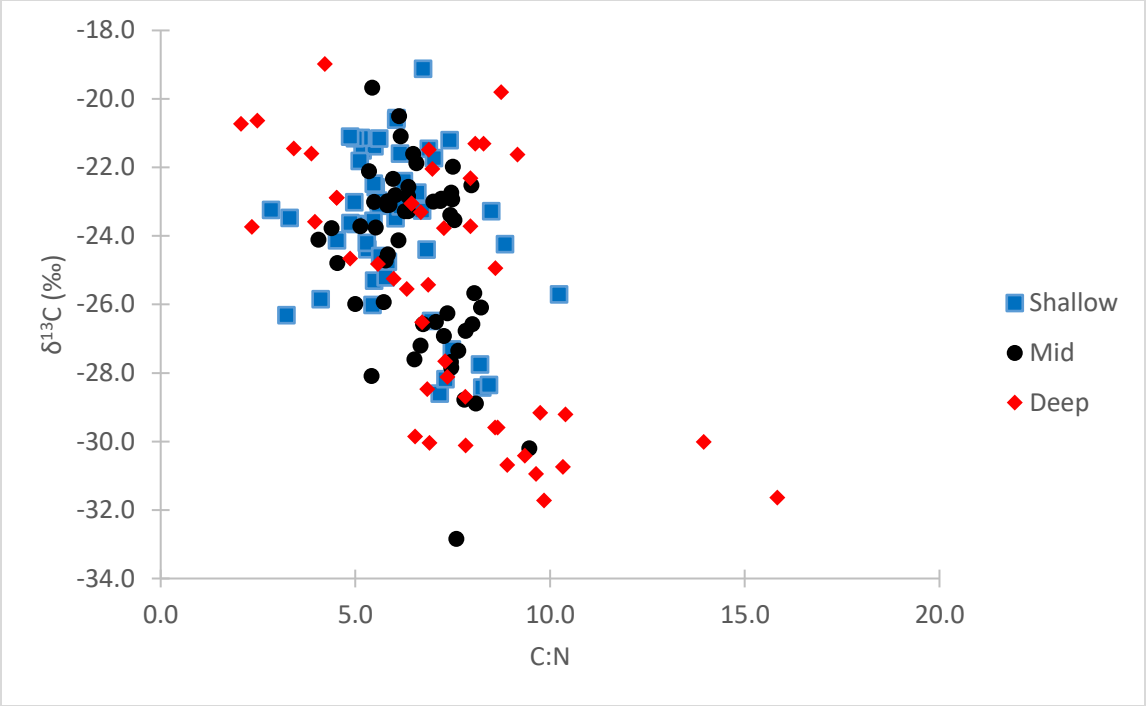


Figure 1.10*: Bi-plot showing POM $\delta^{13}C$ values collected from 2016 bottom water samples against the C:N ratio of the POM.*

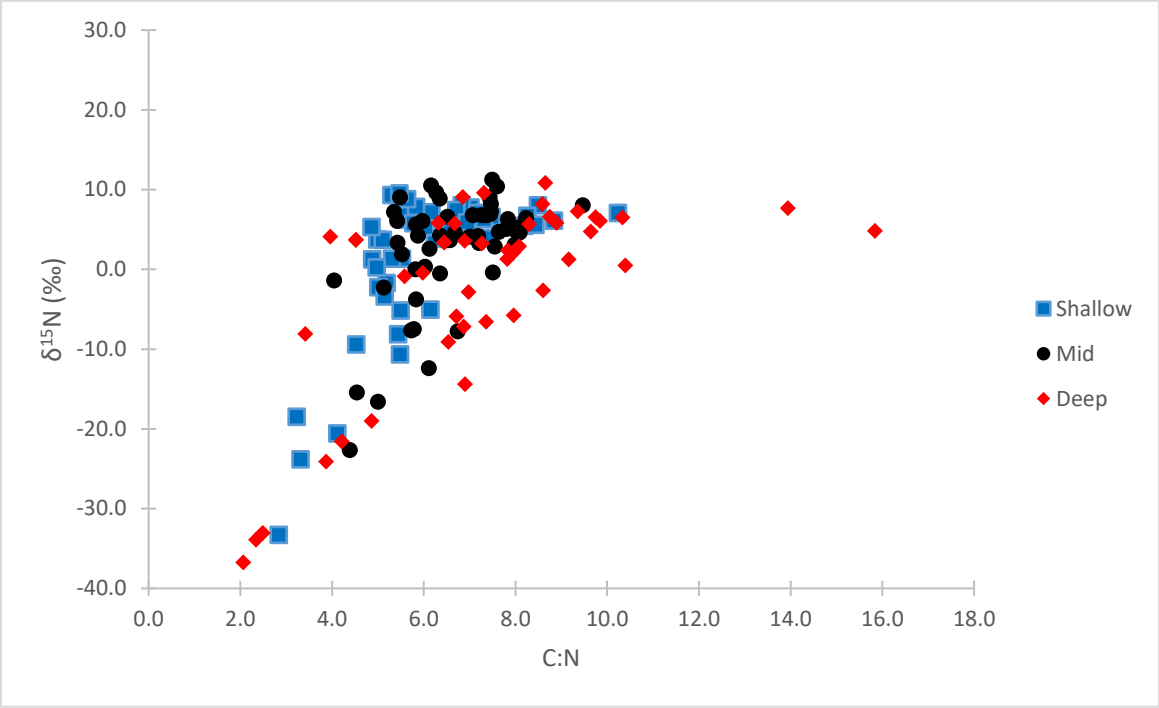


Figure 1.11*: Bi-plot showing POM $\delta^{15}N$ values collected from 2016 bottom water samples against the C:N ratio of the POM.*

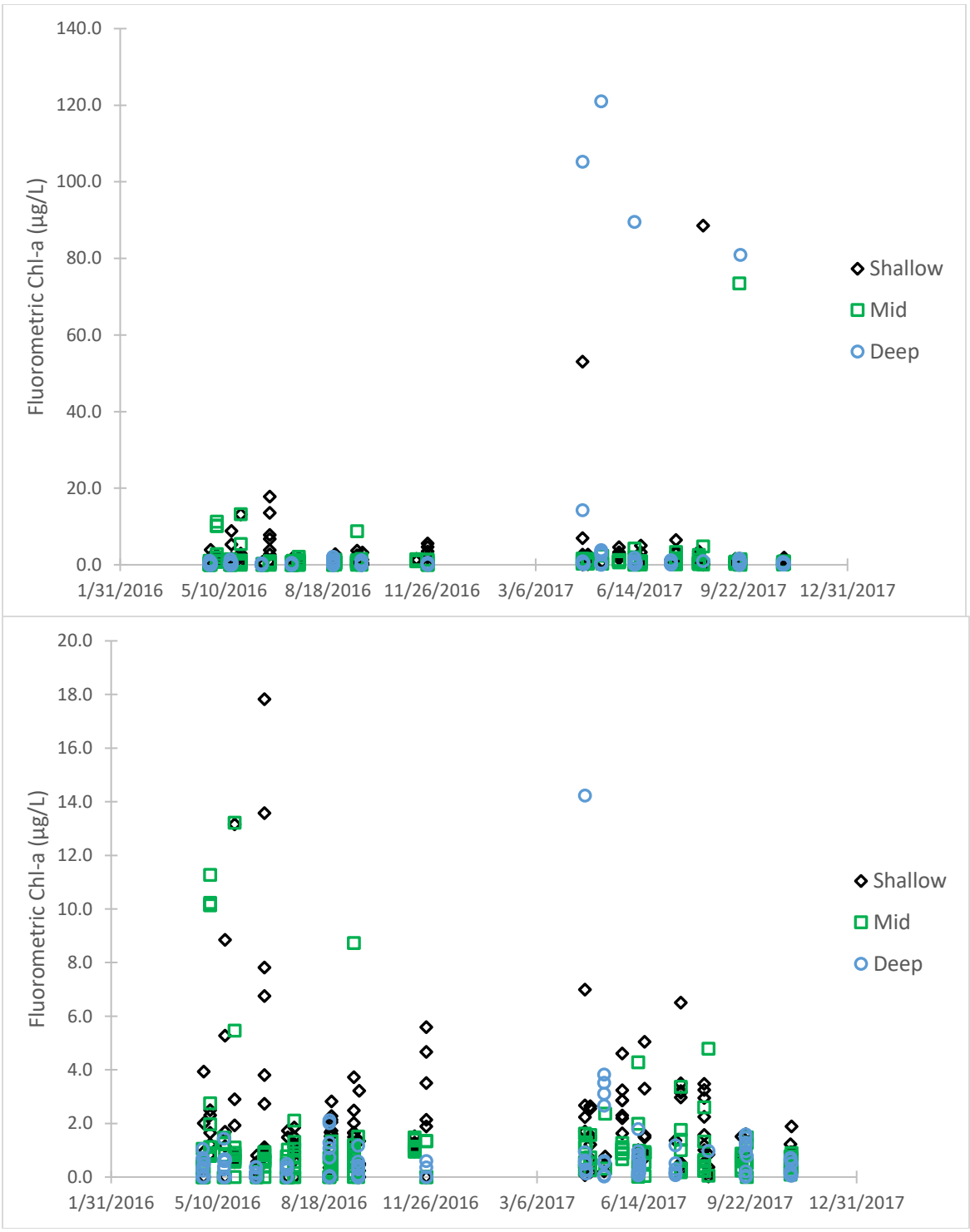


Figure 1.12*: Bi-plots showing the Chl-a values at each station based on sampling date and depth strata.*

The bottom figure is a narrower Chl-a range to show monthly variability without the larger values from 2017. The top figure shows the full Chl-a range.

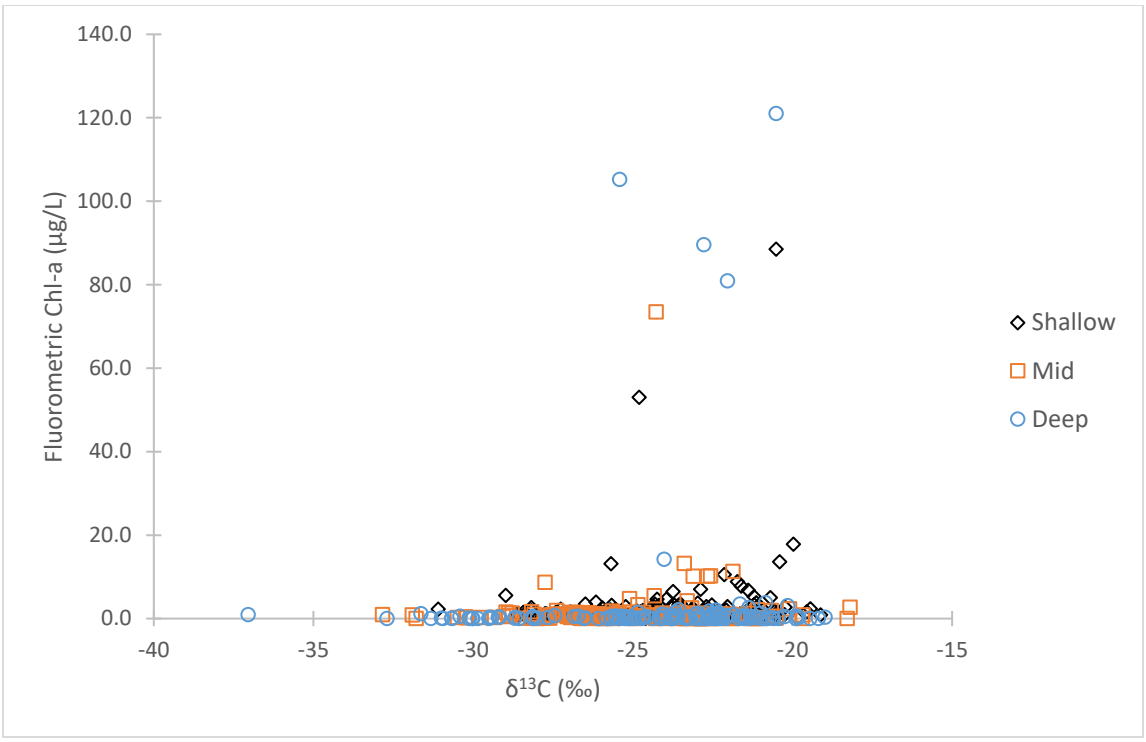


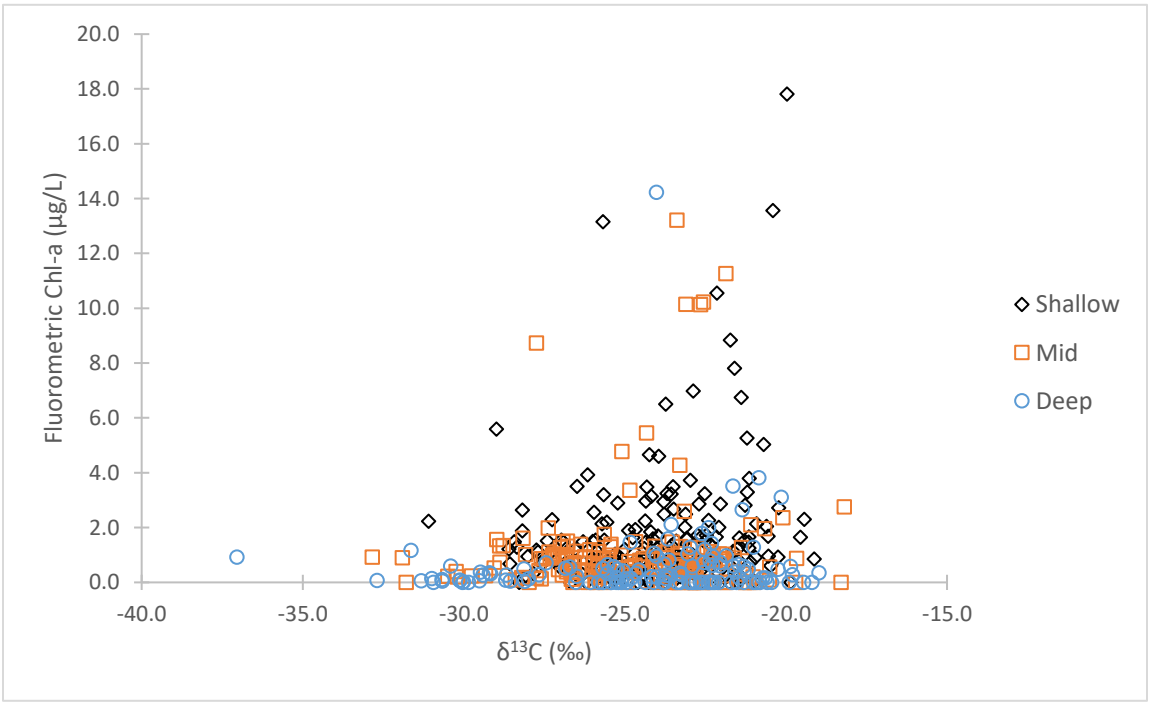


Figure 1.13: *Bi-plots showing the Chl-a values at each station based on depth strata and $\delta^{13}C$ values.*

The bottom figure is a narrower Chl-a range to show monthly variability without the larger values from 2017. The top figure shows the full Chl-a range.

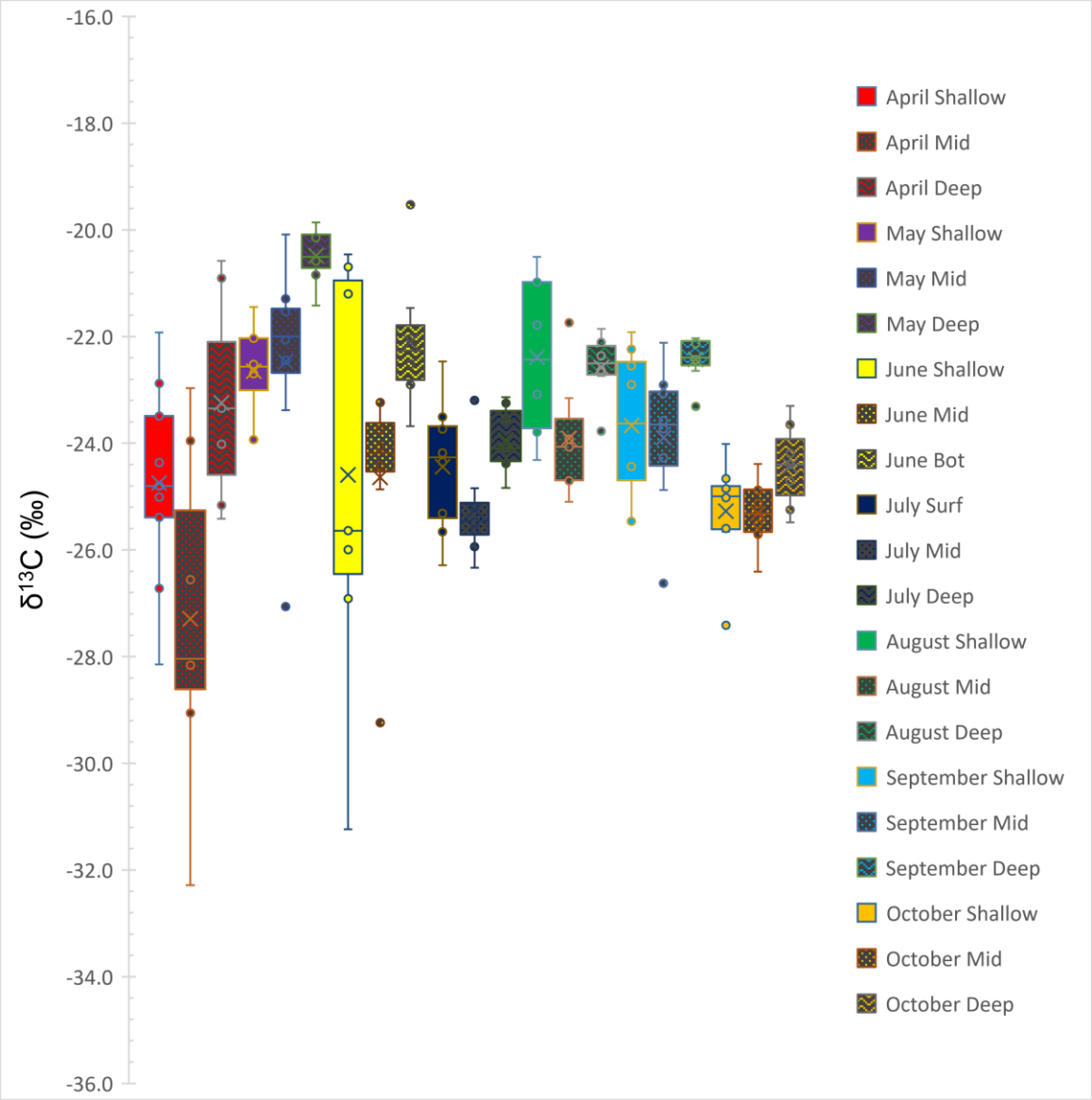


Figure 1.14: *Plot showing the $\delta^{13}C$ values of the POM collected from the surface water during 2017.*

Each color indicates the sampling month while each shading indicates each depth strata. Error bars are in standard deviation.

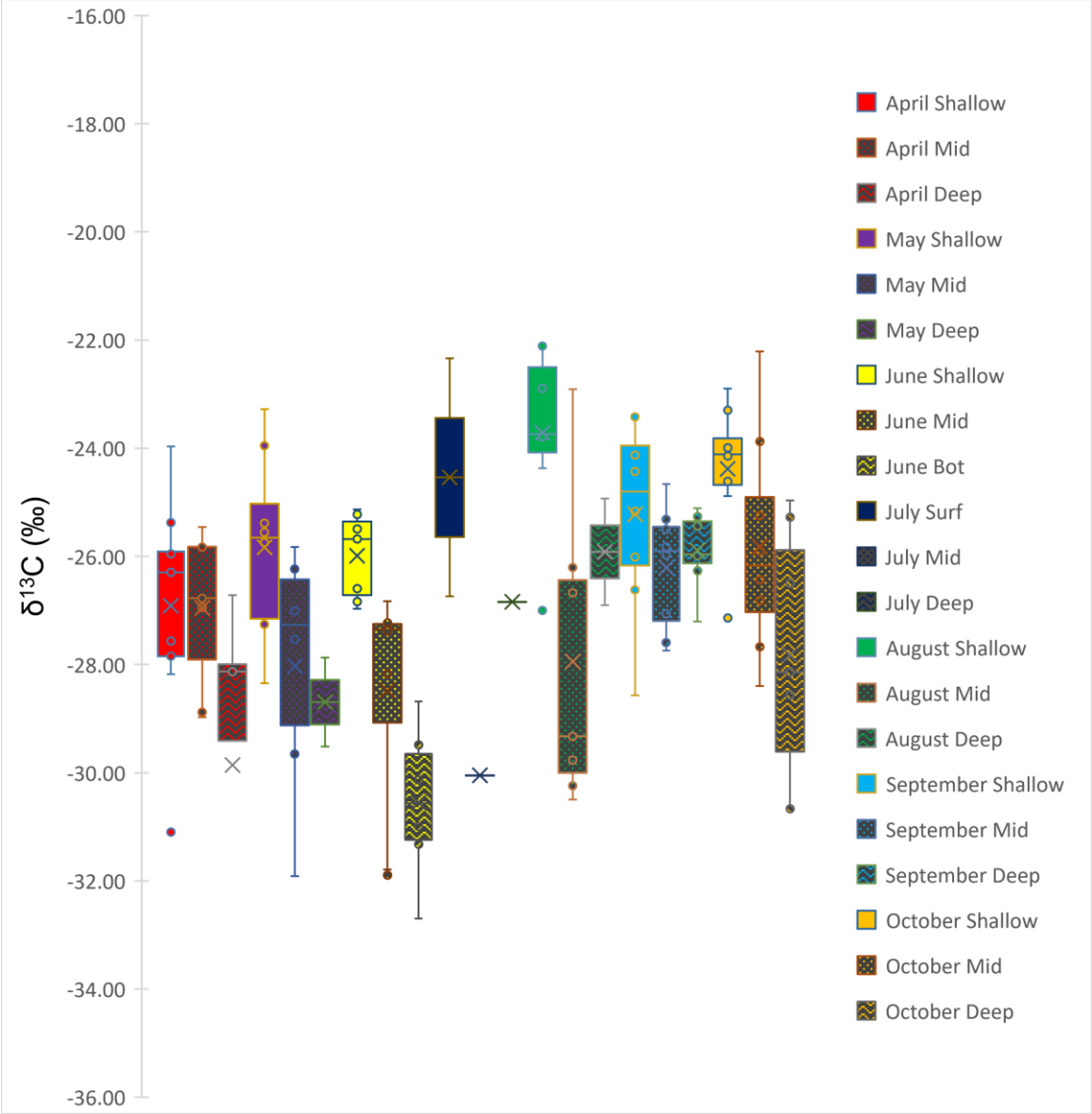


Figure 1.15: *Plot showing the $\delta^{13}C$ values of the POM collected from the bottom water during 2017.*

Each color indicates the sampling month while each shading indicates each depth strata. Error bars are in standard deviation.

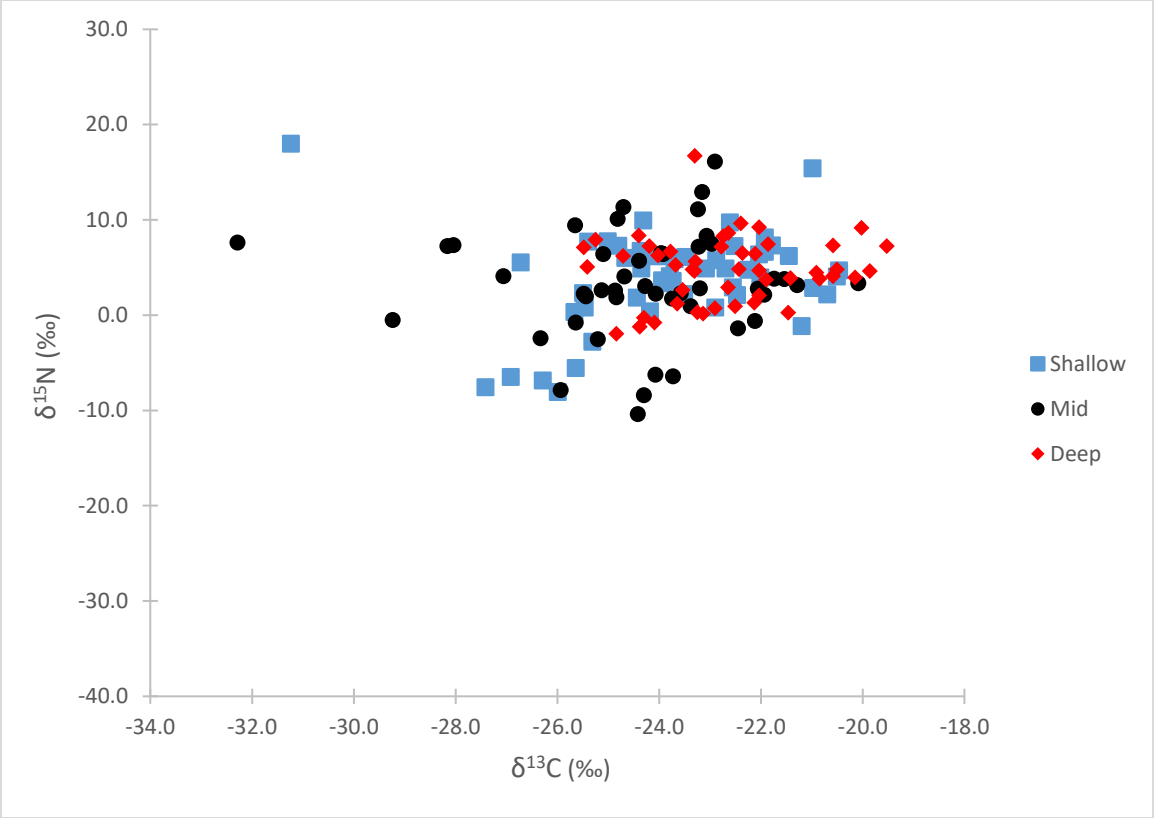


Figure 1.16: *POM stable isotope values sampled from surface water in 2017.*

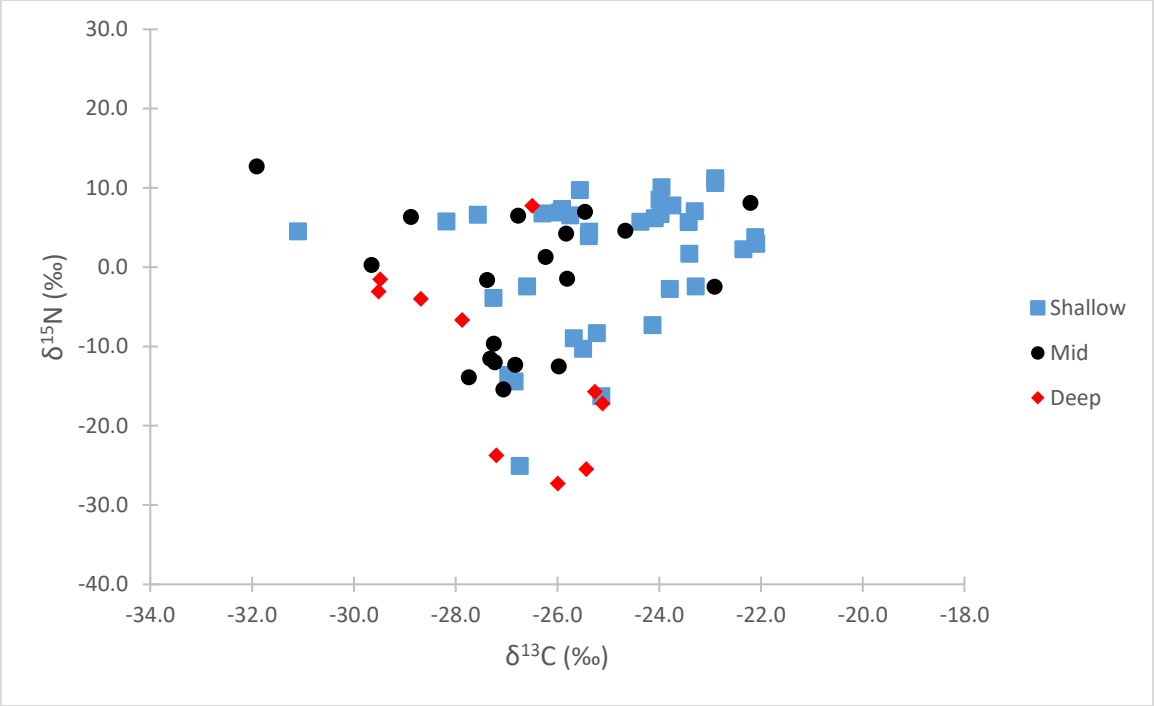


Figure 1.19: *POM stable isotope values sampled from bottom water in 2017.*

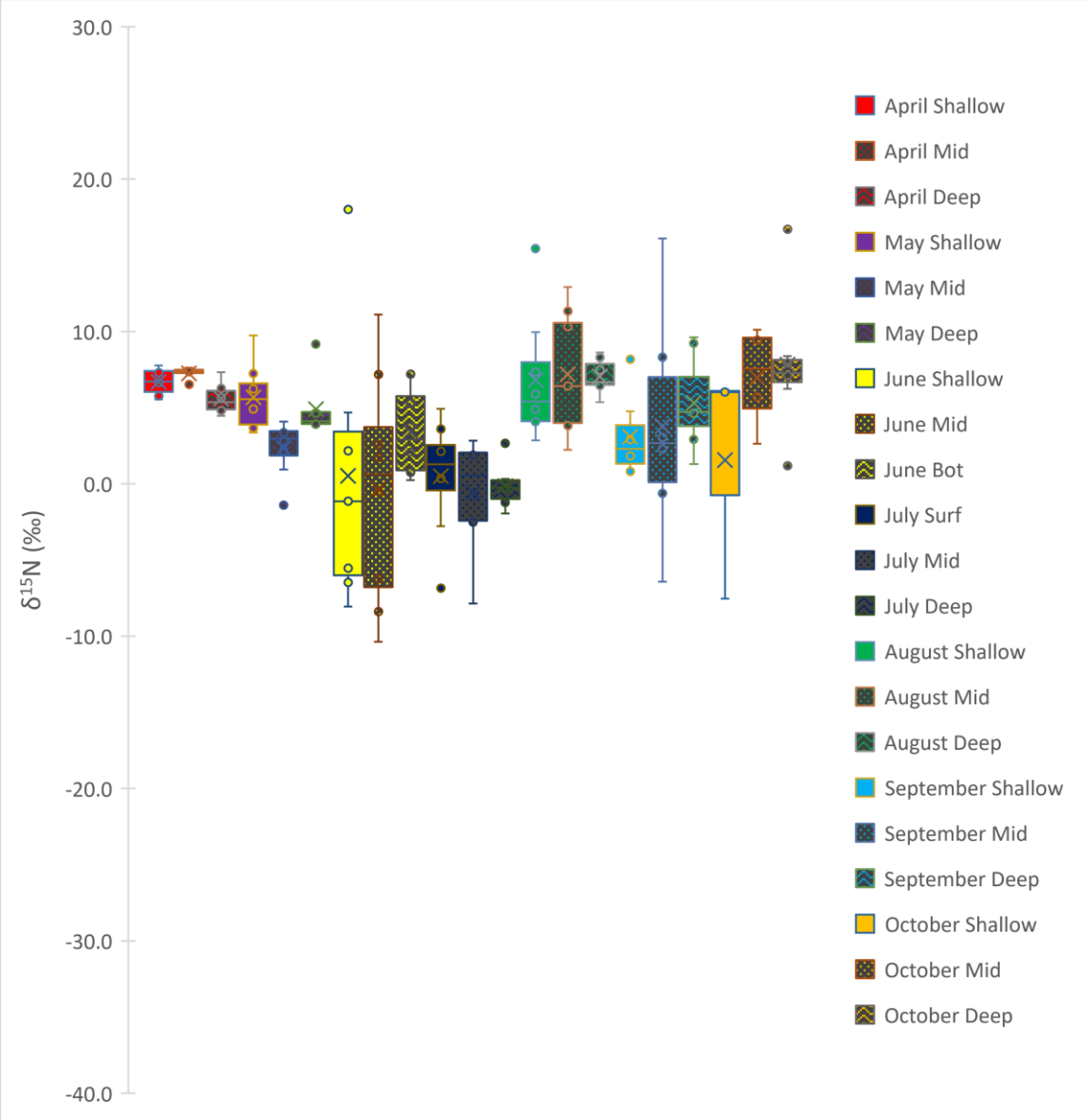


Figure 1.17*: Plot showing the $\delta^{15}N$ values of the POM collected from the surface water during 2017.*

Each color indicates the sampling month while each shading indicates each depth strata. Error bars are in standard deviation.

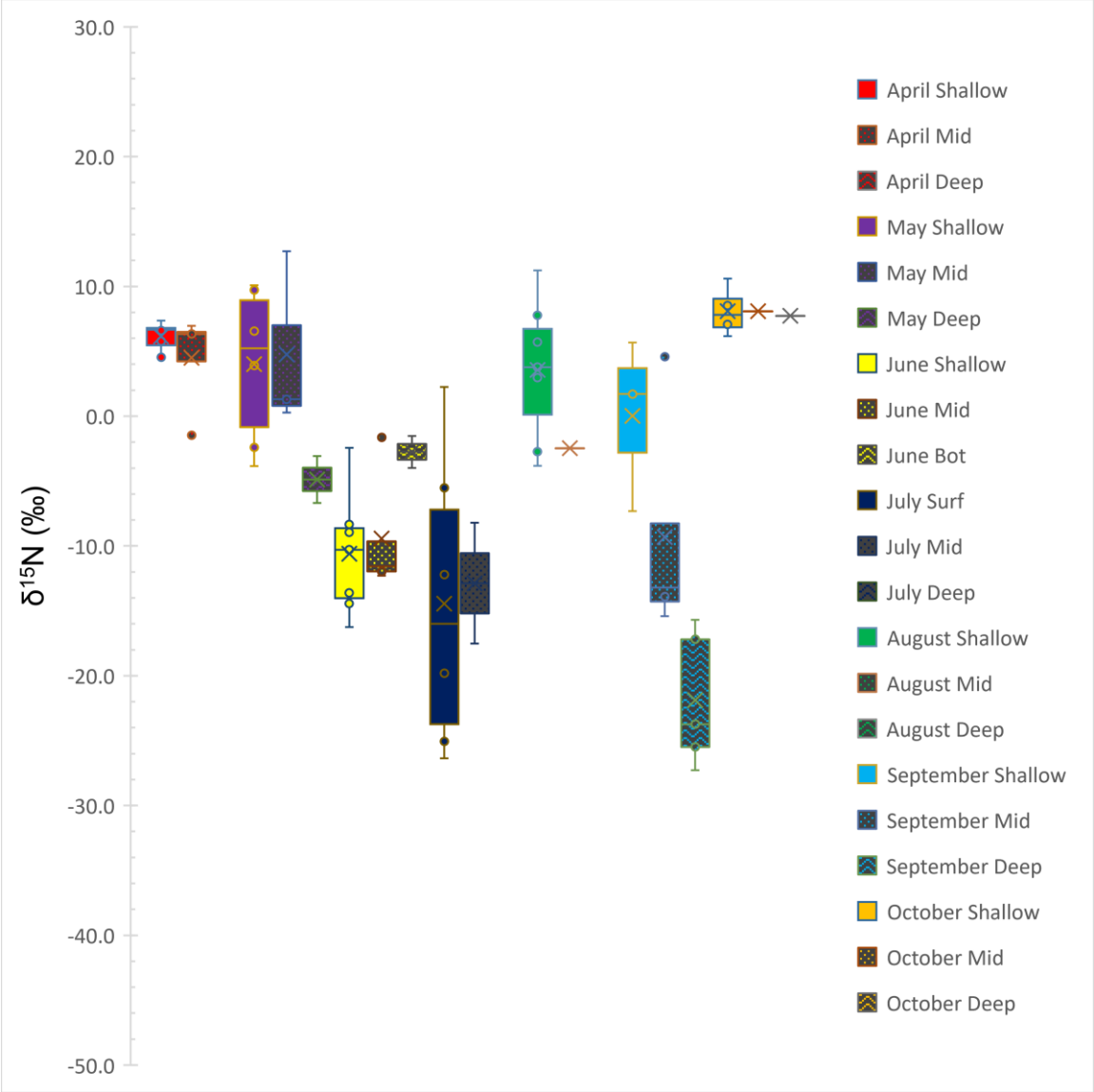


Figure 1.18*: Plot showing the $\delta^{15}N$ values of the POM collected from the bottom water during 2017.*

Each color indicates the sampling month while each shading indicates each depth strata. Error bars are in standard deviation.

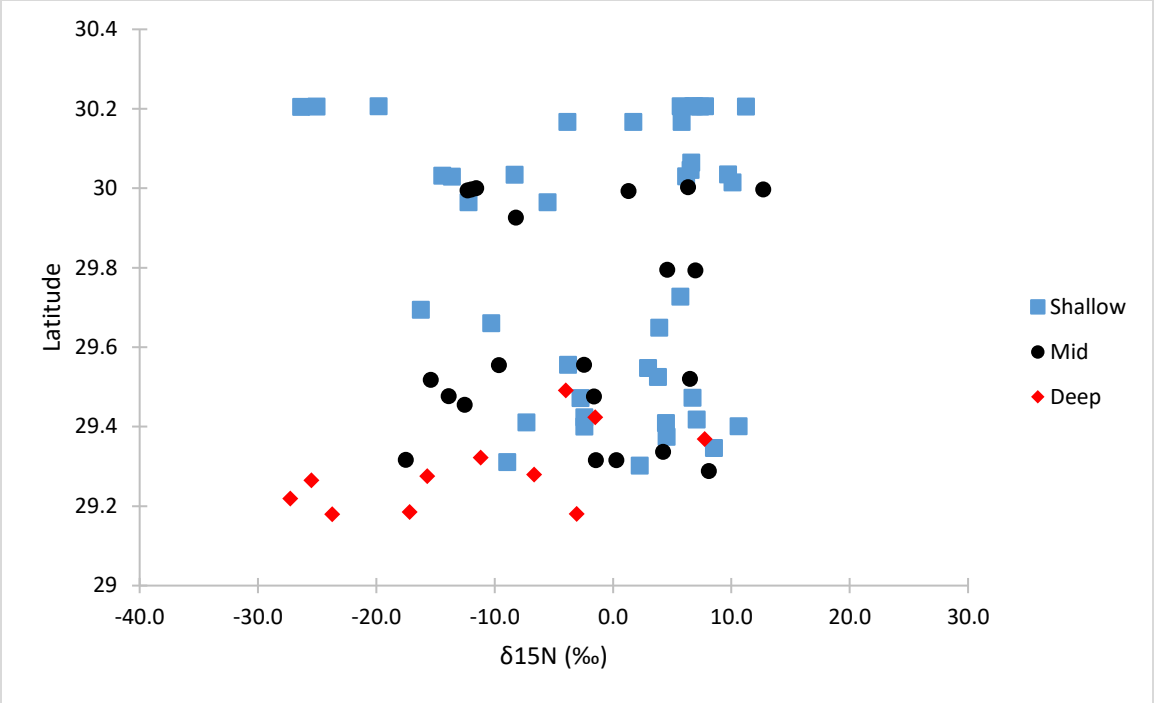


Figure 1.19*: Bi-plot showing the $\delta^{15}N$ values of POM collected from bottom water in 2017 against the sampling latitude.*

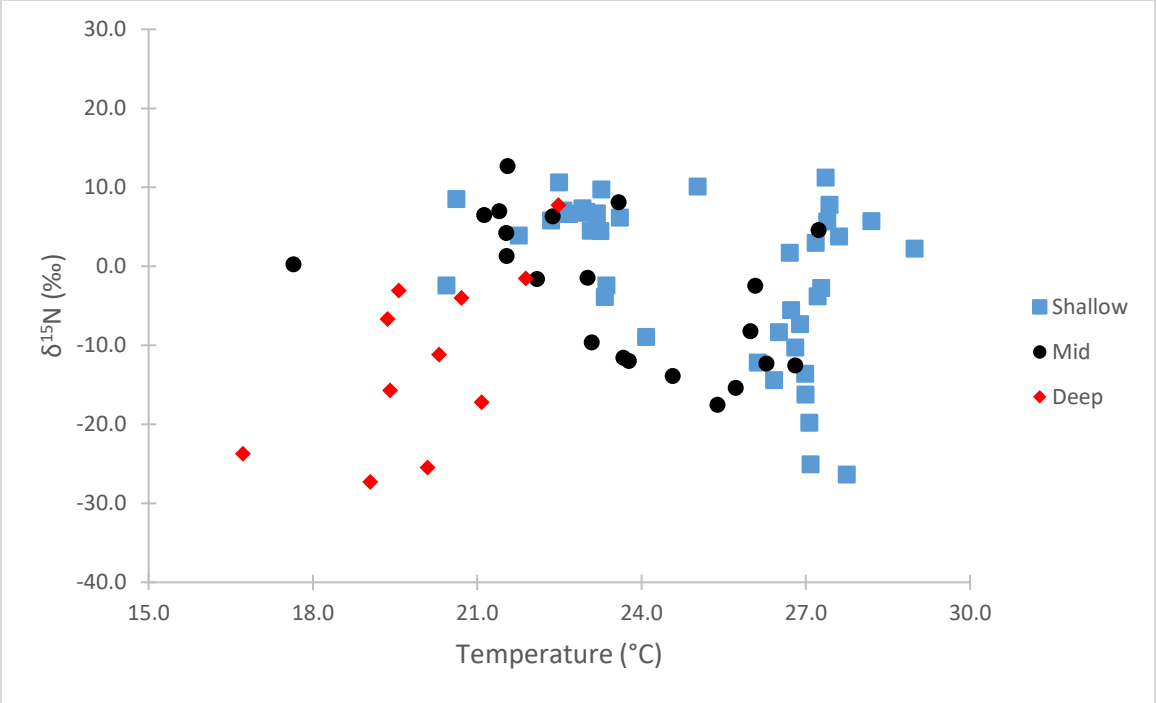


Figure 1.20*: Bi-plot showing the $\delta^{15}N$ values of POM collected from bottom water in 2017 against water temperature.*

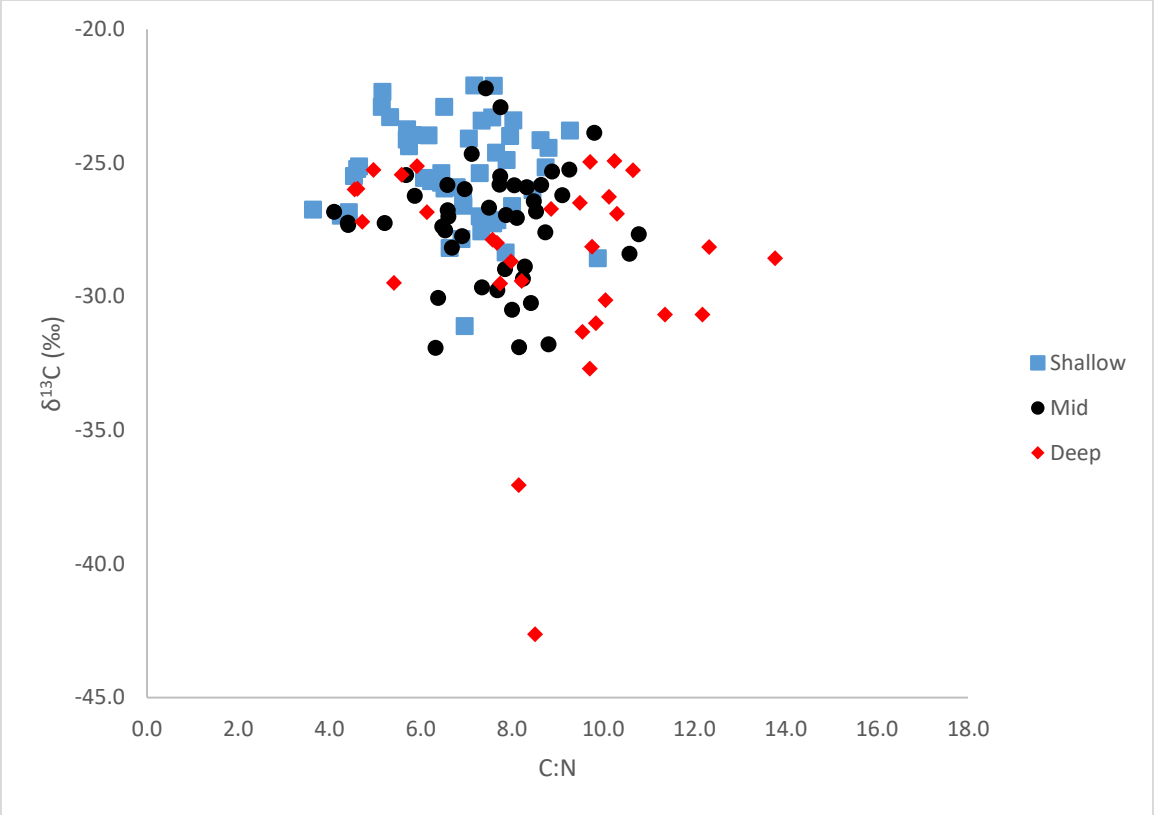


Figure 1.21: *Bi-plot showing the δ13C values of POM collected from bottom water in 2017 against the C:N ratio of the POM.*

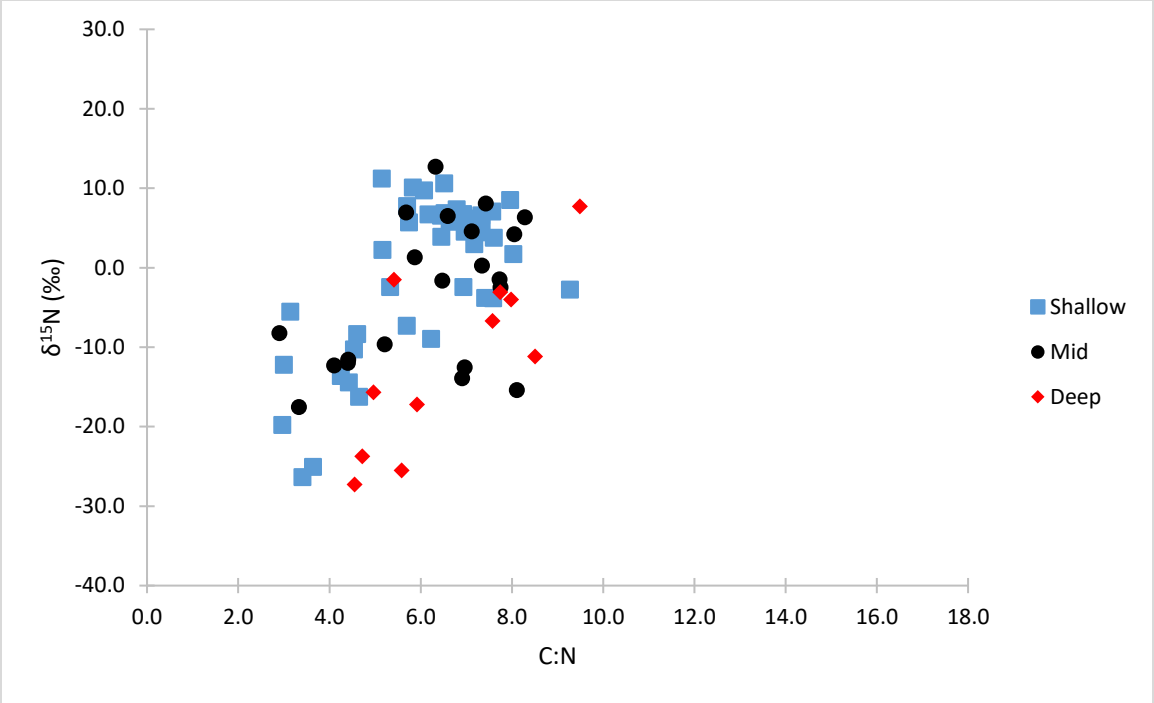


Figure 1.22: *Bi-plot showing the $\delta^{15}N$ values of POM collected from bottom water in 2017 against the C:N ratio of the POM.*

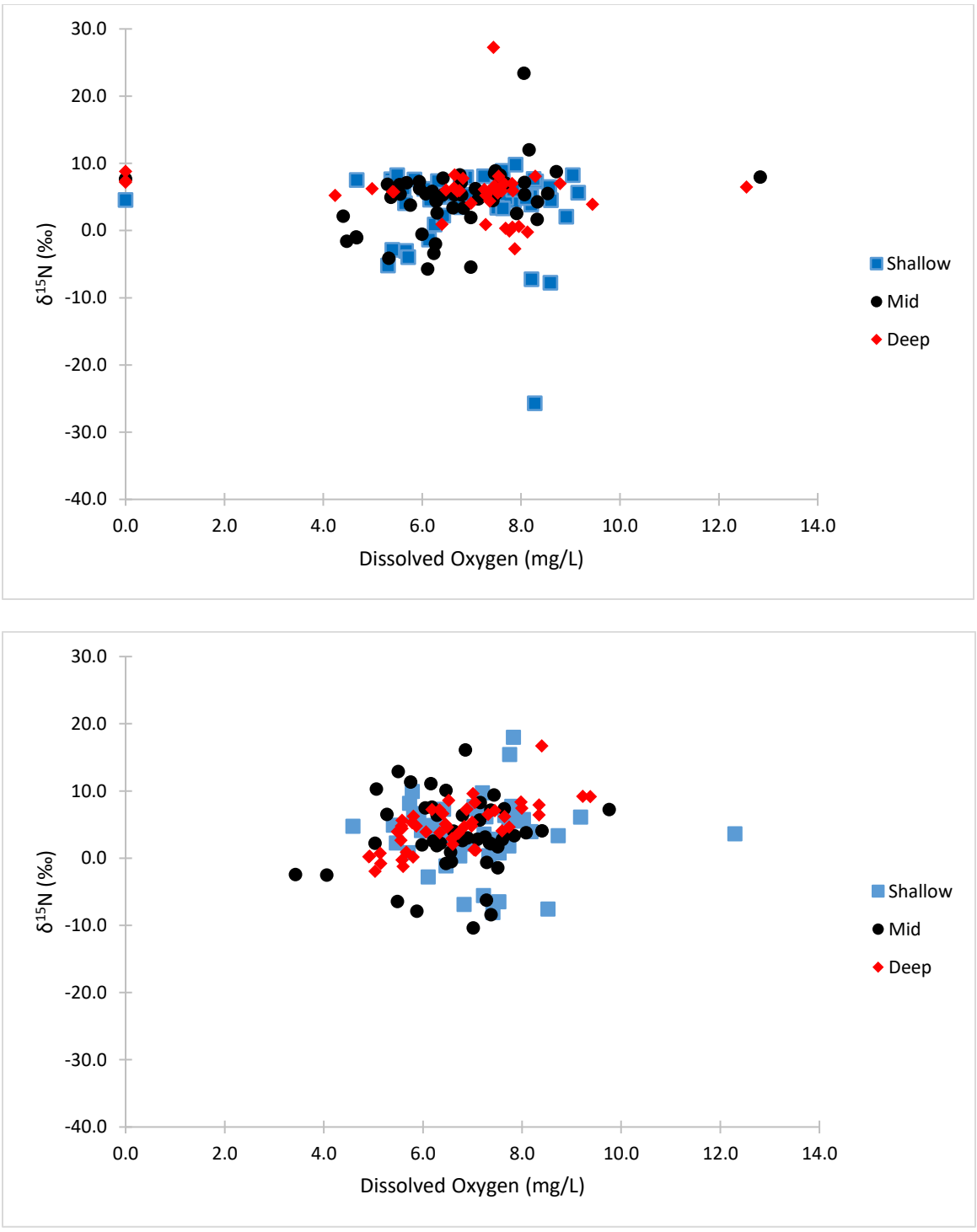


Figure 1.23: *Bi-plots showing the $\delta^{15}N$ values of POM collected from surface water in 2016 (Top) and 2017 (Bottom) against the dissolved oxygen content of the surface water.*

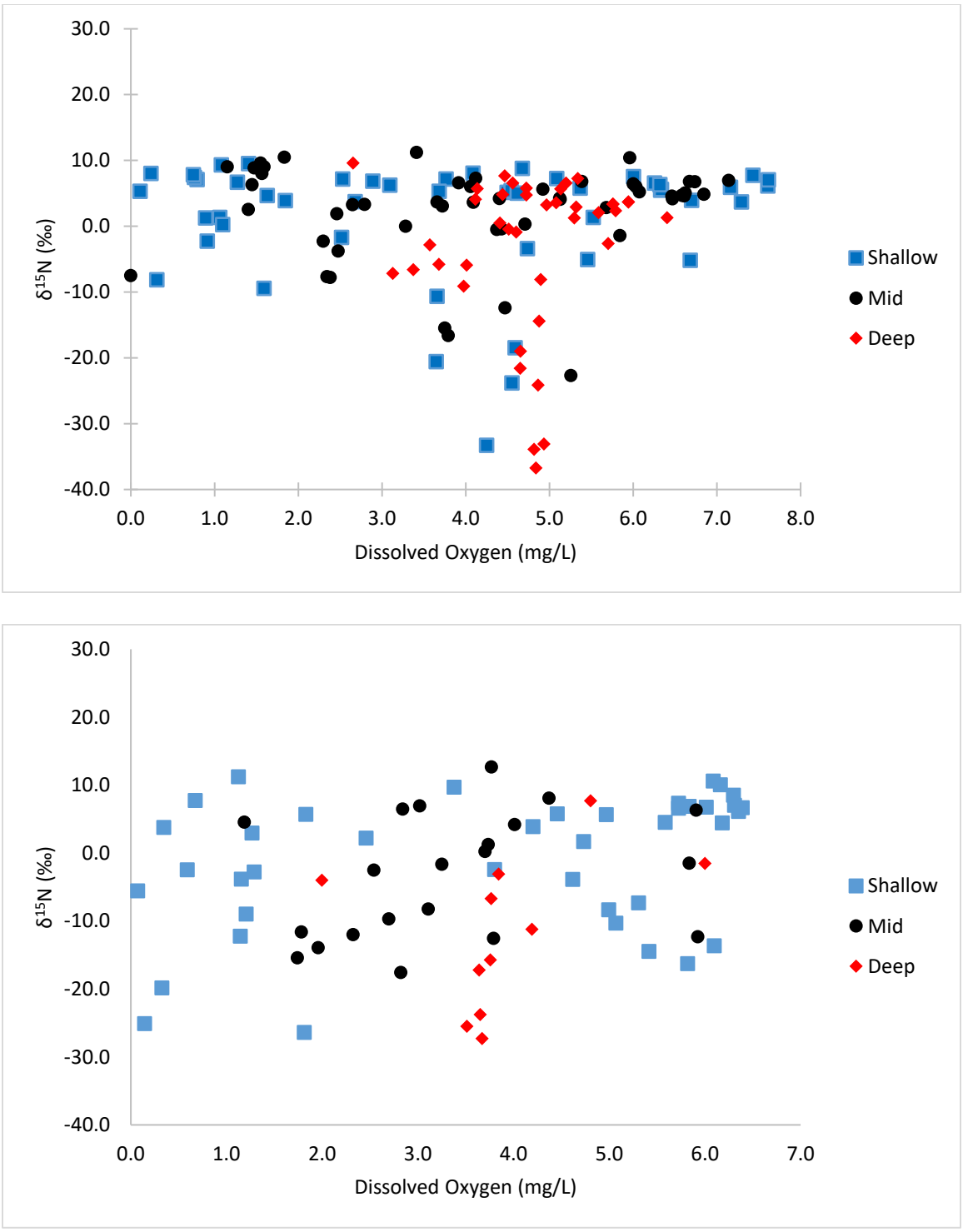


Figure 1.24: *Bi-plots showing the $\delta^{15}N$ values of POM collected from bottom water in 2016 (Top) and 2017 (Bottom) against the dissolved oxygen content of the bottom water.*

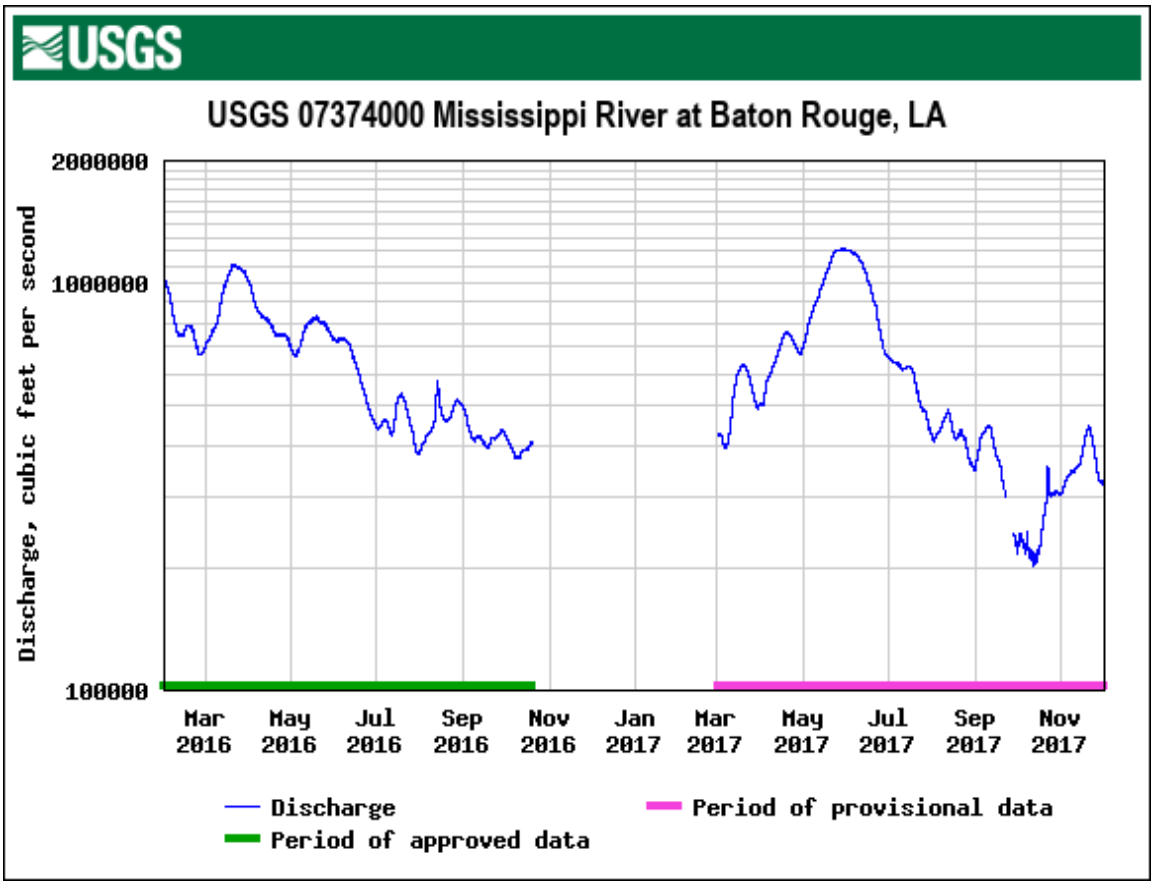


Figure 1.25*: Mississippi River discharge data collected by USGS for 2016 and 2017.*

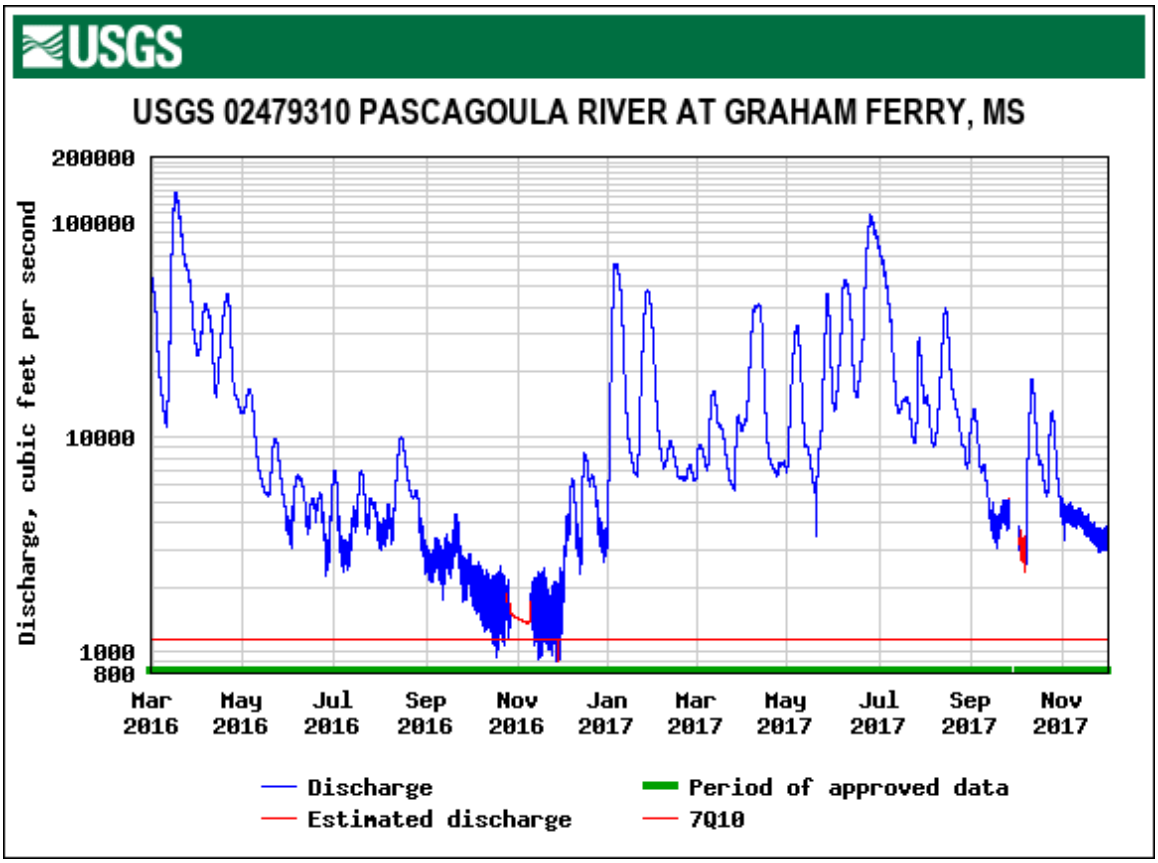


Figure 1.26*: Pascagoula River discharge data collected by USGS for 2016 and 2017.*

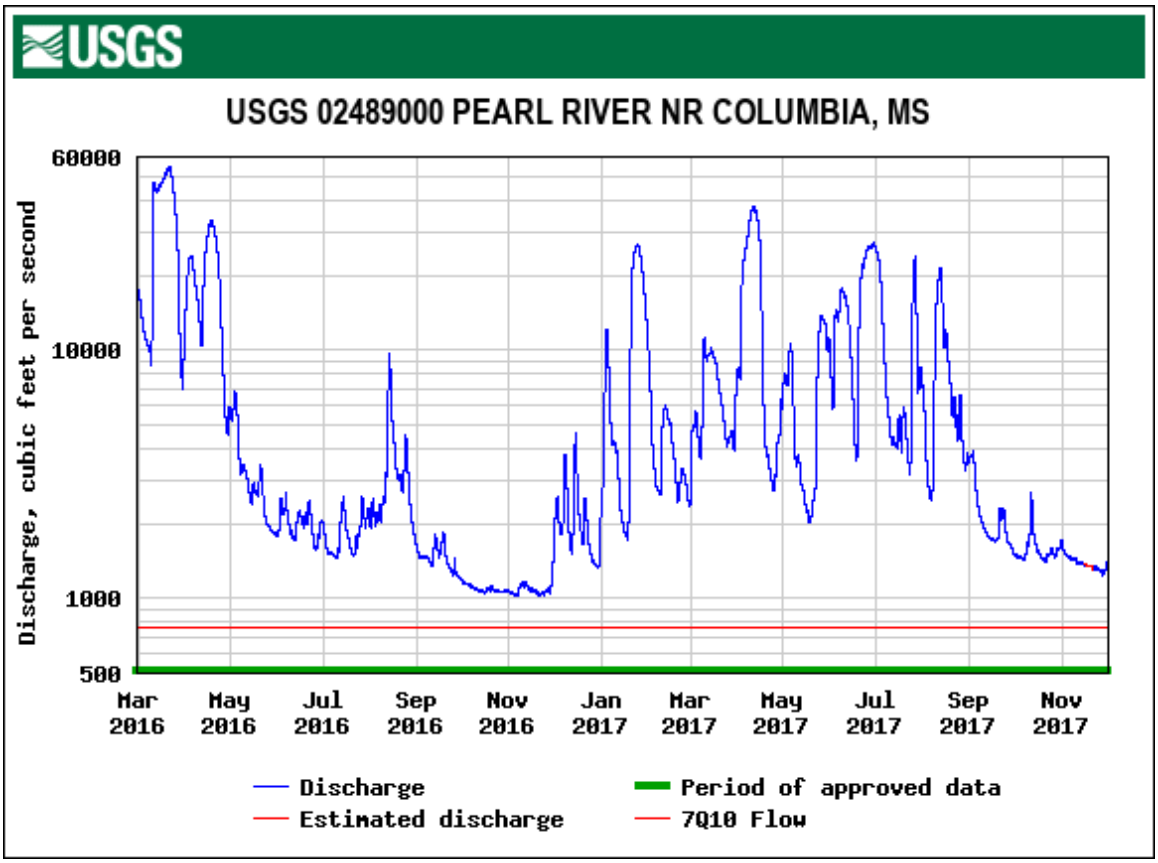


Figure 1.27: *Pearl River discharge data collected by USGS for 2016 and 2017.*

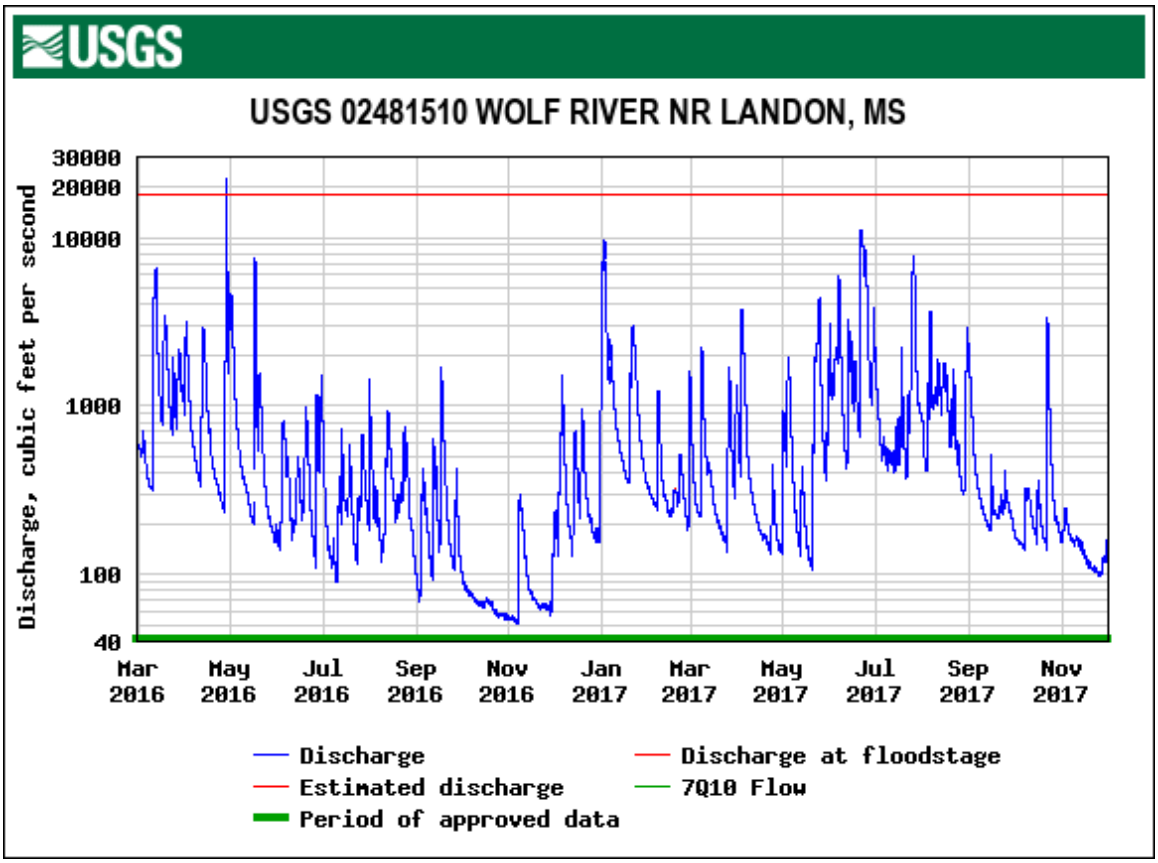

Figure 1.28: *Wolf River discharge data collected by USGS for 2016 and 2017.*

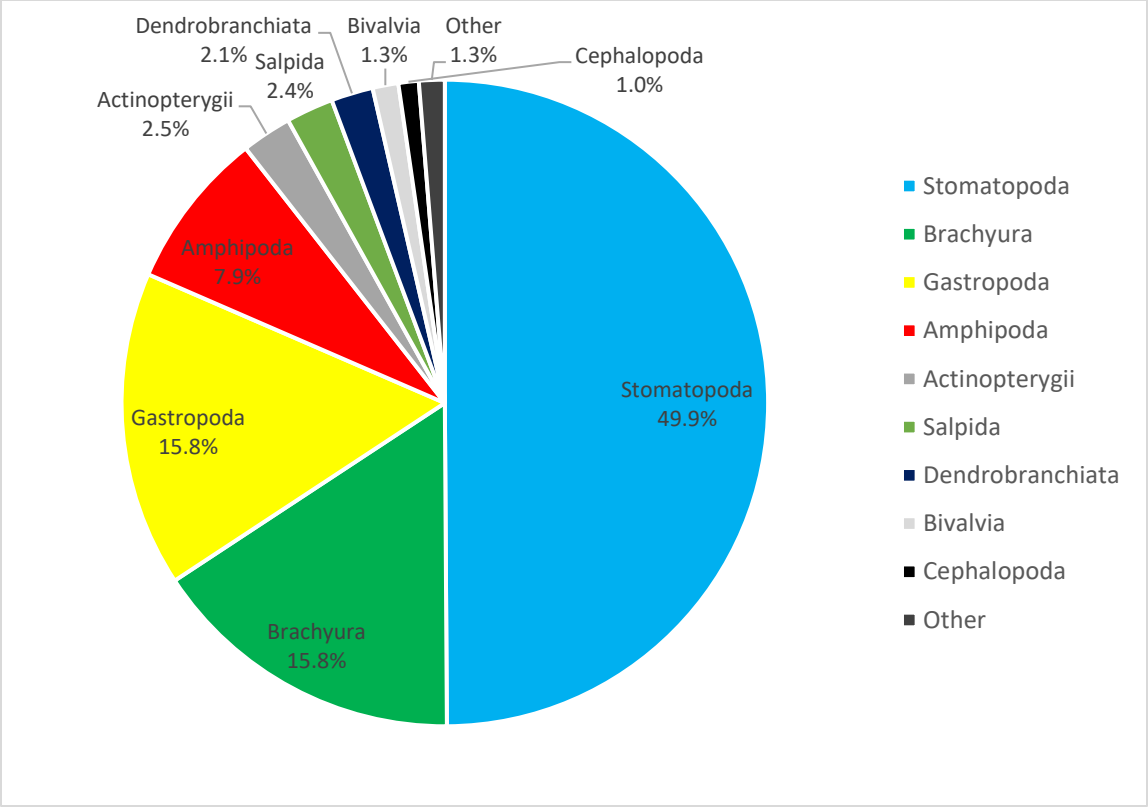


Figure 2.1*: 2016 stomach content analysis results based upon visual identification and DNA barcoding.*

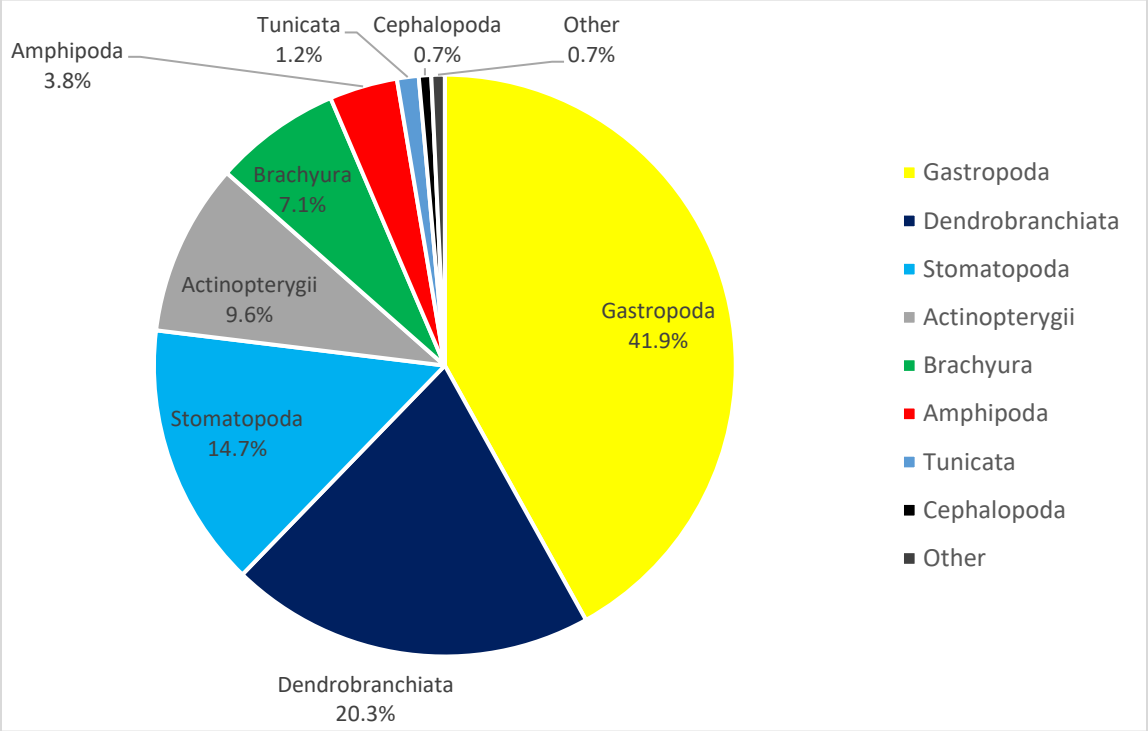


Figure 2.2: *2017 stomach content analysis results based upon visual identification and DNA barcoding.*

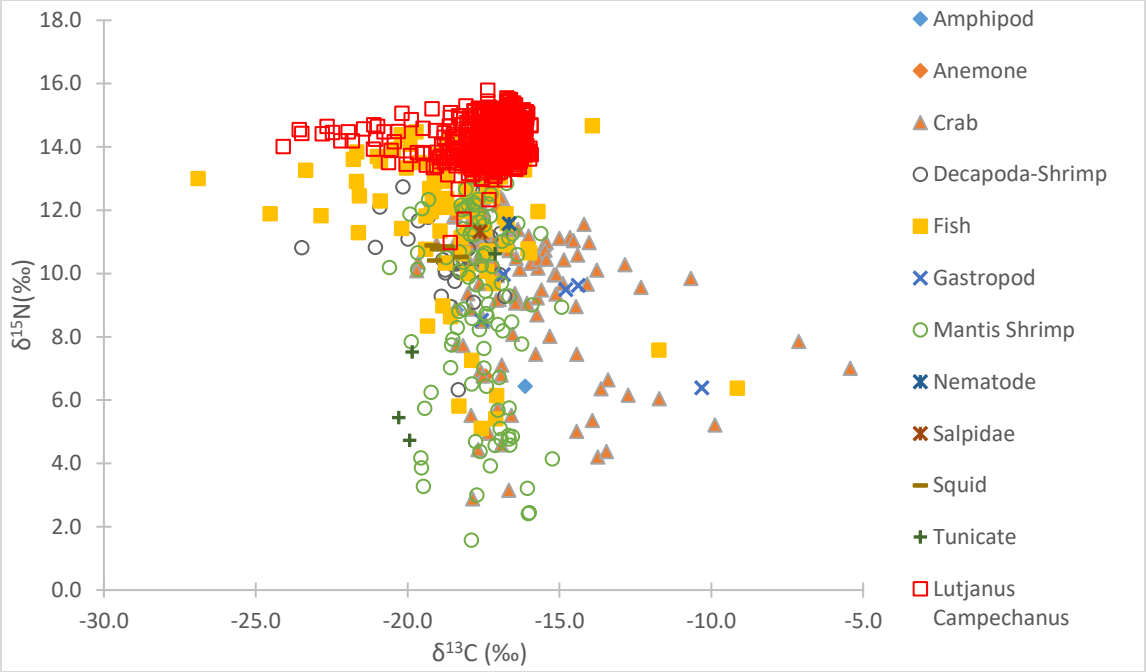


Figure 2.3: *All broad prey items in isotope space along with the predatory red snapper.*

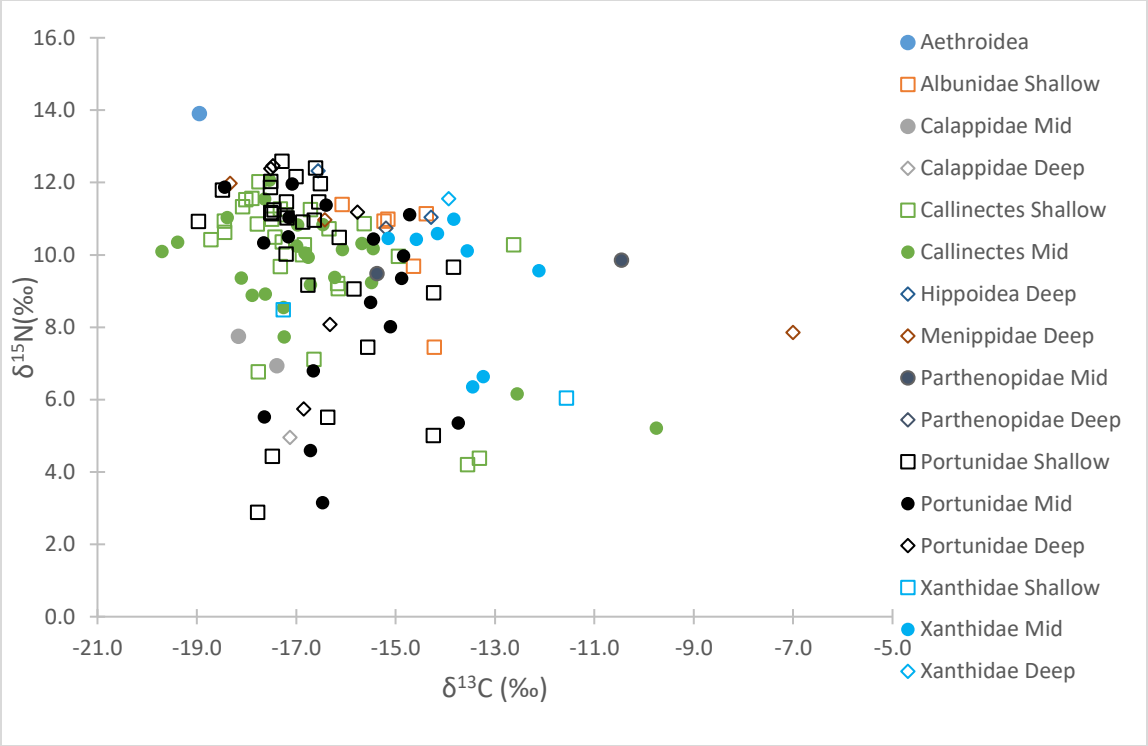


Figure 2.4: *All the Brachyura prey items from 2016 and 2017 in isotope space based upon depth strata sampled.*

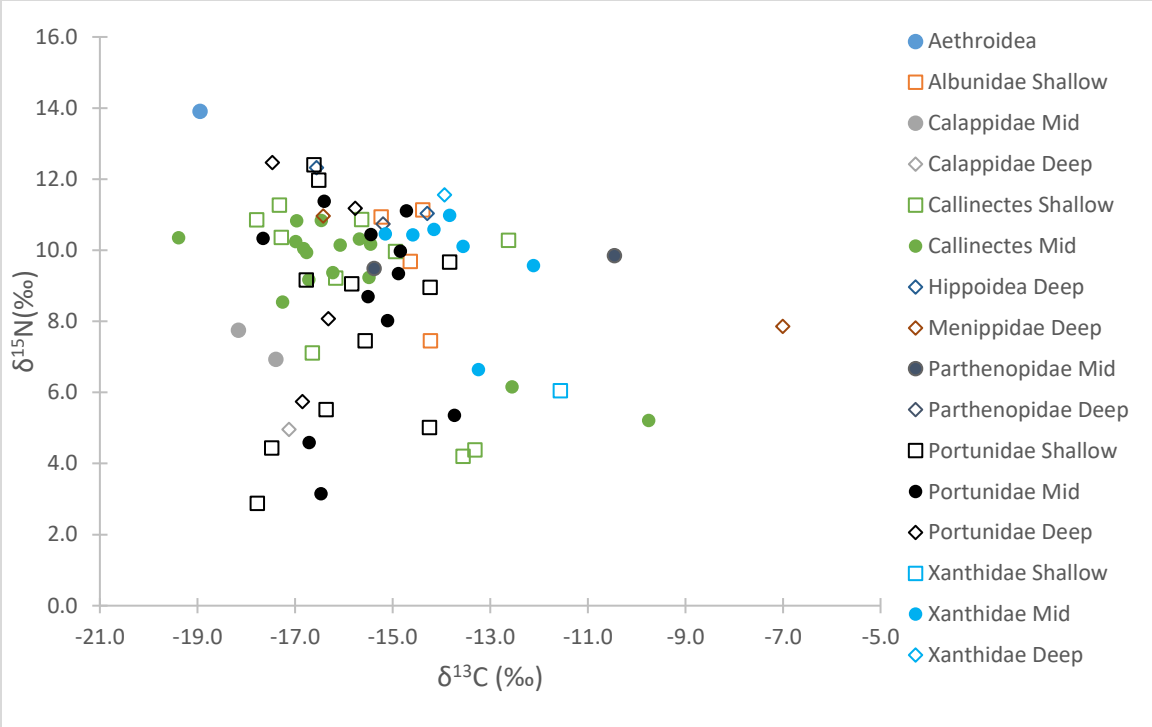


Figure 2.5*: 2016 Brachyura prey items in isotope space based on grouping and depth strata collected from*

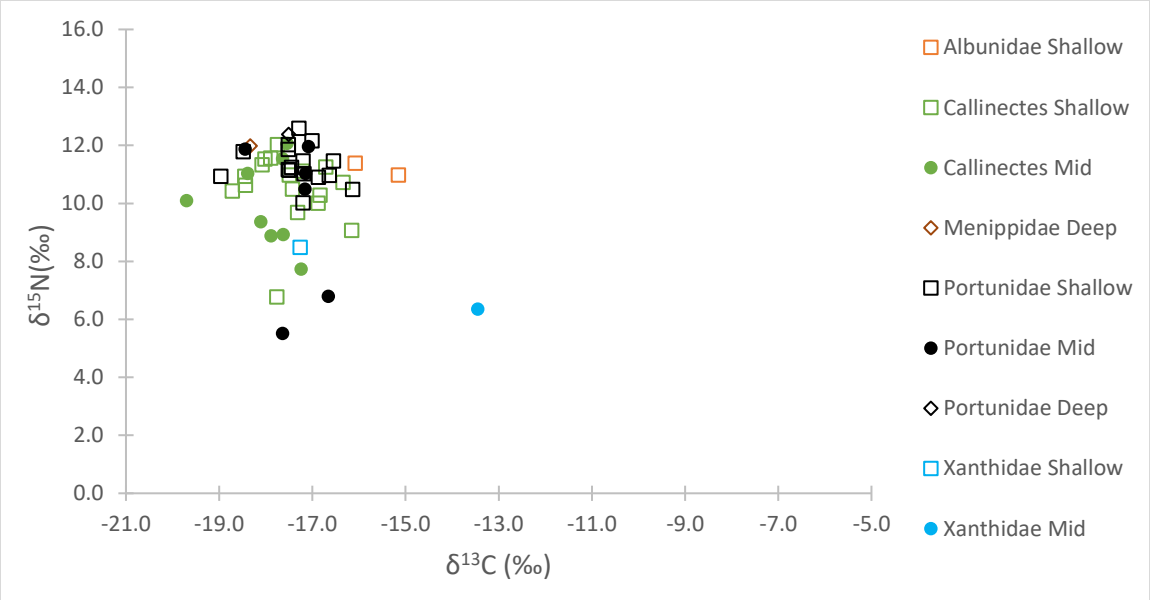


Figure 2.6: *2017 Brachyura prey items in isotope space based on grouping and depth strata collected from*

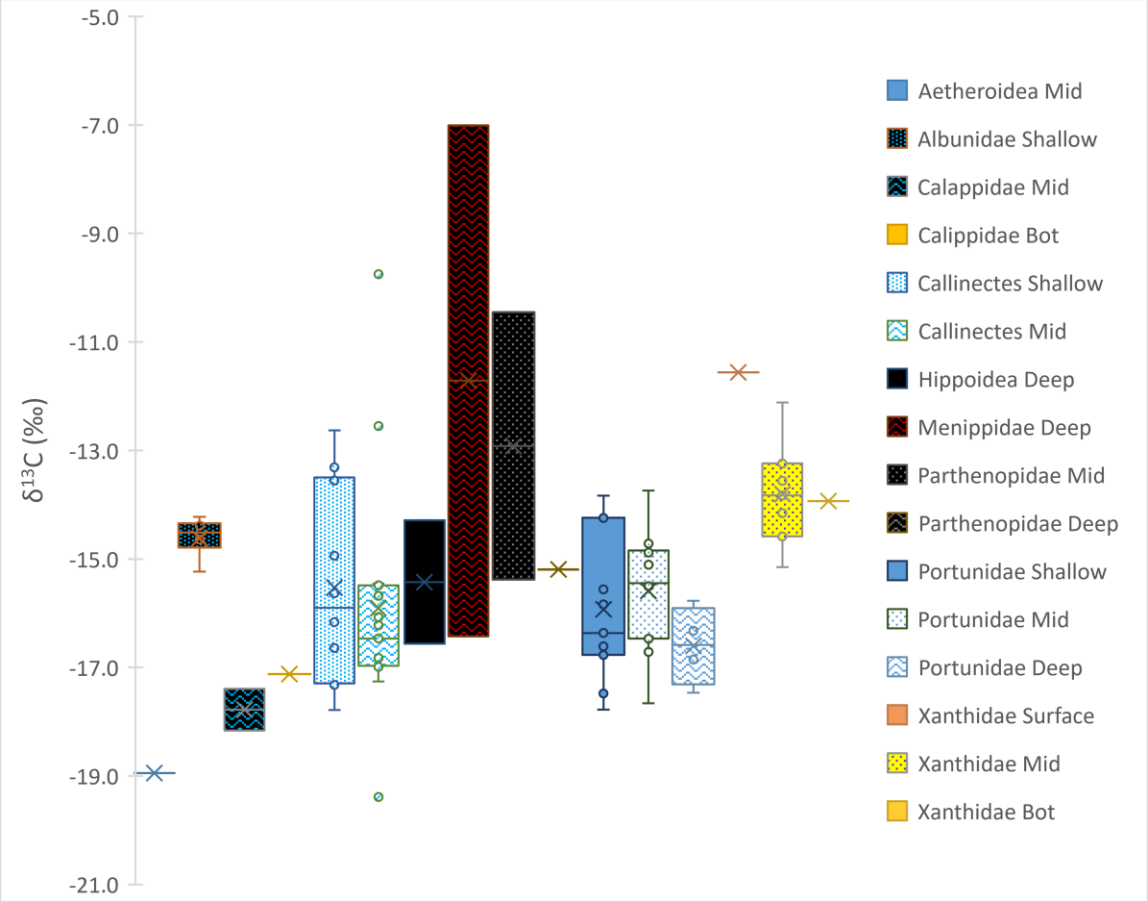


Figure 2.7: *2016 Brachyura prey items by $\delta^{13}C$ value and by depth strata sampled.*

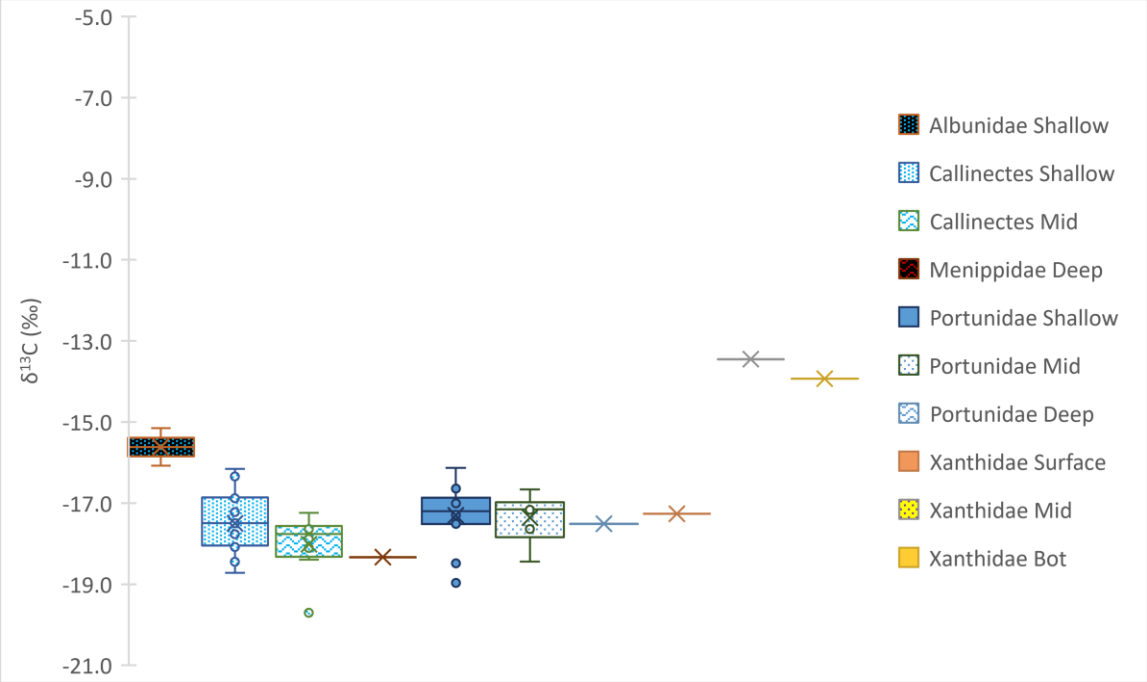


Figure 2.8: *2017 Brachyura prey items by $\delta^{13}C$ value and by depth strata sampled.*

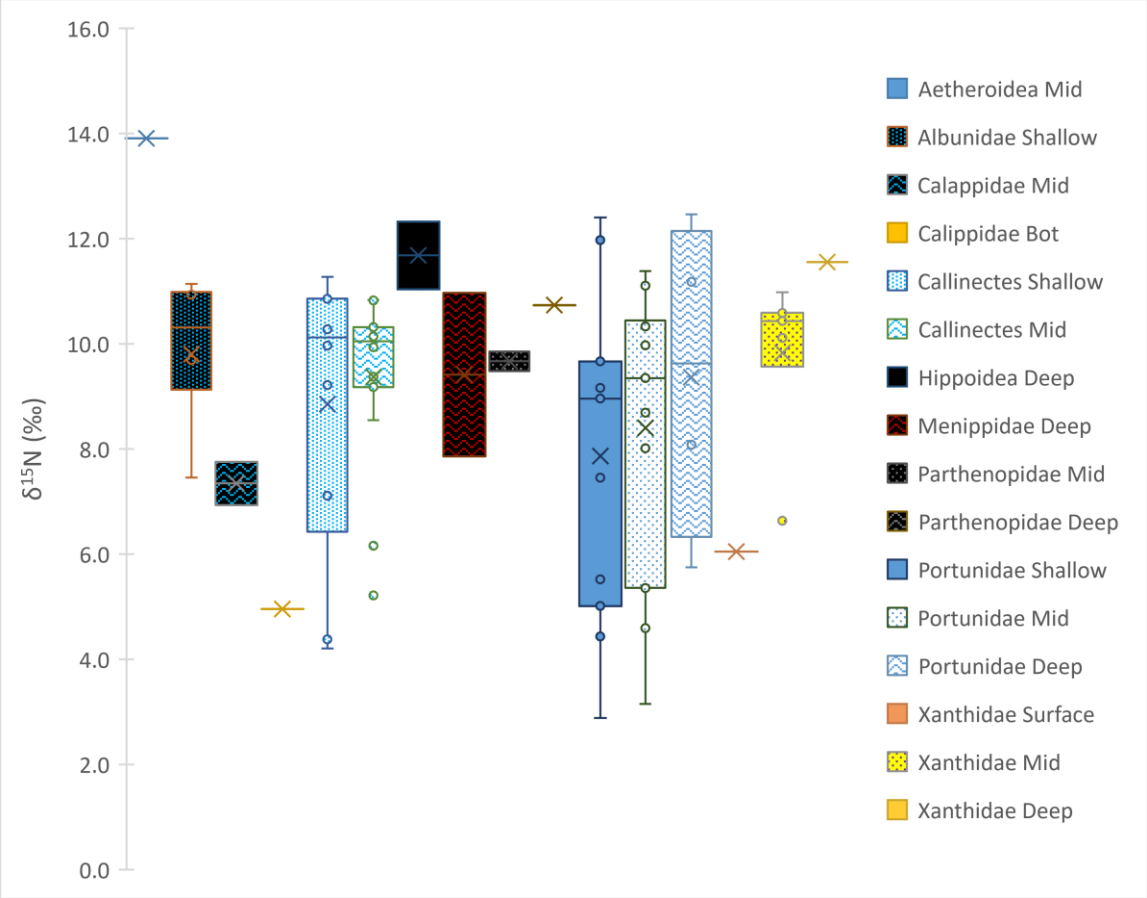


Figure 2.9: *2016 Brachyura prey $\delta^{15}N$ values by Brachyura type and depth strata.*

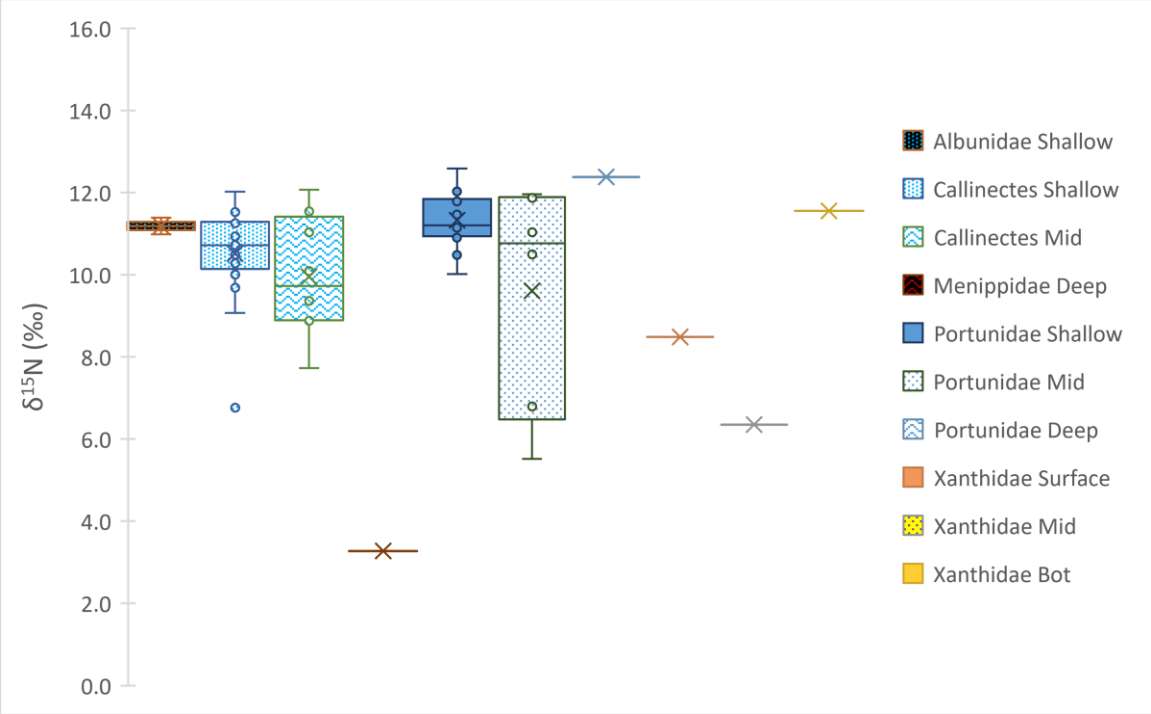


Figure 2.10: *2017 Brachyura prey $\delta^{15}N$ values by Brachyura type and depth strata.*

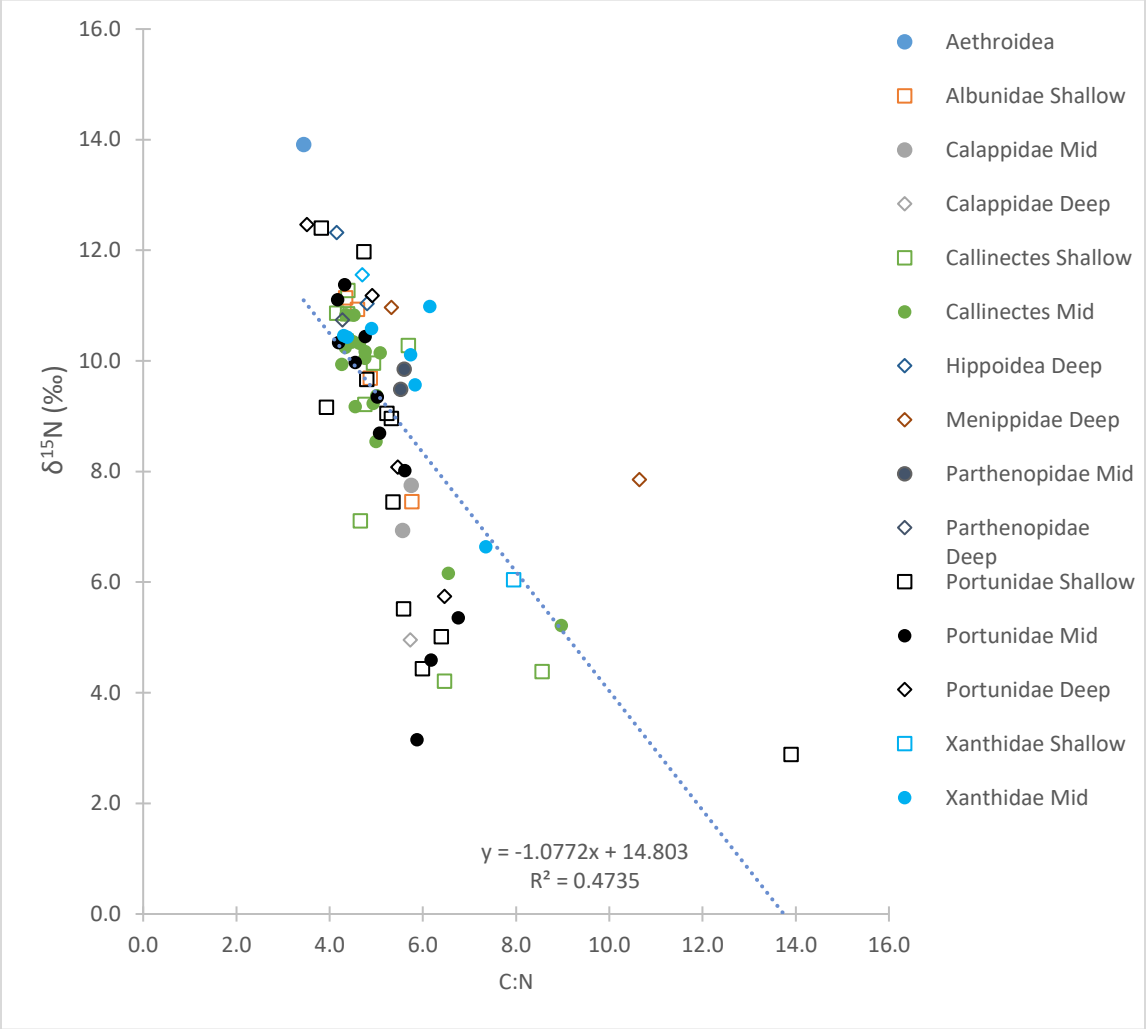


*Figure 2.11:* 2016 Brachyura prey $\delta^{15}N$ values by Brachyura type and depth strata against C:N ratio

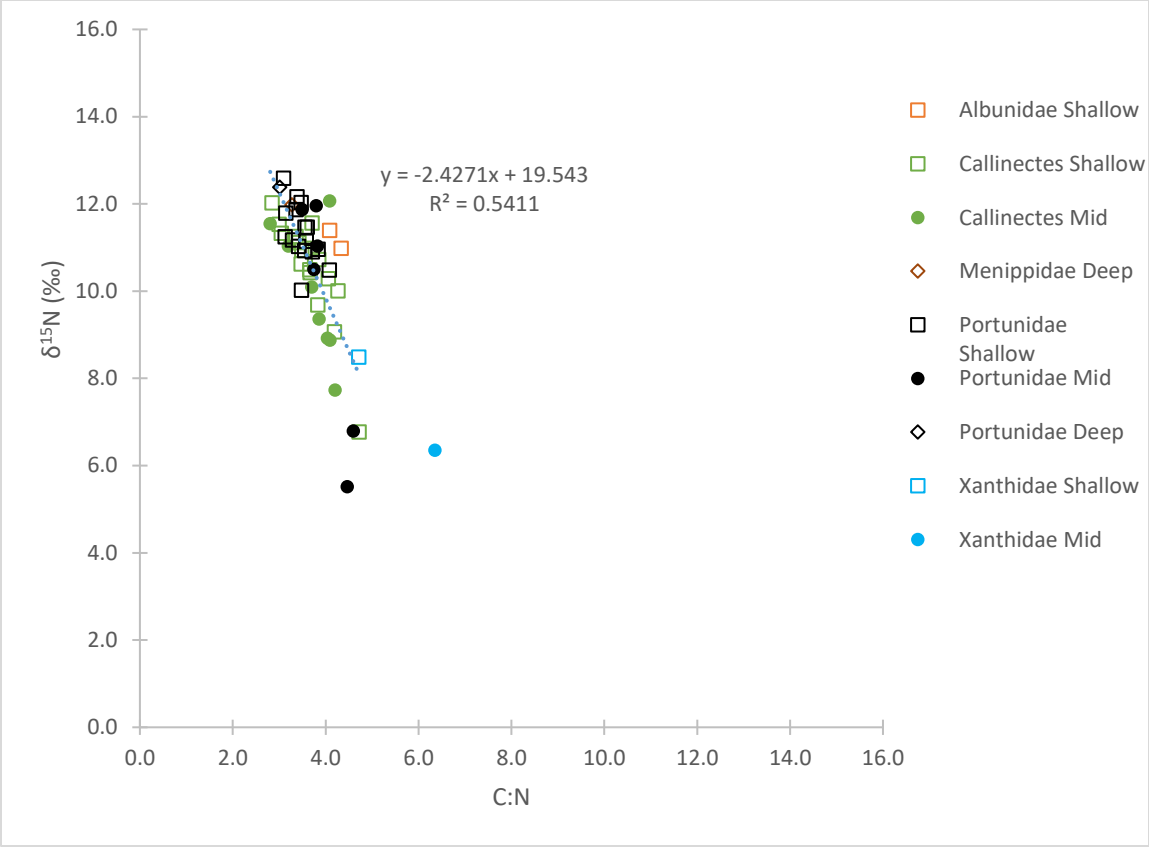


Figure 2.12*: 2017 Brachyura prey $\delta^{15}N$ values by Brachyura type and depth strata against C:N ratio*

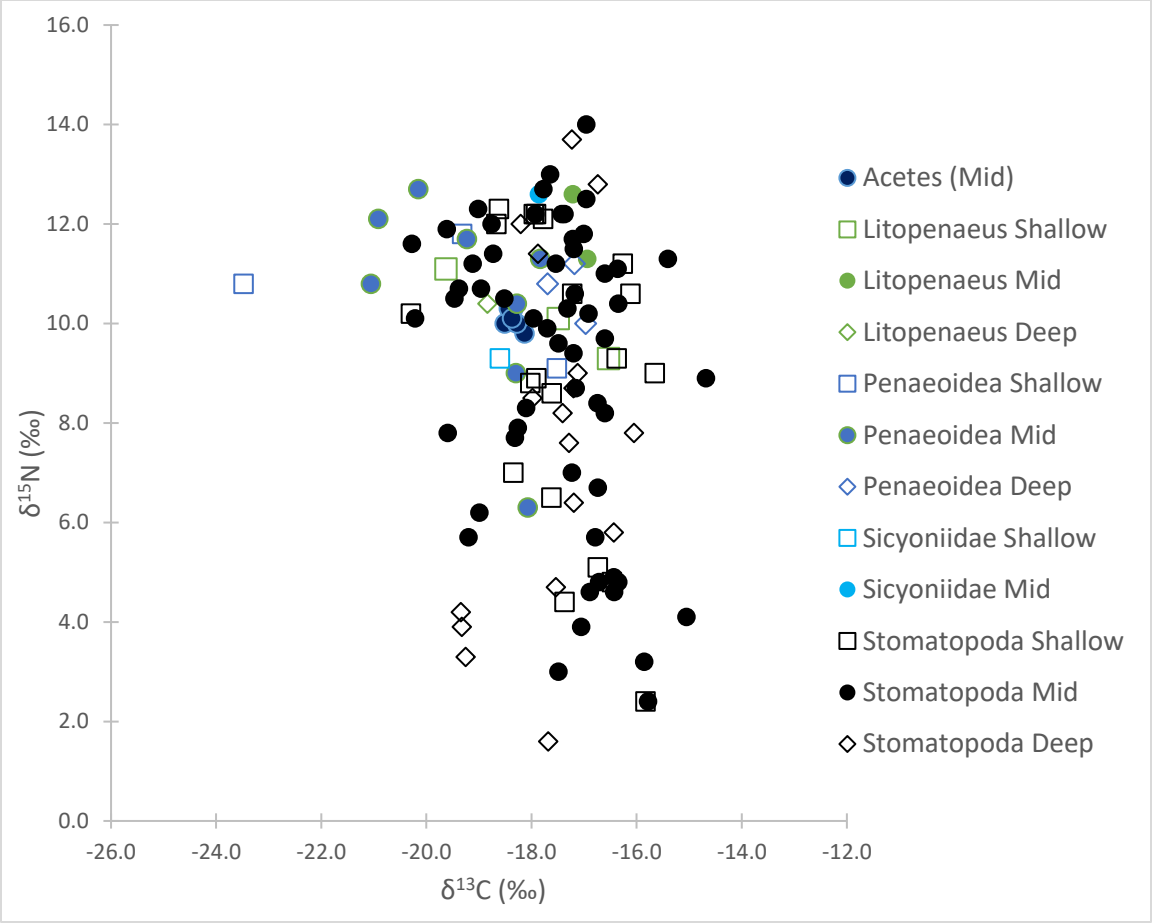


Figure 2.13: *2016 and 2017 Dendrobranchiata and Stomatopoda prey items in isotope space based upon depth strata collected from and prey type.*

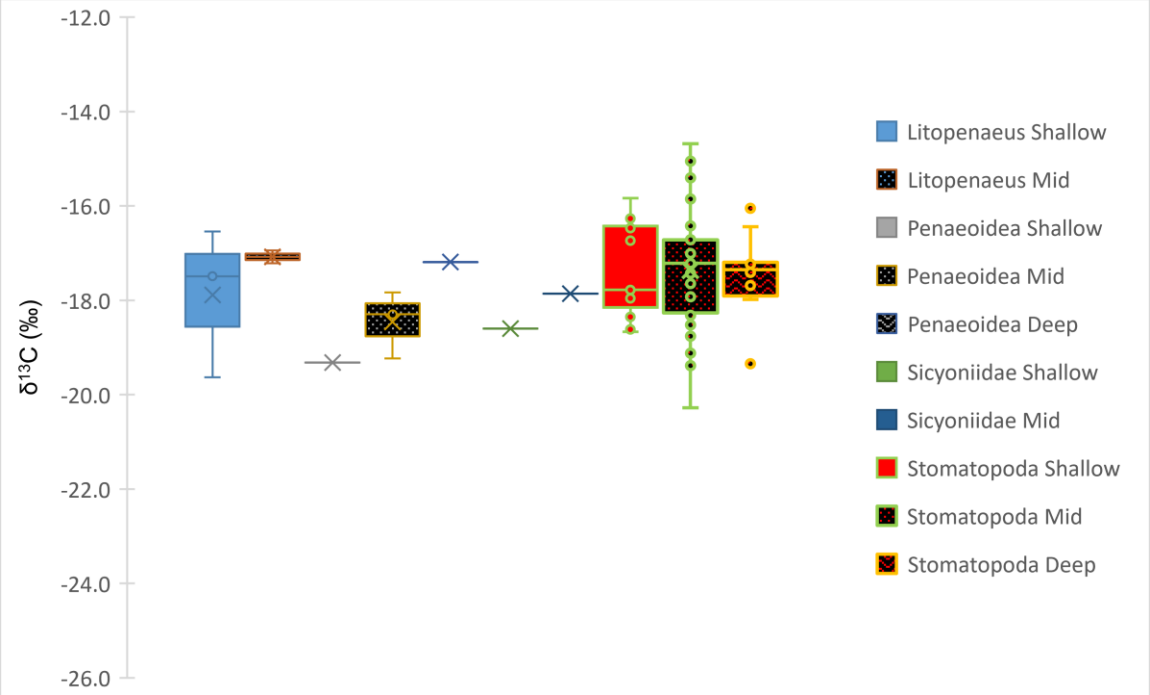


Figure 2.14: *$\delta^{13}C$ values of Dendrobranchiata and Stomatopoda prey items collected in 2016 based upon prey type and depth strata sampled.*

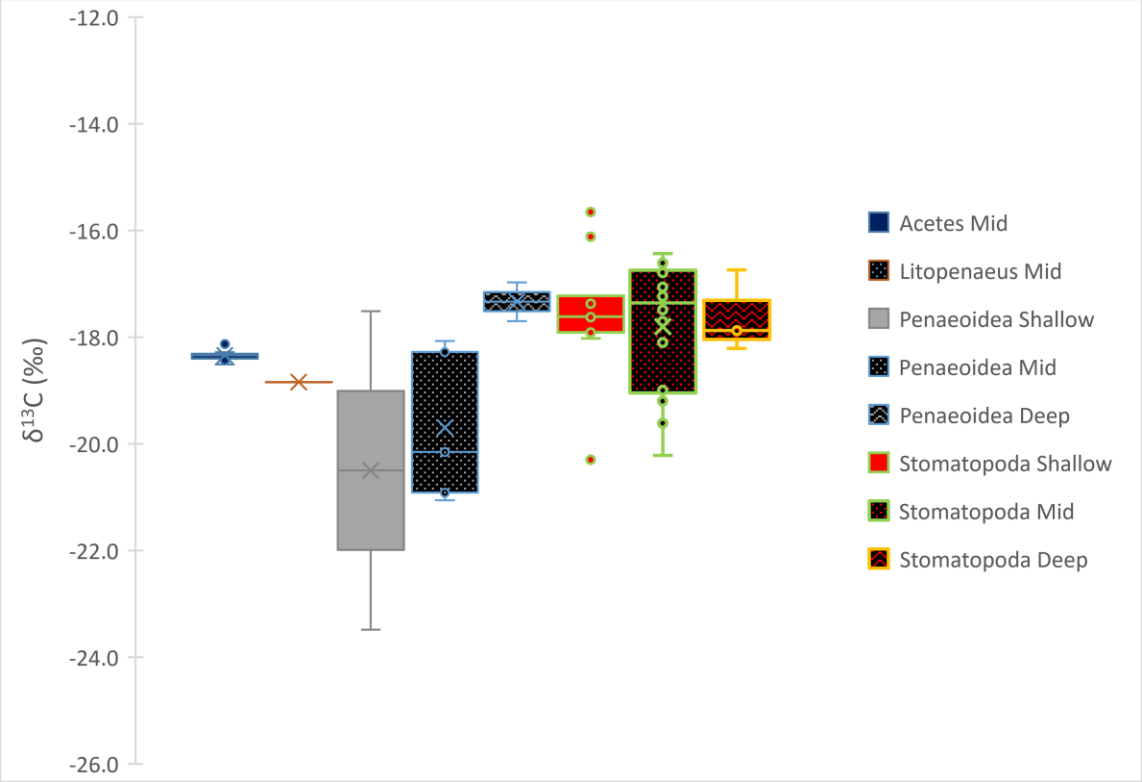


Figure 2.15: *$\delta^{13}C$ values of Dendrobranchiata and Stomatopoda prey items collected in 2017 based upon prey type and depth strata sampled.*

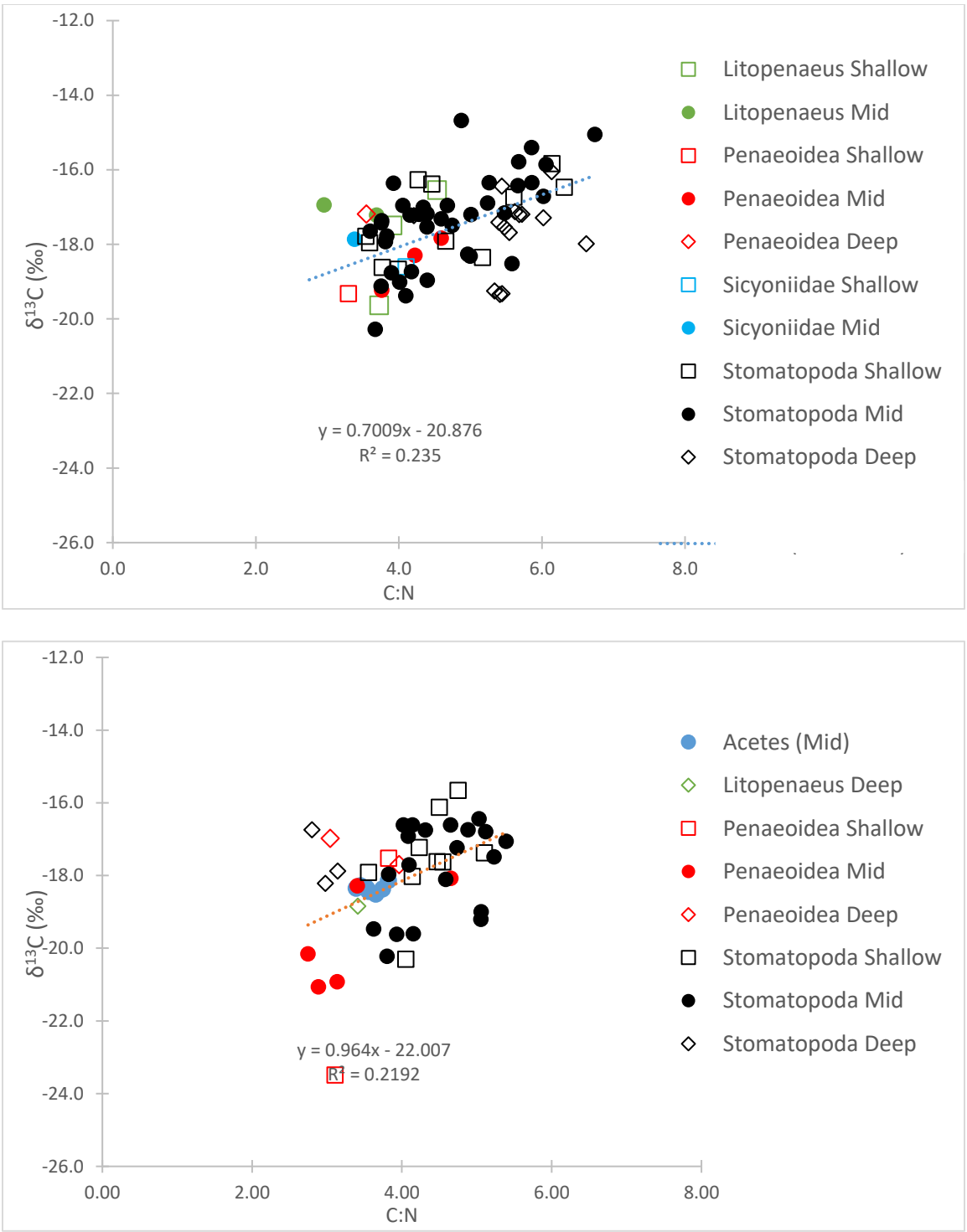


Figure 2.16: *$\delta^{13}C$ values of Dendrobranchiata and Stomatopoda prey items collected in 2016 (Top) and 2017 (Bottom) based upon prey type and depth strata sampled against C:N ratio.*

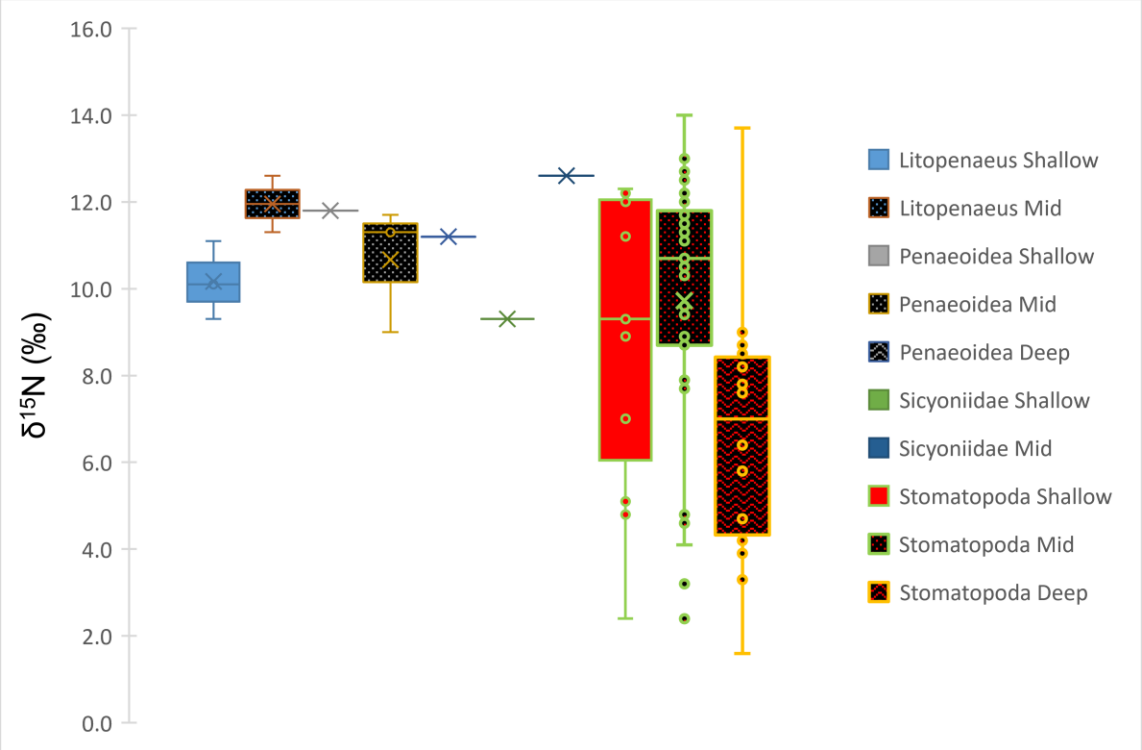


Figure 2.17*: $\delta^{15}N$ values of Dendrobranchiata and Stomatopoda prey items collected in 2016 based upon prey type and depth strata sampled.*

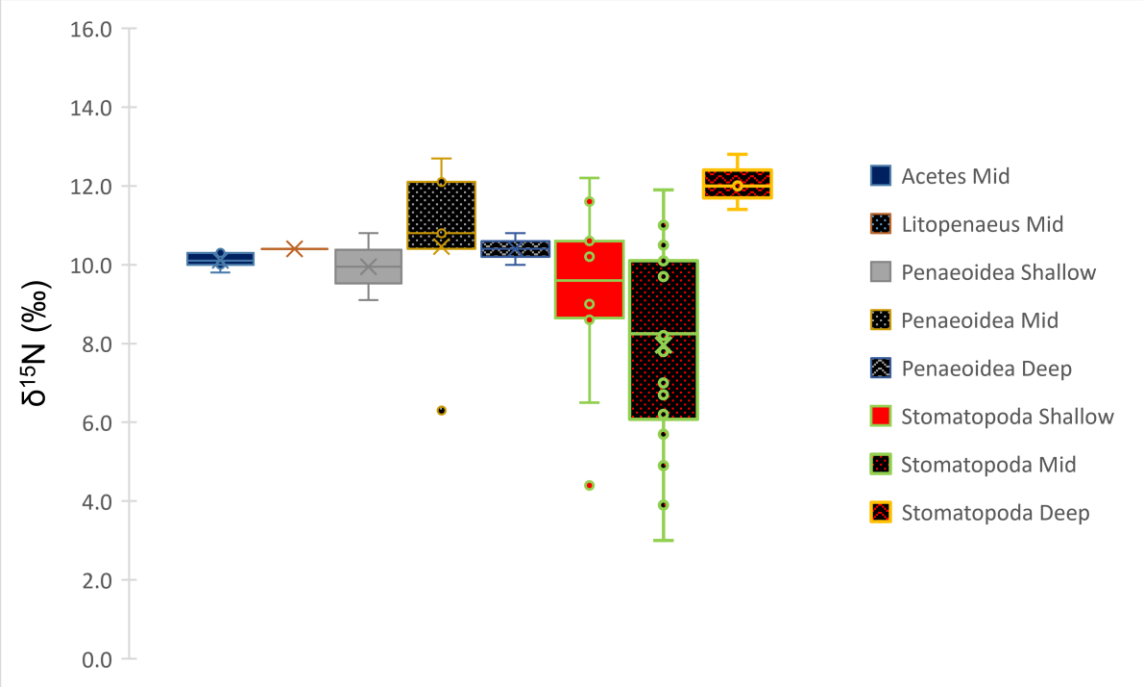


Figure 2.18: *$\delta^{15}N$ values of Dendrobranchiata and Stomatopoda prey items collected in 2017 based upon prey type and depth strata sampled.*

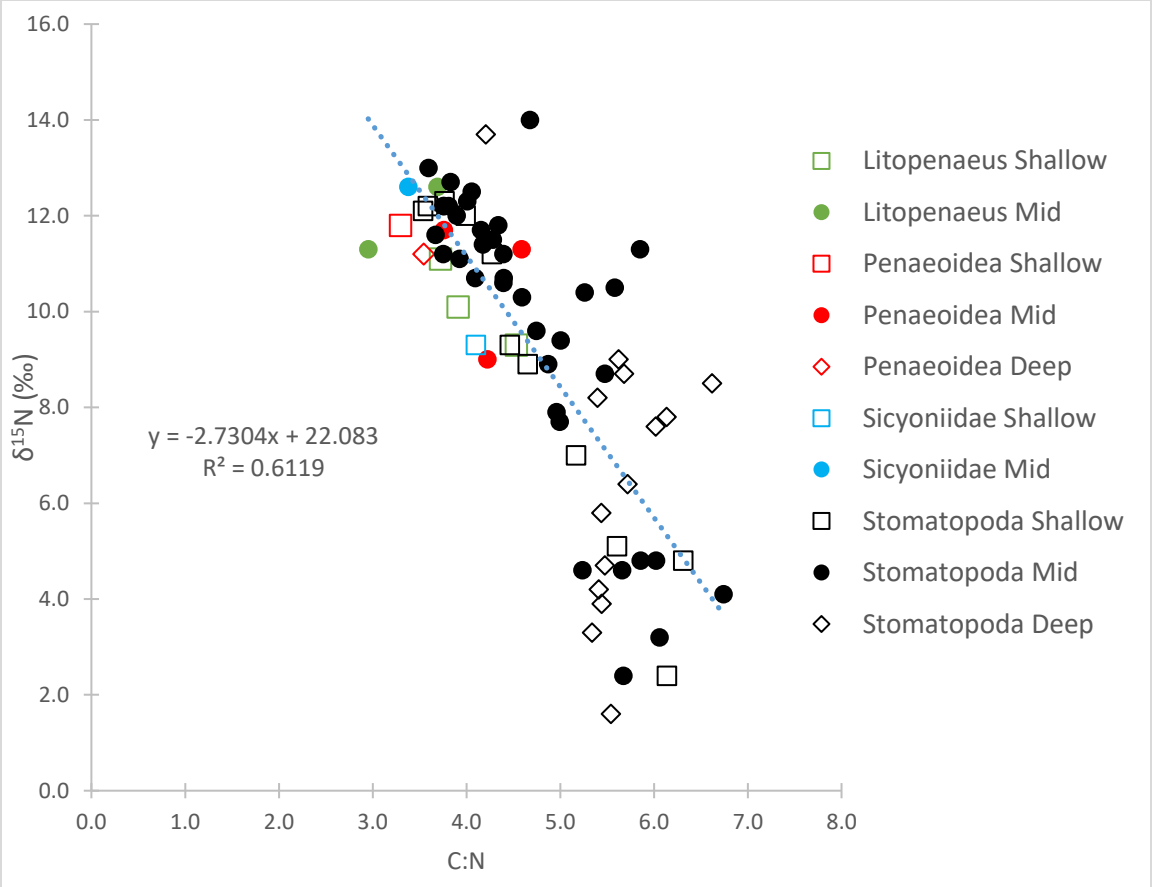


Figure 2.19*: $\delta^{15}N$ values of Dendrobranchiata and Stomatopoda prey items collected in 2016 based upon prey type and depth strata sampled compared with the C:N ratio of the prey.*

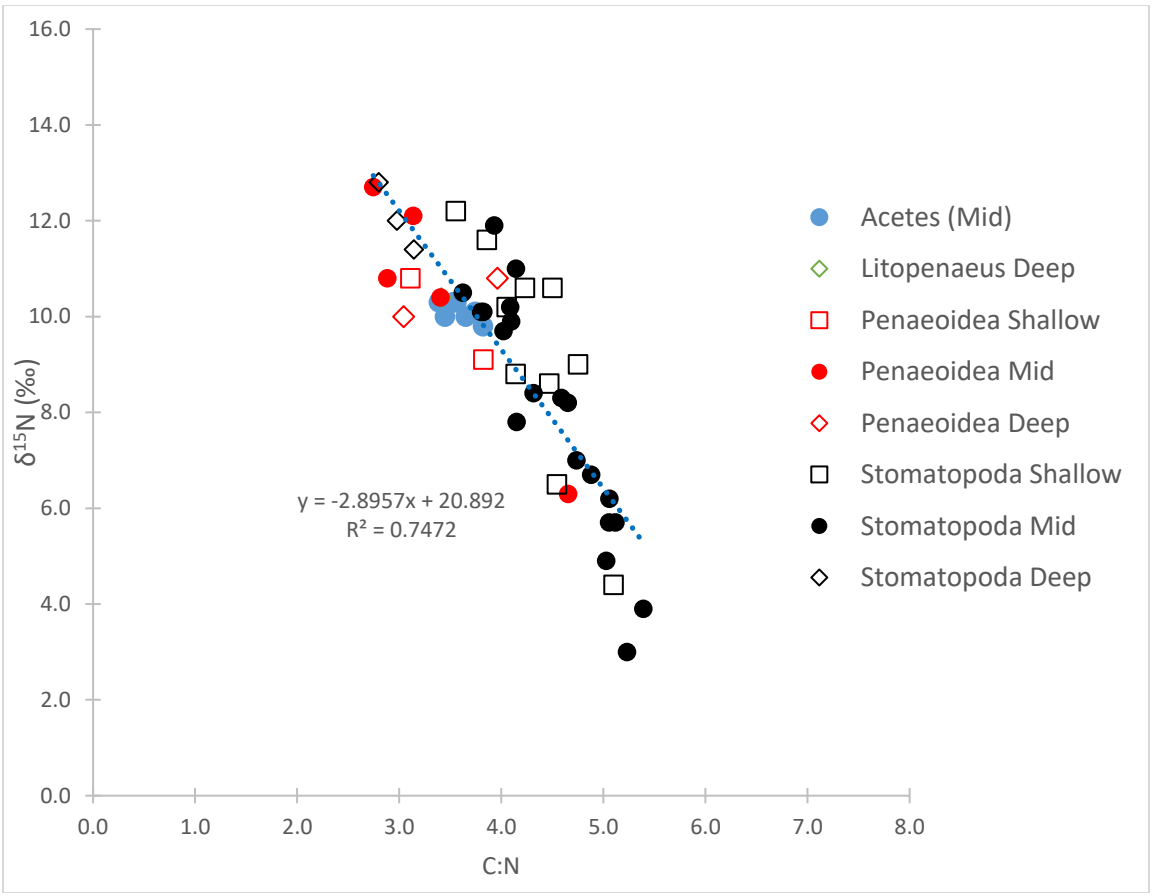


Figure 2.20: *$\delta^{15}N$ values of Dendrobranchiata and Stomatopoda prey items collected in 2017 based upon prey type and depth strata sampled compared with the C:N ratio of the prey.*

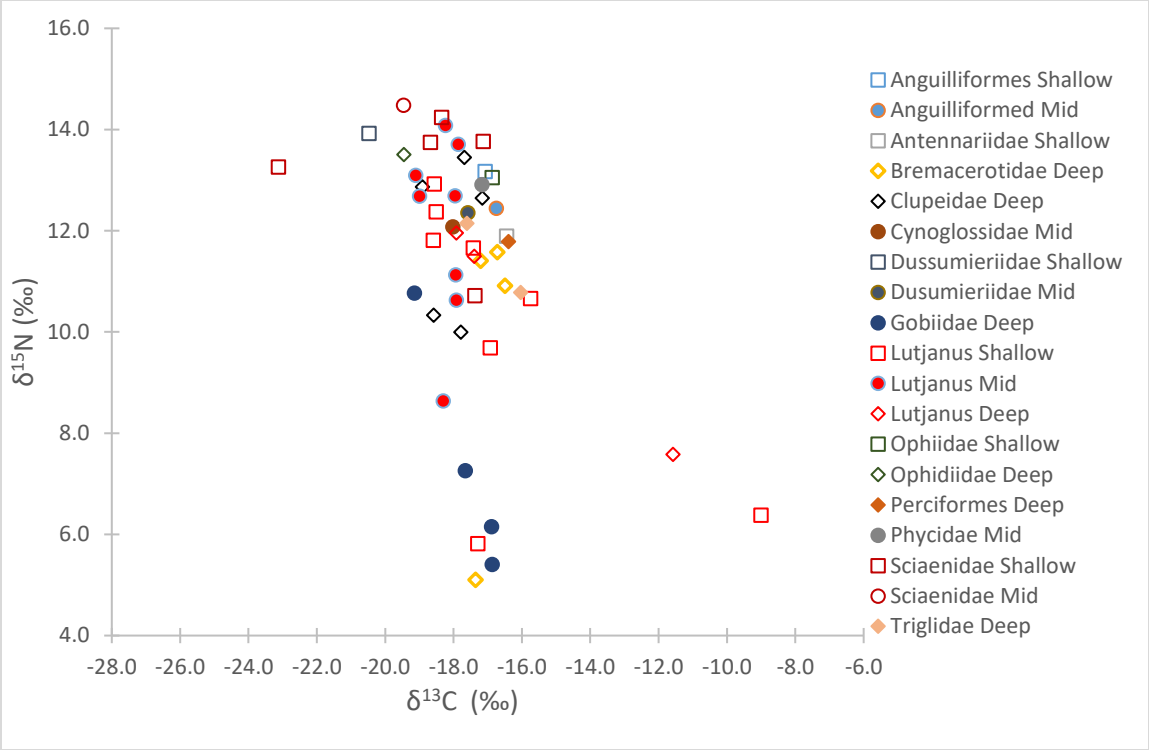


Figure 2.21*: Actinopterygii prey items collected in 2016 in isotopes space based upon Actinopterygii prey type and depth strata.*

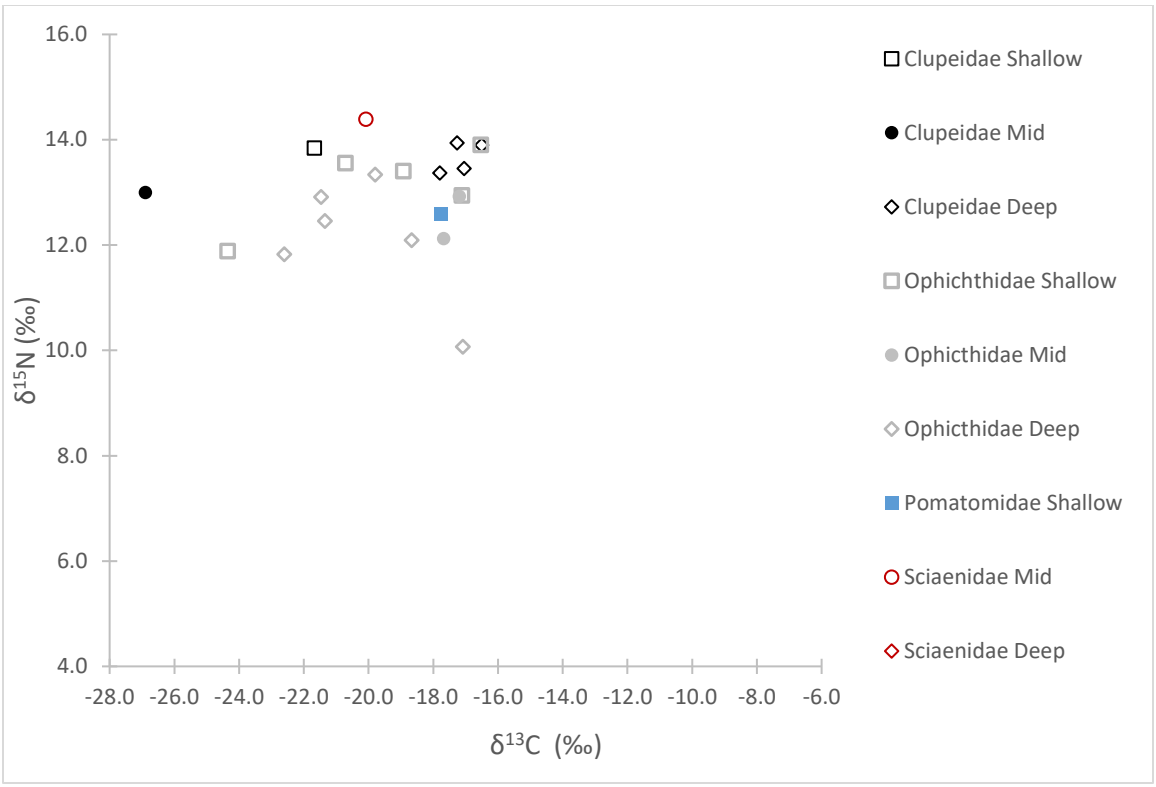


Figure 2.22: *Actinopterygii prey items collected in 2017 in isotopes space based upon fish prey type and depth strata.*

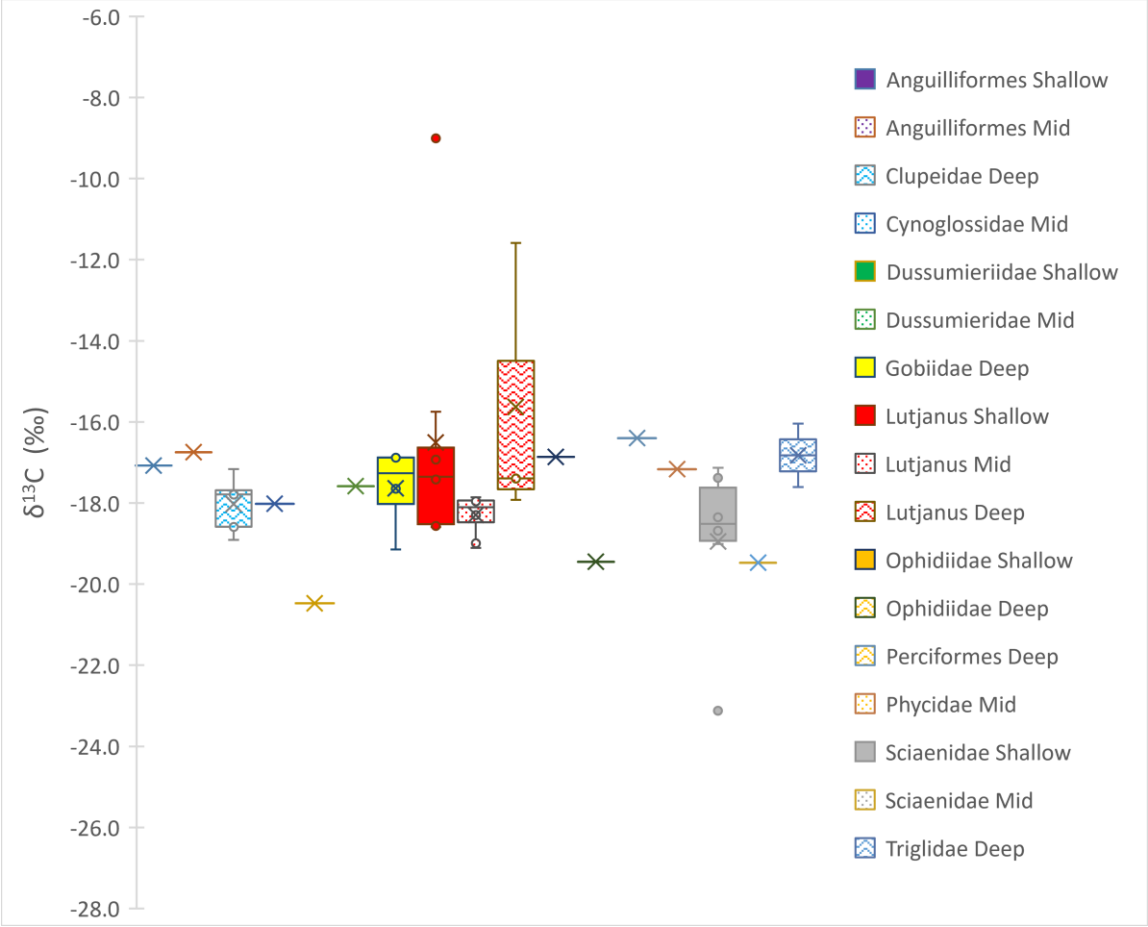


Figure 2.23*: $\delta^{13}C$ values of Actinopterygii prey items from 2016 based on depth strata sampled and Actinopterygii type.*

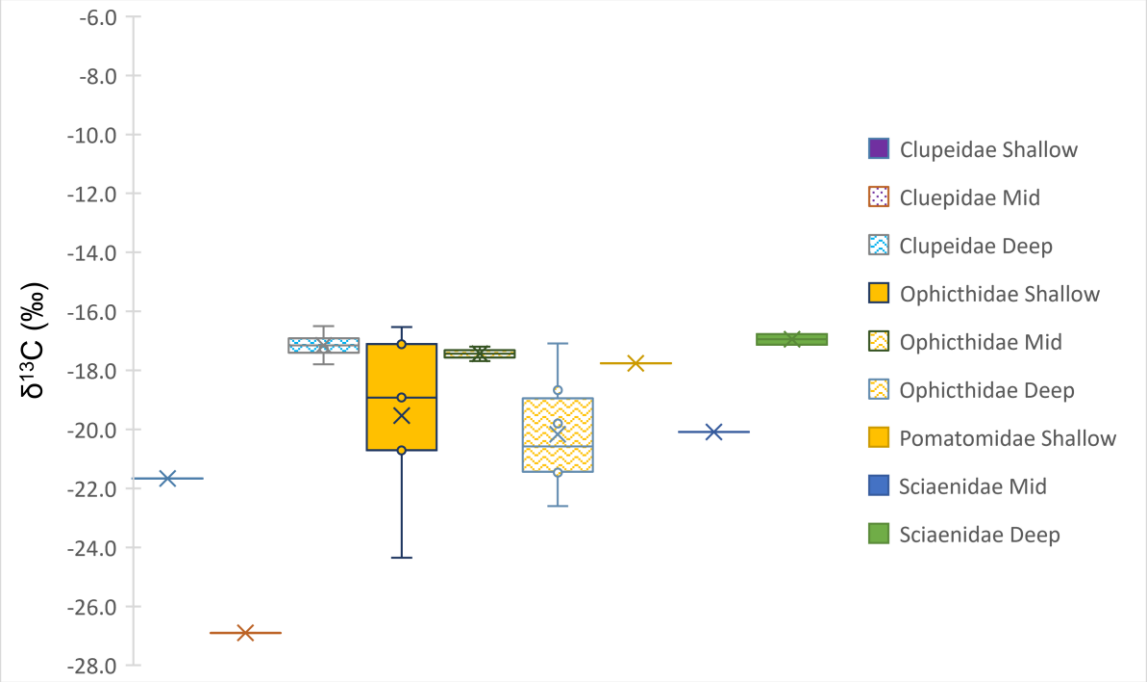


Figure 2.24: *$\delta^{13}C$ values of Actinopterygii prey items from 2017 based on depth strata sampled and Actinopterygii type.*

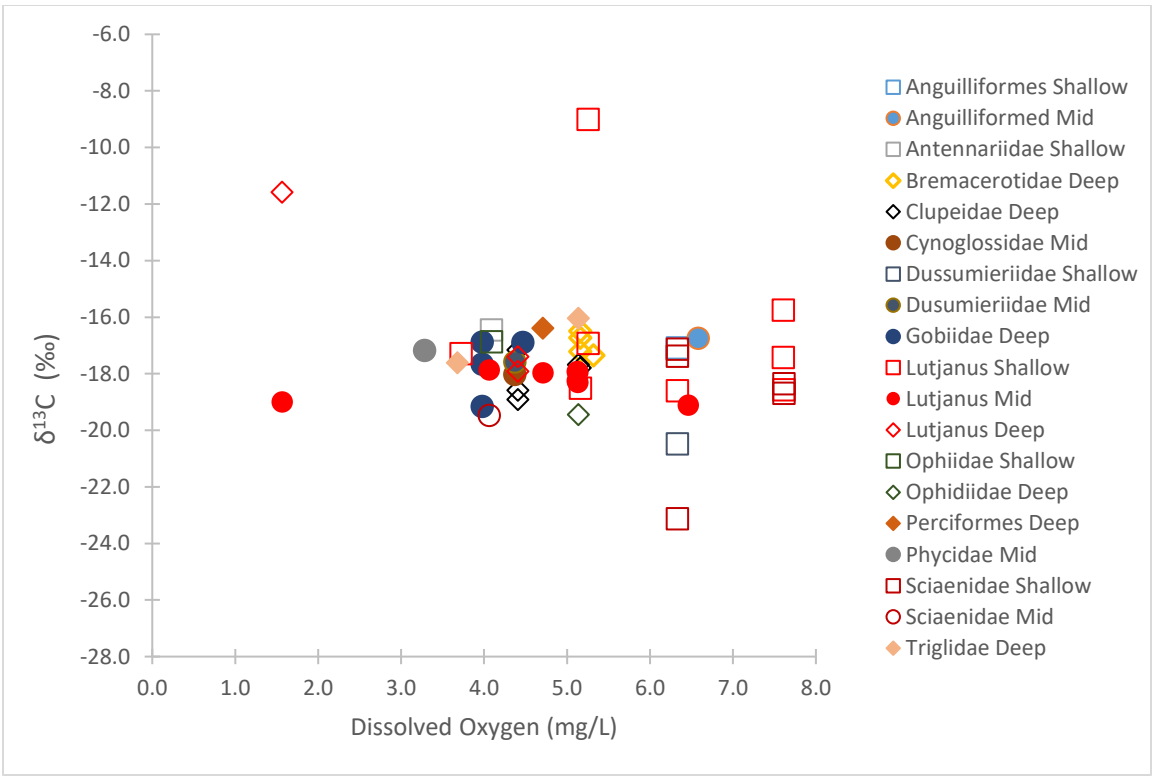


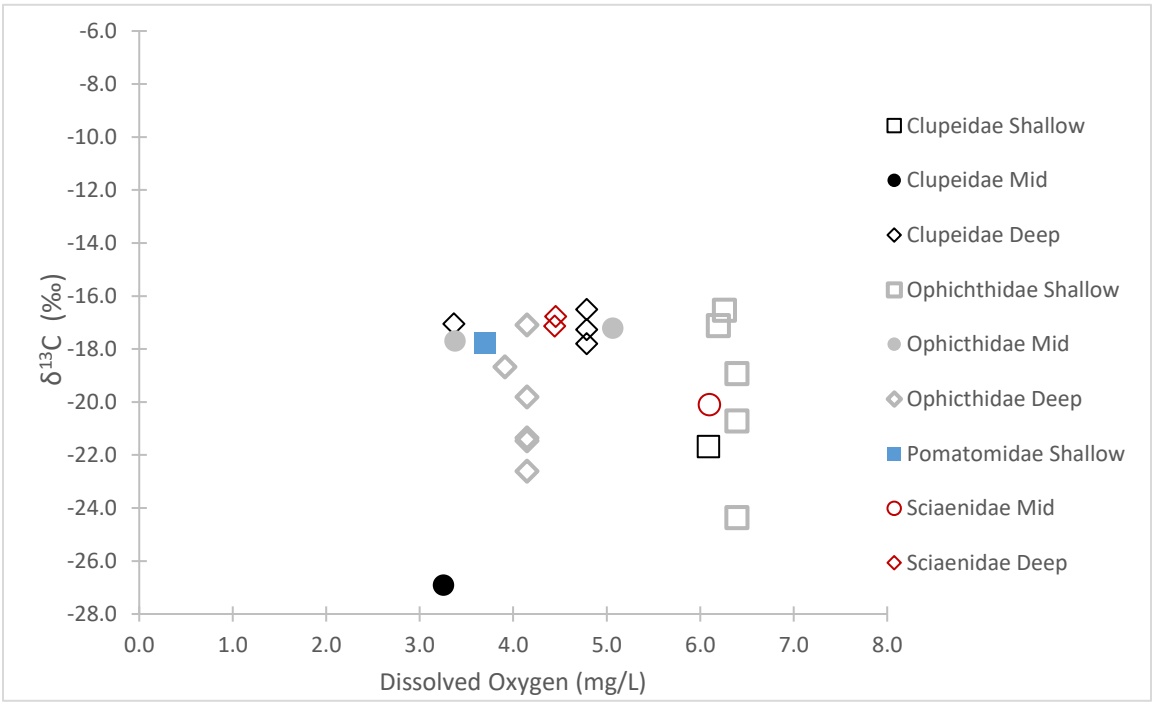


Figure 2.25: *Figure showing the 2016 (top) and 2017 (bottom) Actinopterygii prey $\delta^{13}C$ values against dissolved oxygen content of the water*

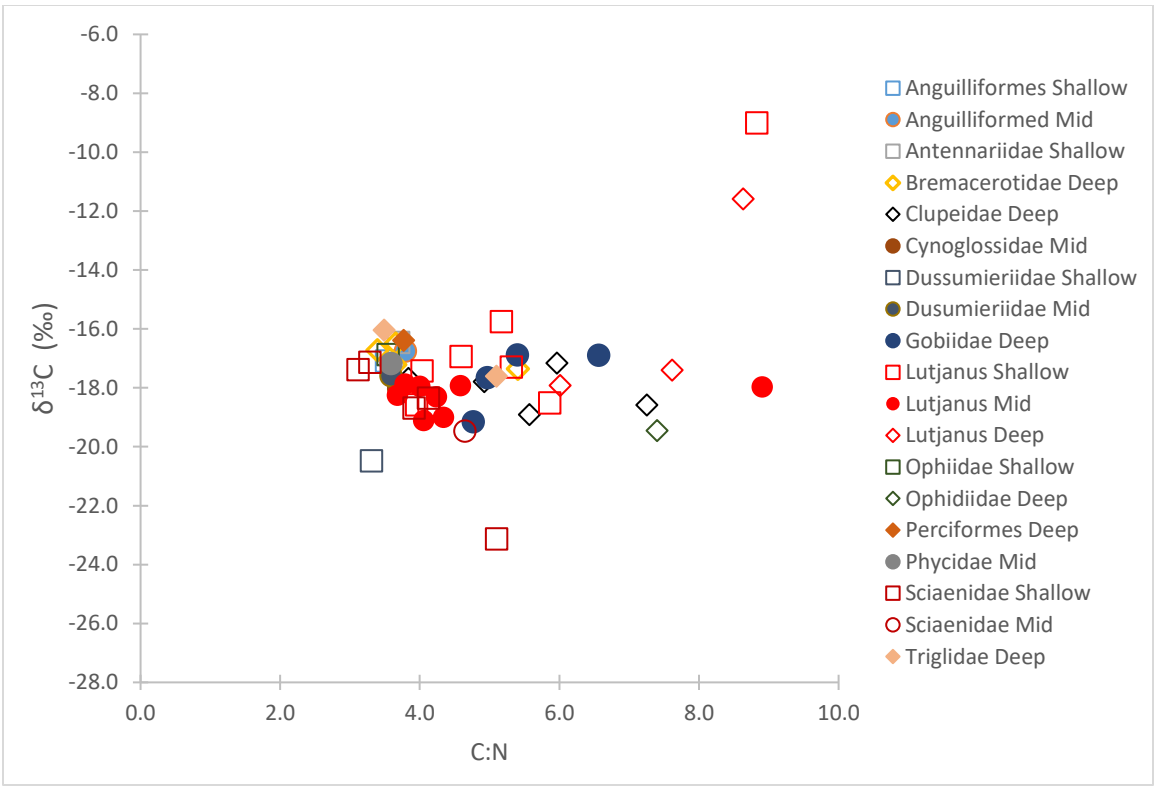


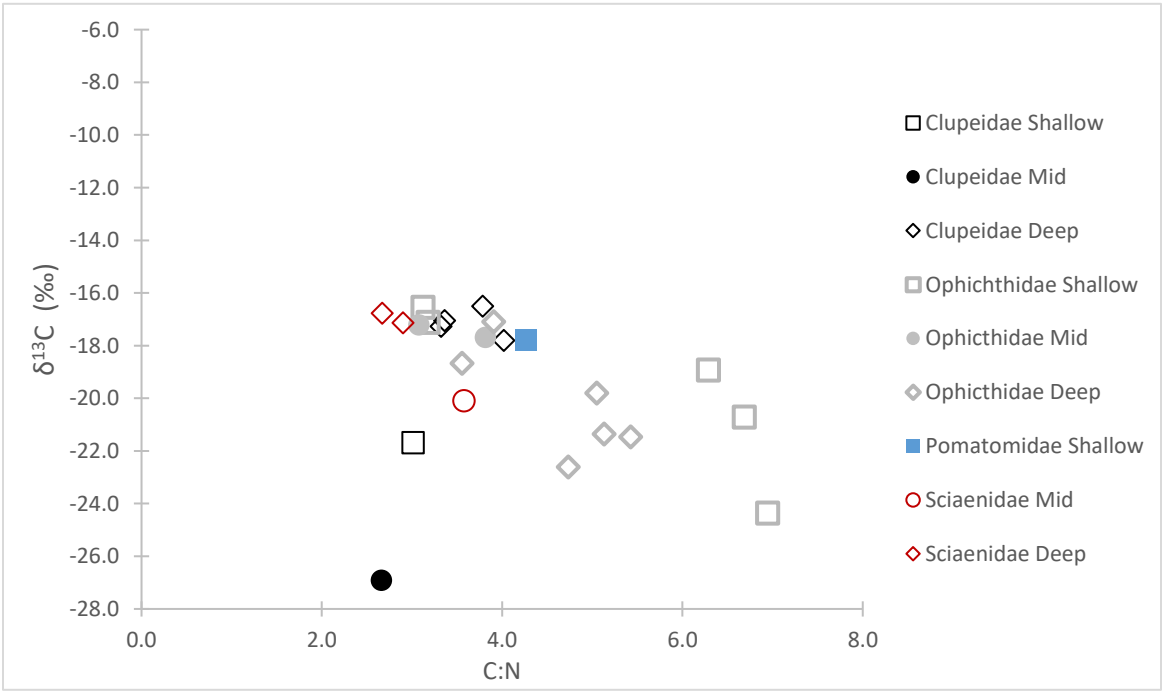


Figure 2.26: *$\delta^{13}C$ values of the Actinopterygii prey items collected in 2016 (Top) and 2017 (Bottom) against their C:N ratio.*

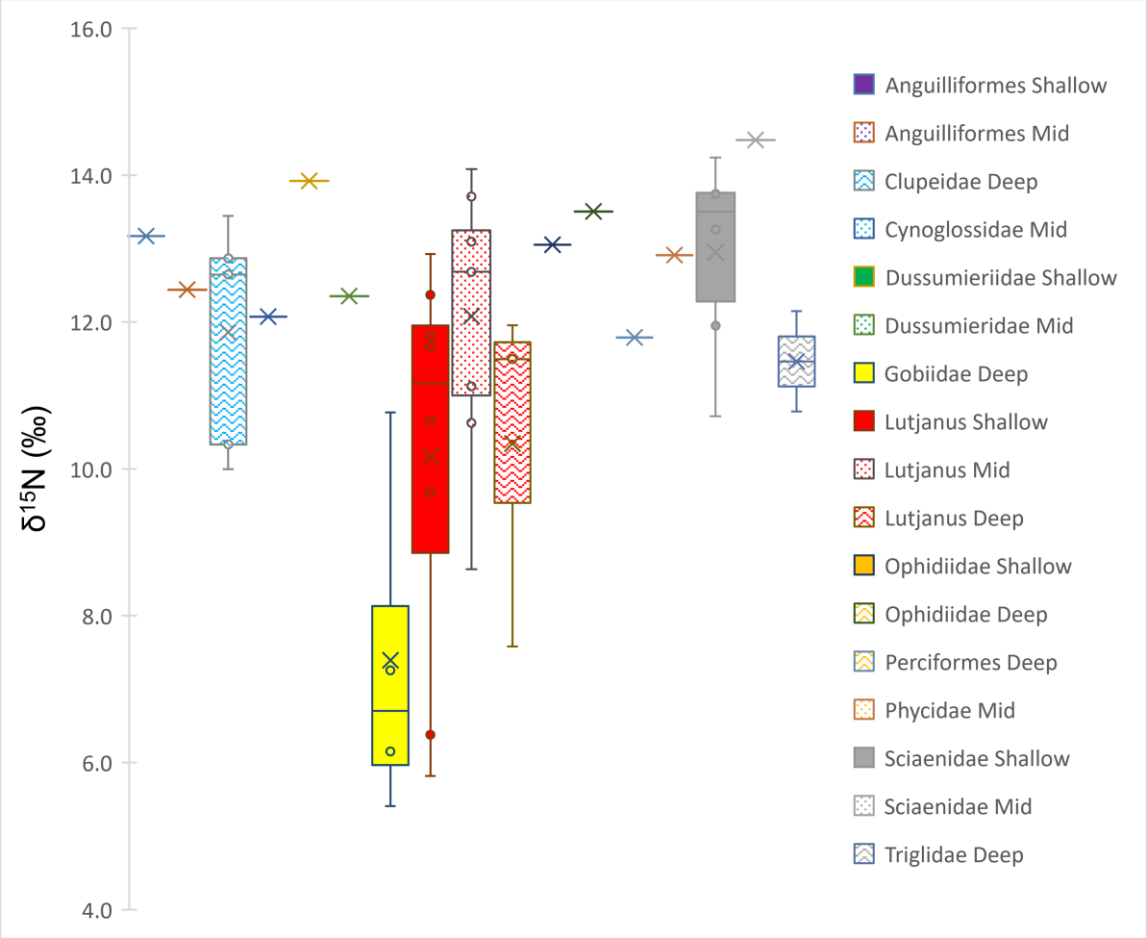


Figure 2.27*: $\delta^{15}N$ values of the Actinopterygii prey items collected in 2016 based on the type of prey Actinopterygii and depth strata*

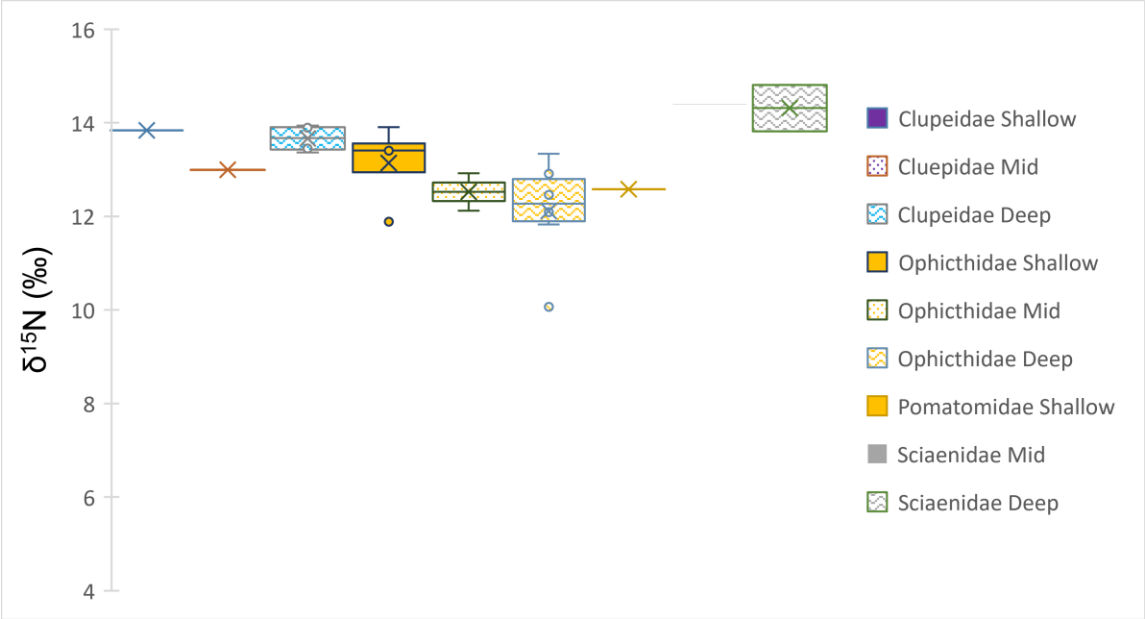


Figure 2.28: *$\delta^{15}N$ values of the Actinopterygii prey items collected in 2017 based on the type of prey Actinopterygii and the depth strata sampled from.*

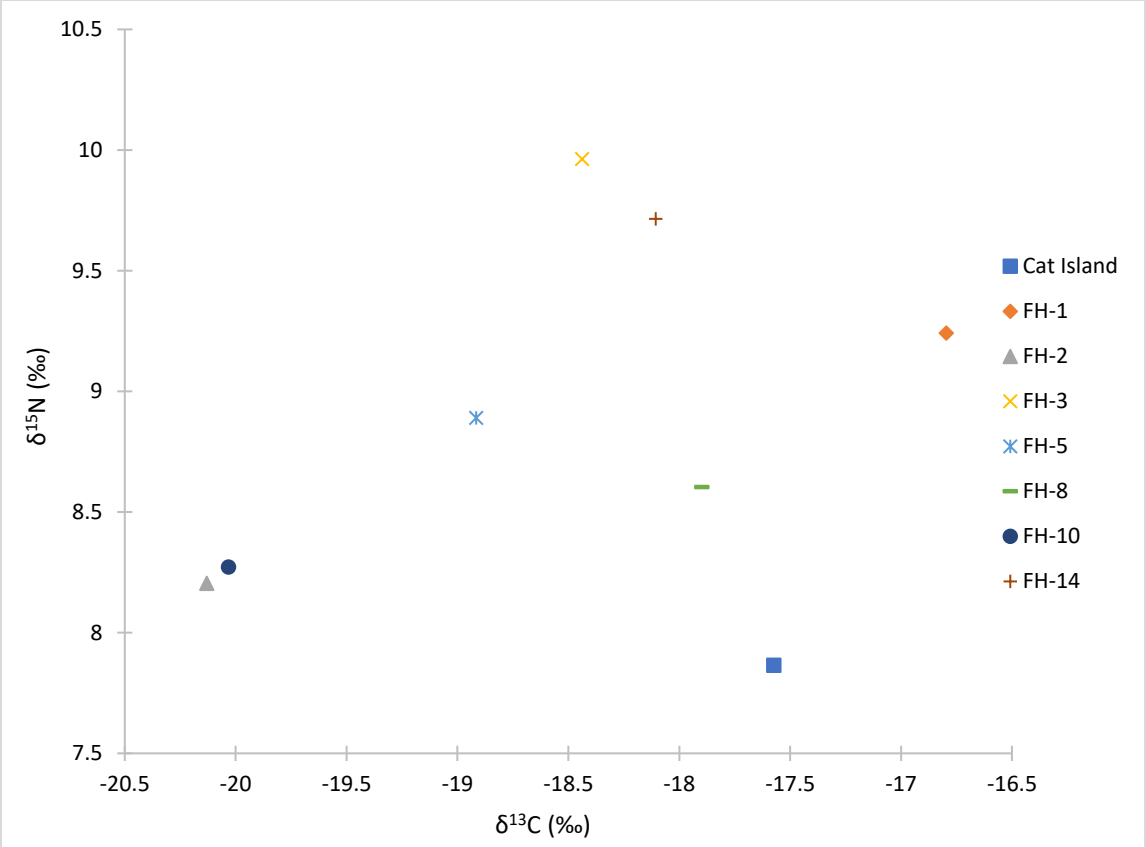


Figure 2.29*: Bi-plot showing the stable isotope values of biofilm collected in April and May of 2017.*

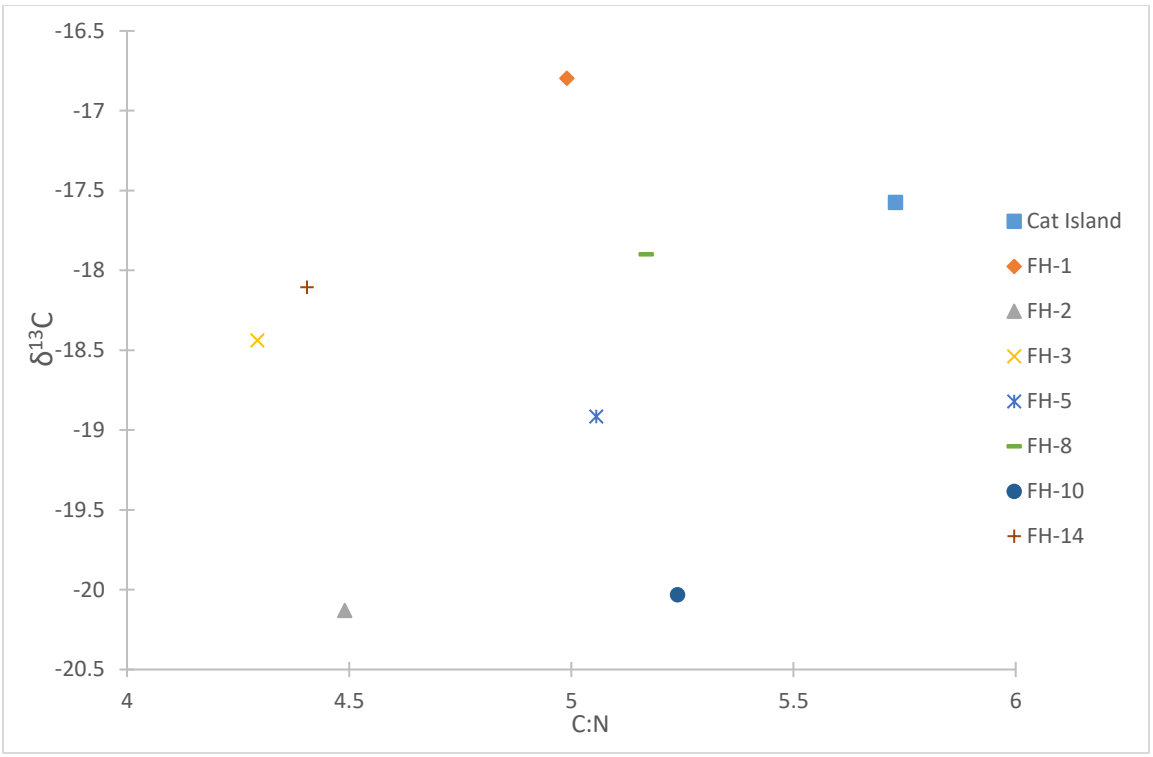


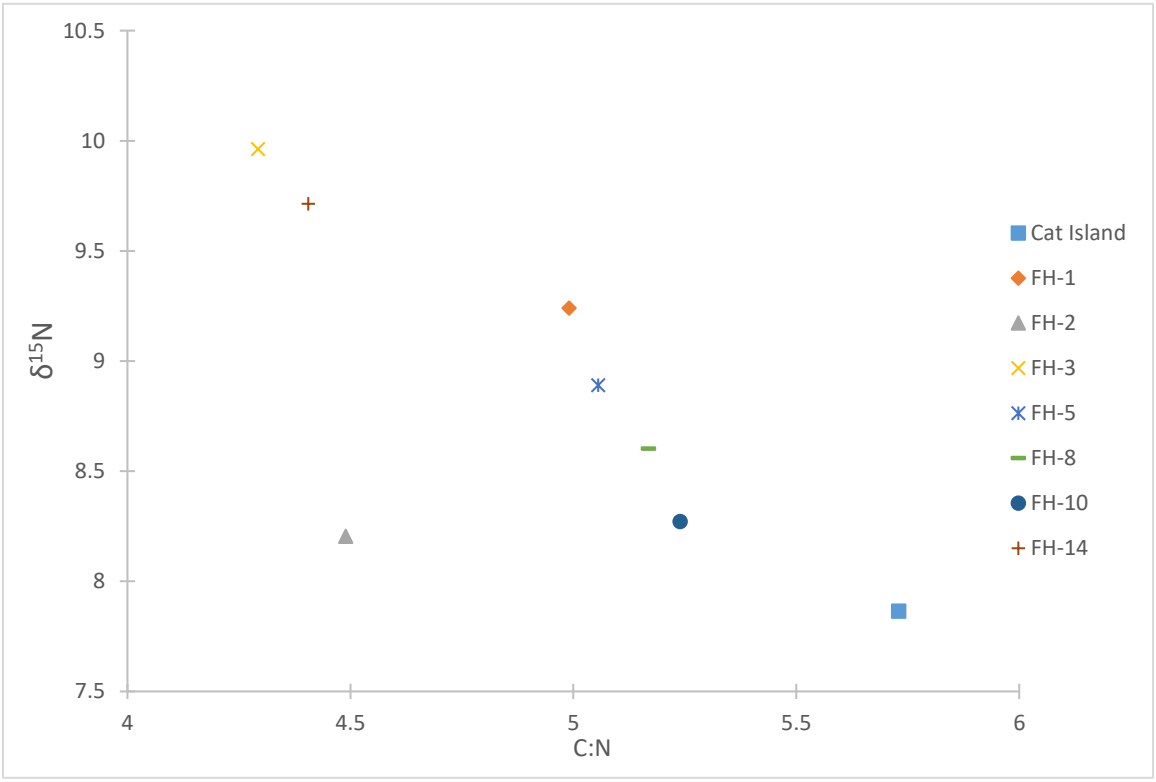


Figure 2.30*: Bi-plot showing biofilm $\delta^{13}C$ (‰, Top) and $\delta^{15}N$ (‰, Bottom) values against C:N ratios.*

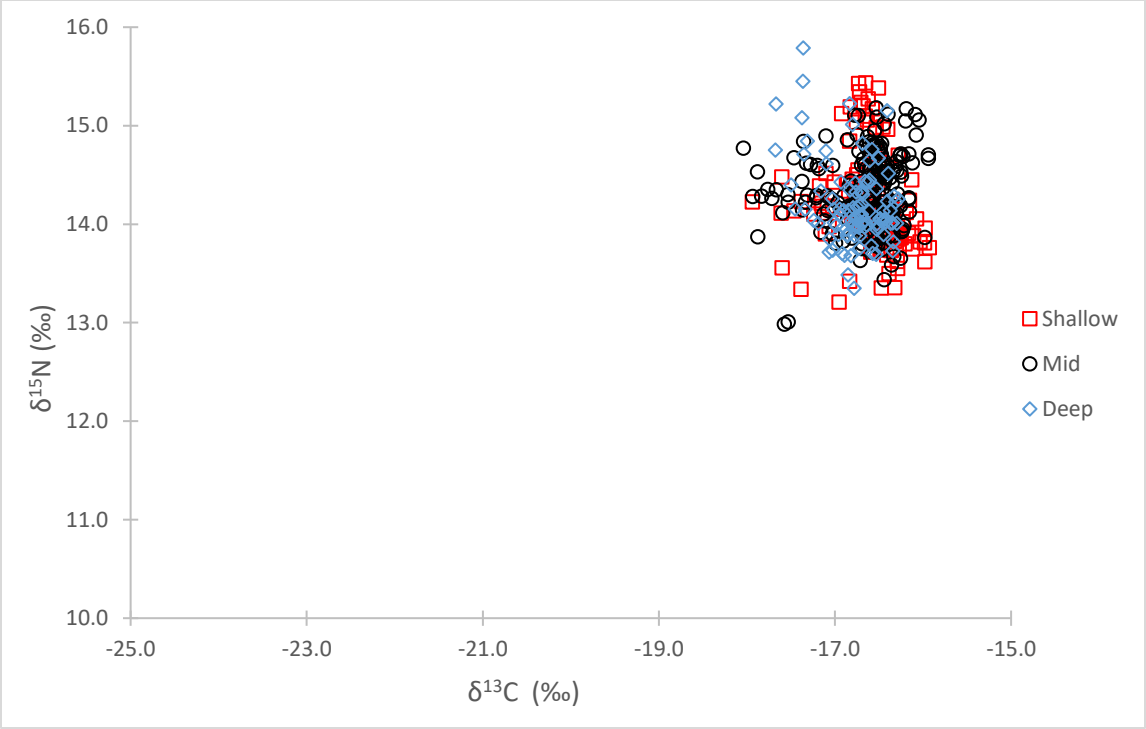


Figure 2.31*: Stable isotope values of red snapper sampled in 2016 based upon depth strata.*

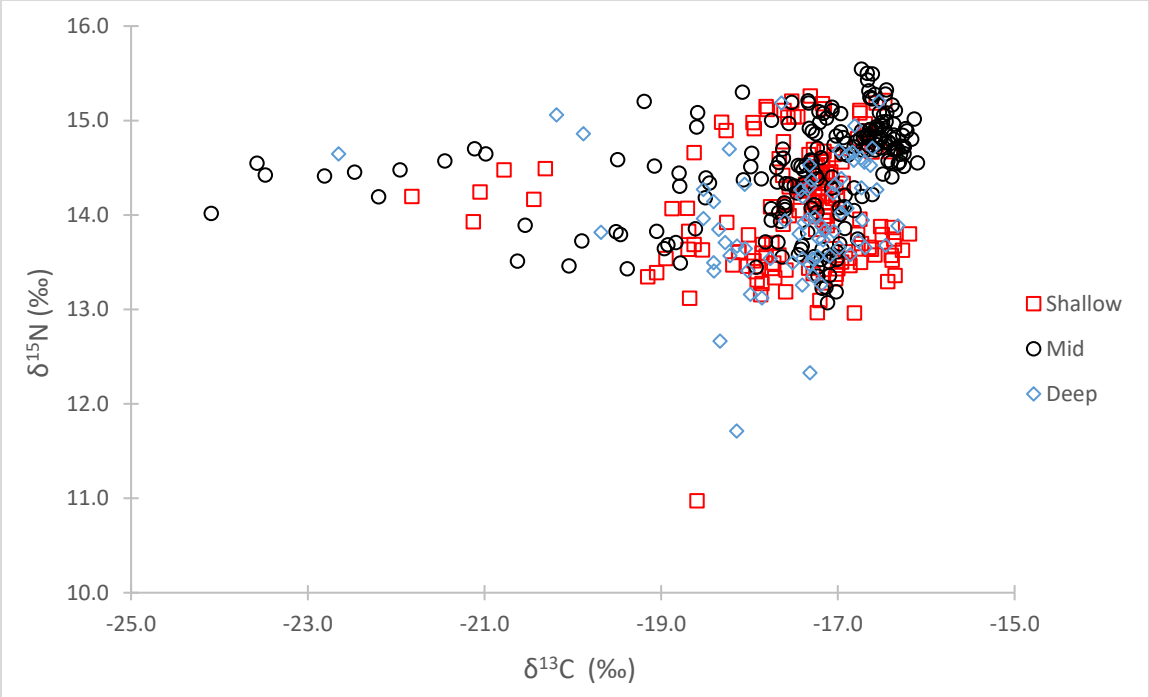


Figure 2.32*: Stable isotope values of red snapper sampled in 2017 based upon depth strata.*

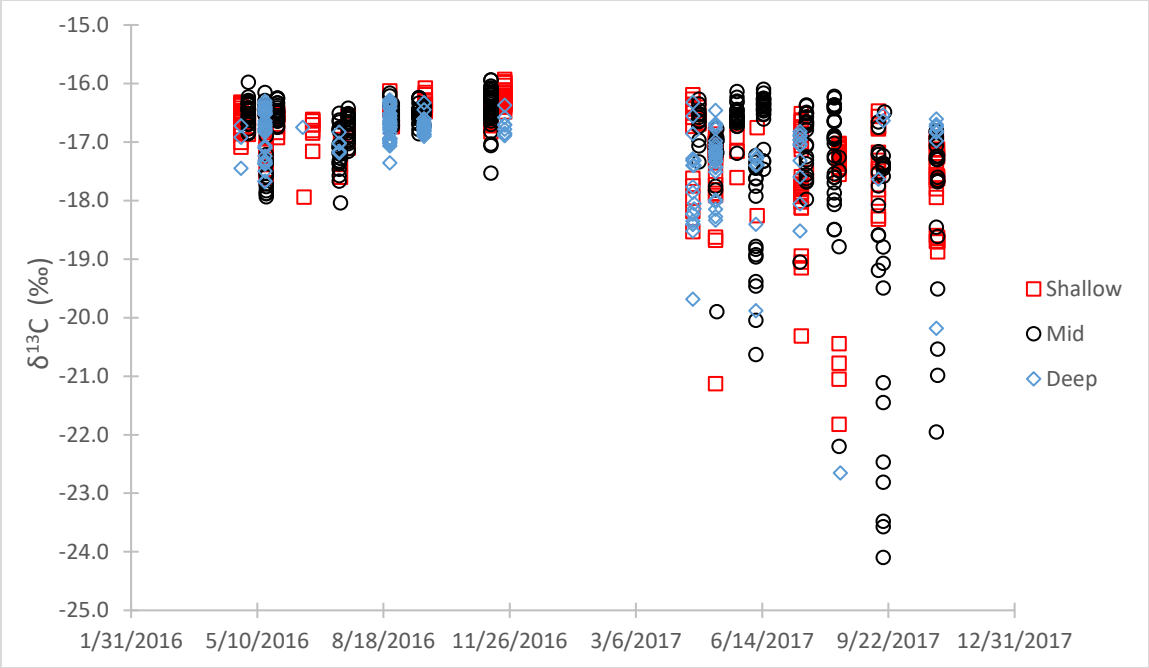


Figure 2.33: *$\delta^{13}C$ values of red snapper sampled in 2016 and 2017 based upon depth strata and sampling date.*

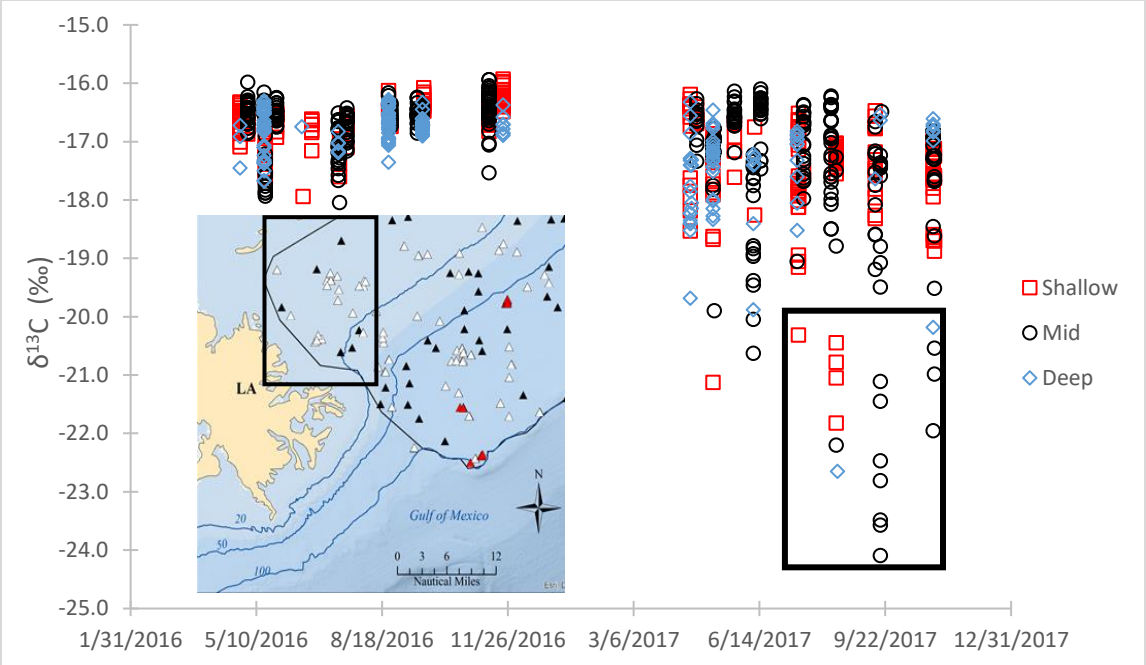


Figure 2.34: *Biplot indicating 2016 and 2017 predatory red snapper δ13C values by sampling date with a sampling map indicating the sampling locations the δ13C depleted red snapper sampled in 2017.*

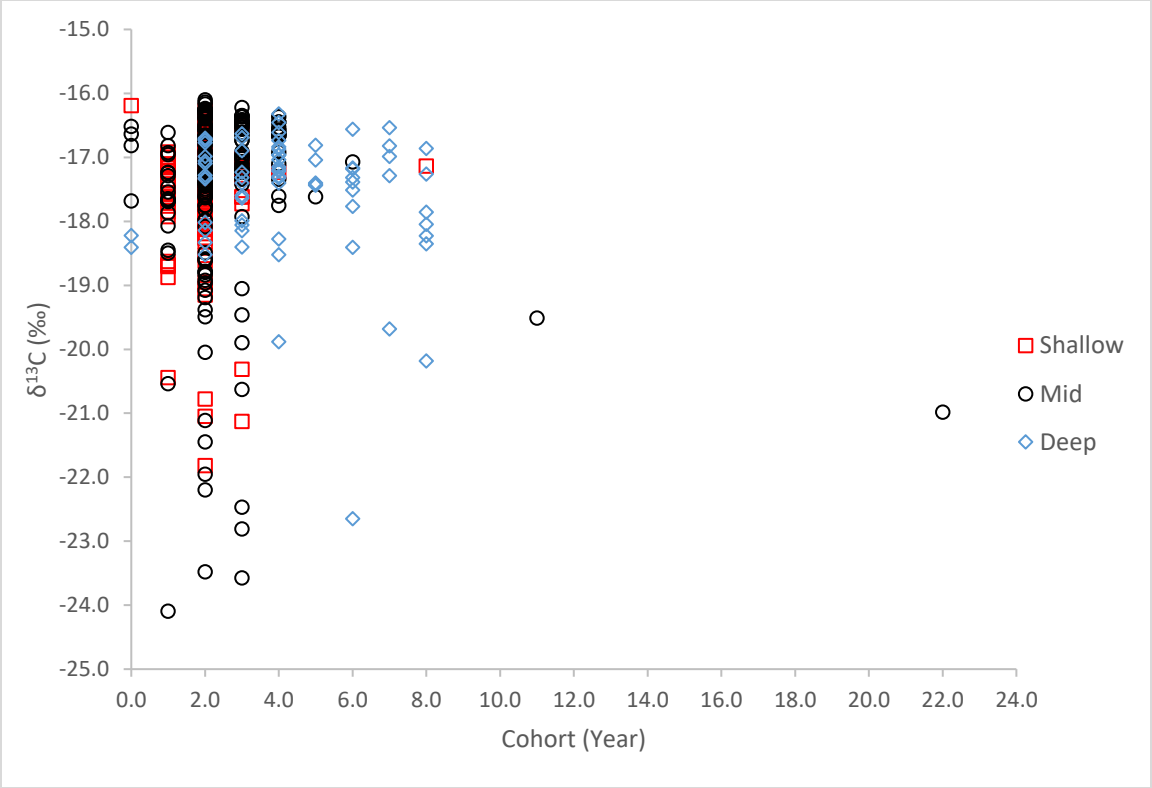

Figure 2.35: *Predatory red snapper sampled in 2017 by $\delta^{13}C$ values and cohort.*

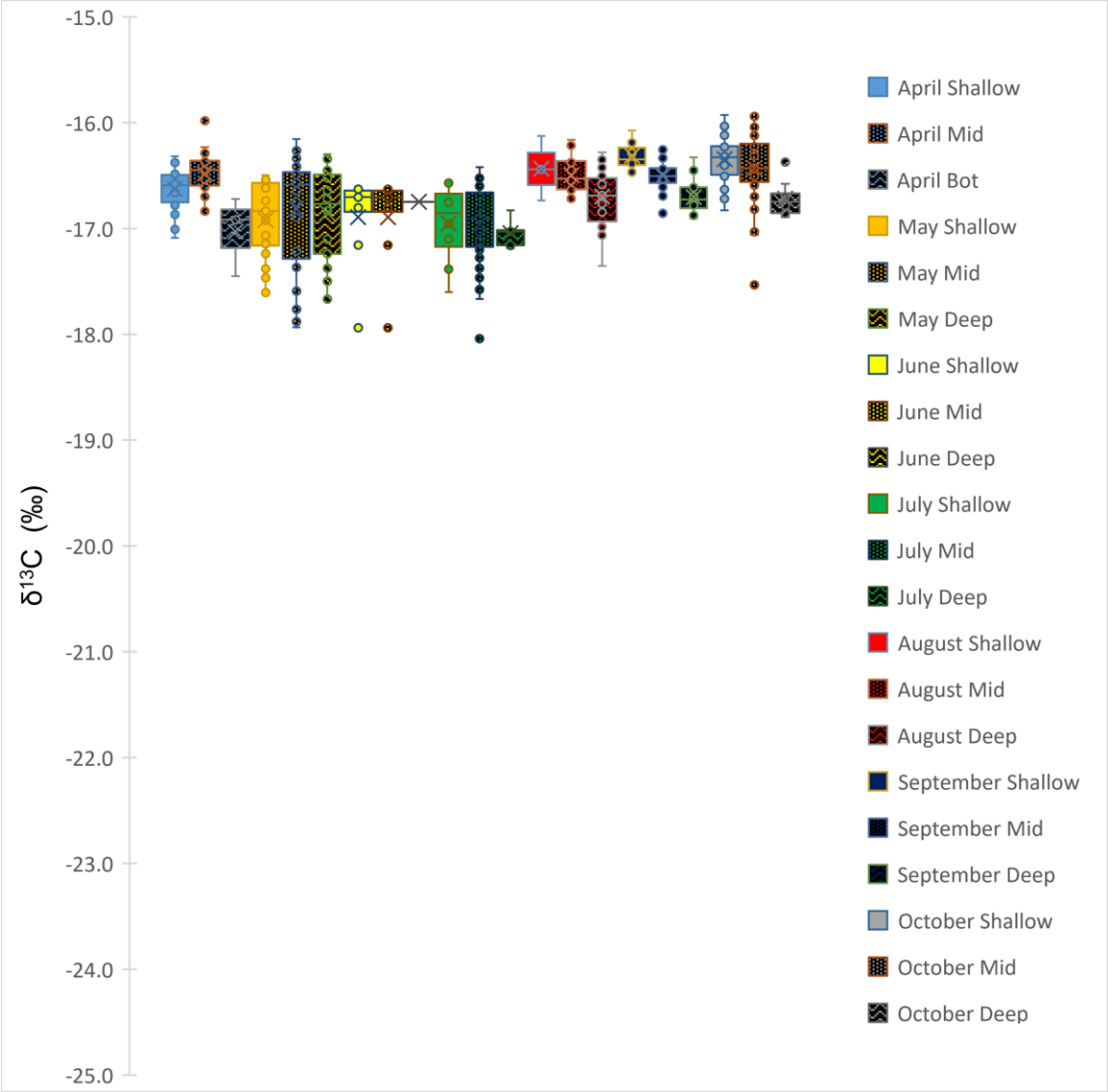


Figure 2.36: *$\delta^{13}C$ values of red snapper sampled in 2016 based upon depth strata and sampling month.*

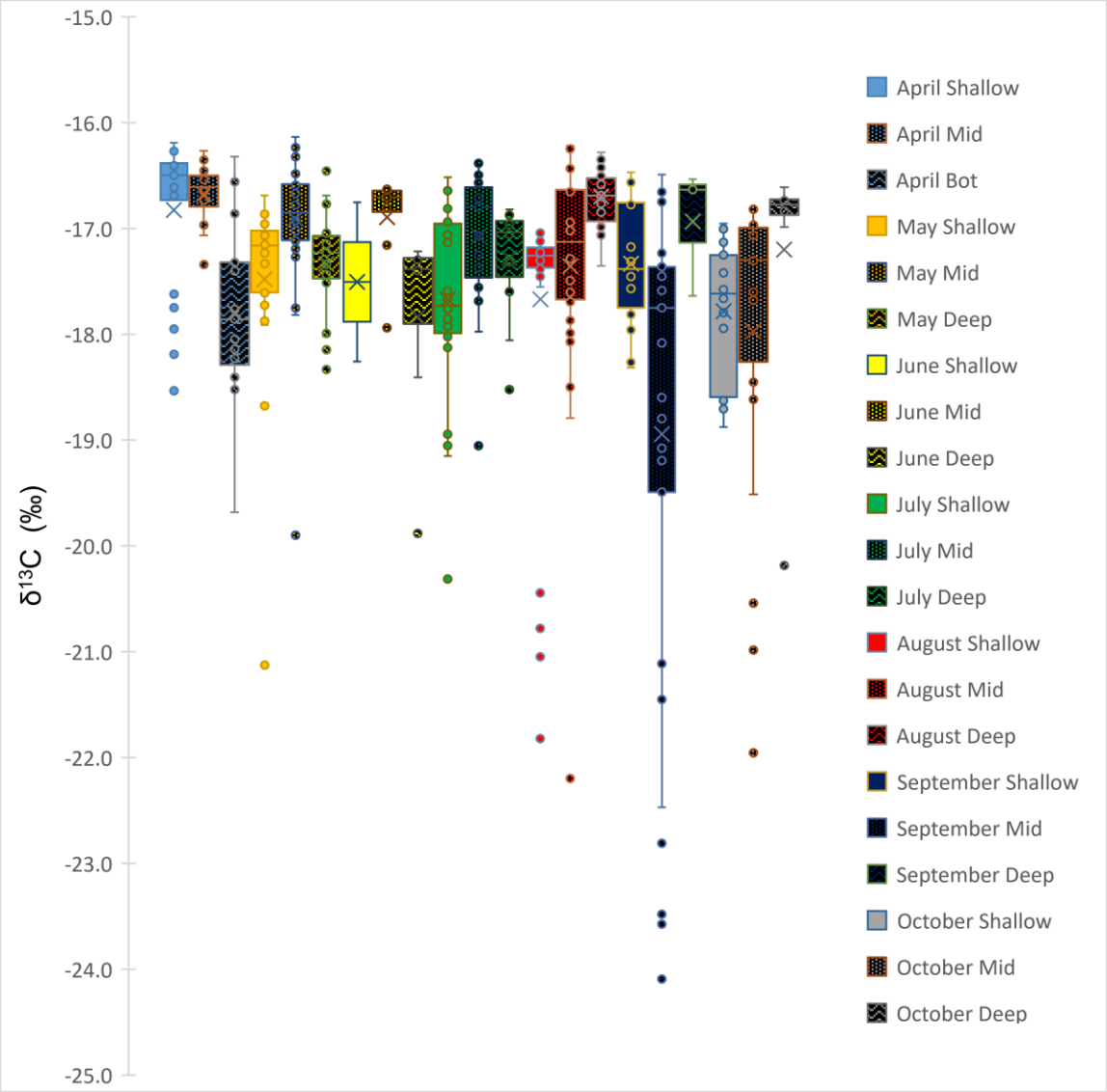


Figure 2.37: *$\delta^{13}C$ values of red snapper sampled in 2017 based upon depth strata and sampling month.*

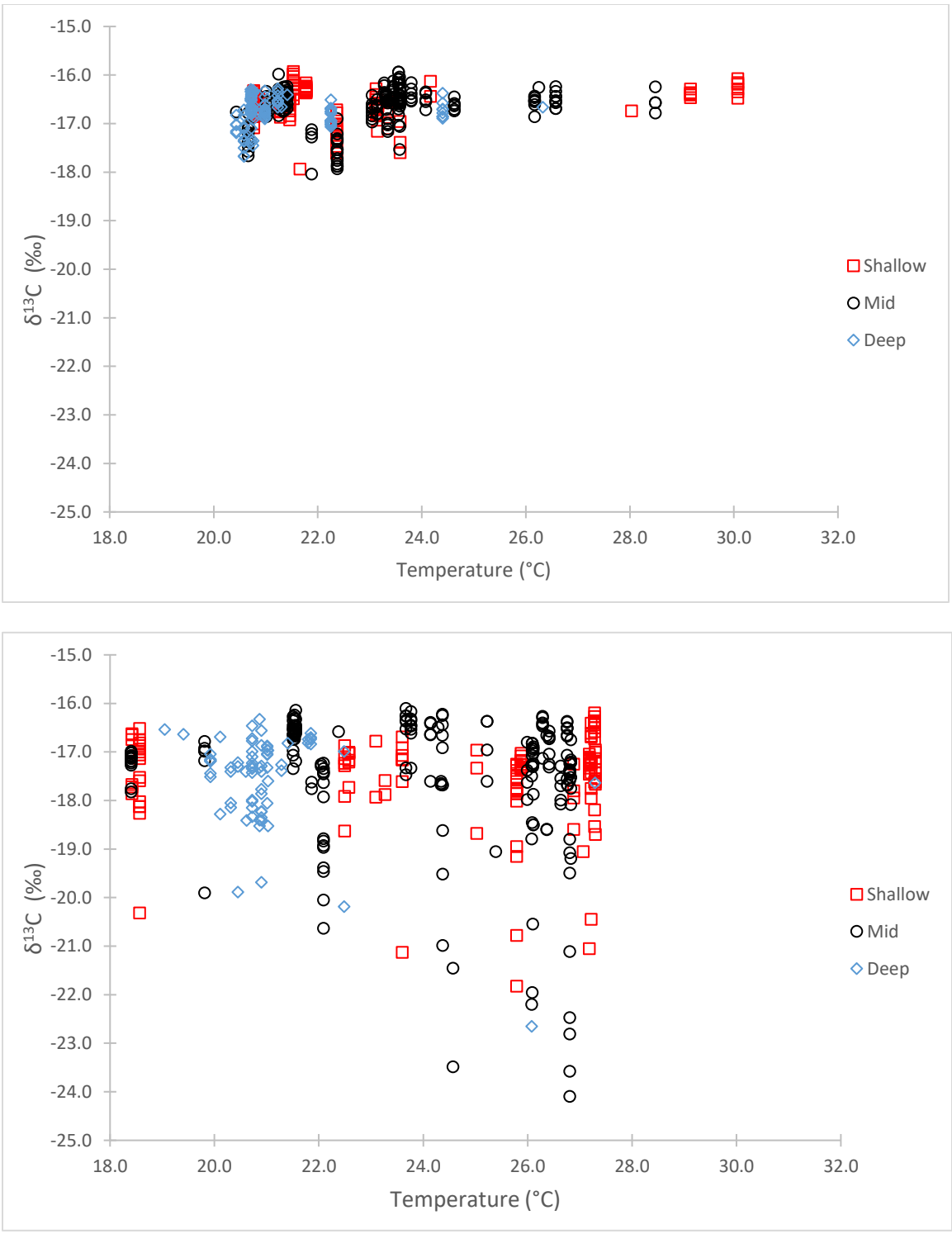


Figure 2.38: *$\delta^{13}C$ values of red snapper sampled in 2016 (top) and 2017 (bottom) based upon depth strata against the bottom water temperature at each station.*

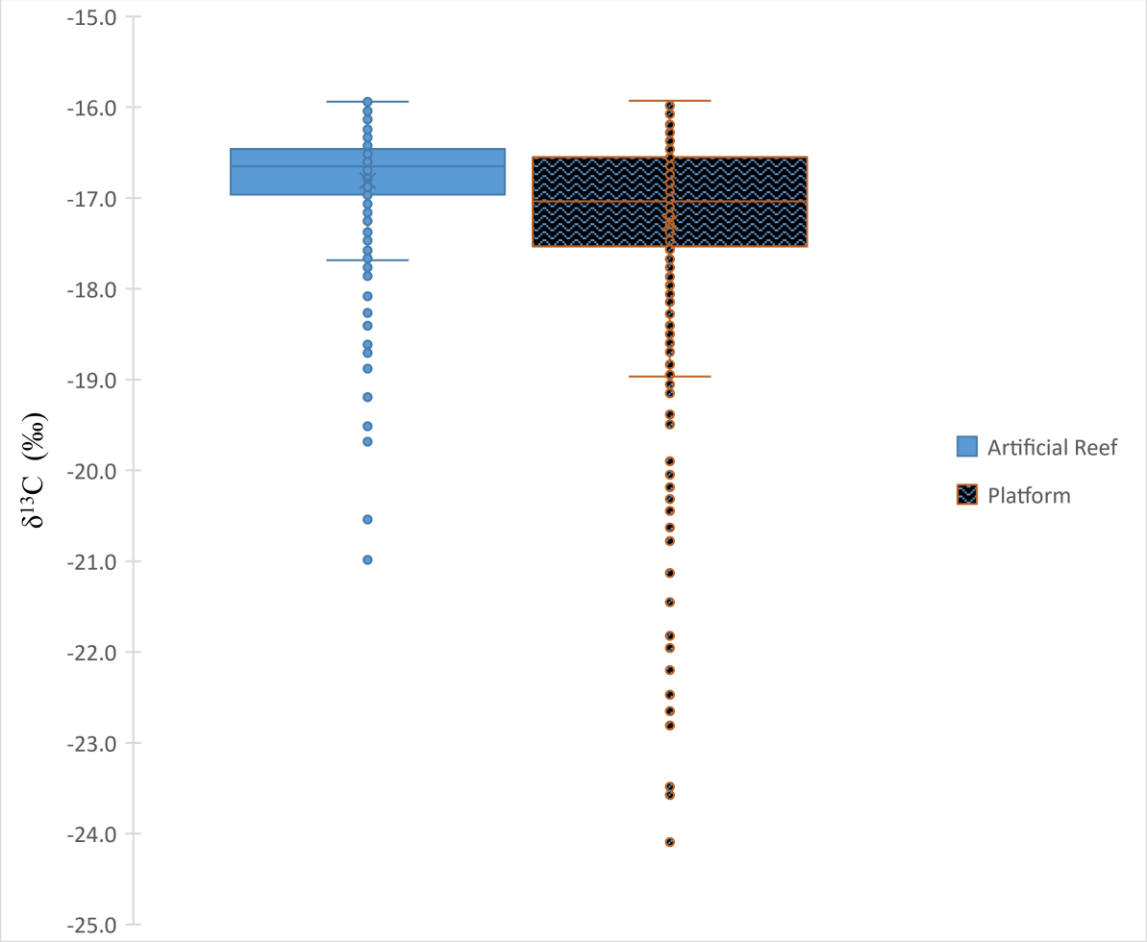


Figure 2.39*: $\delta^{13}C$ values of red snapper sampled in 2016 and 2017 based upon structure present at the sampling station.*

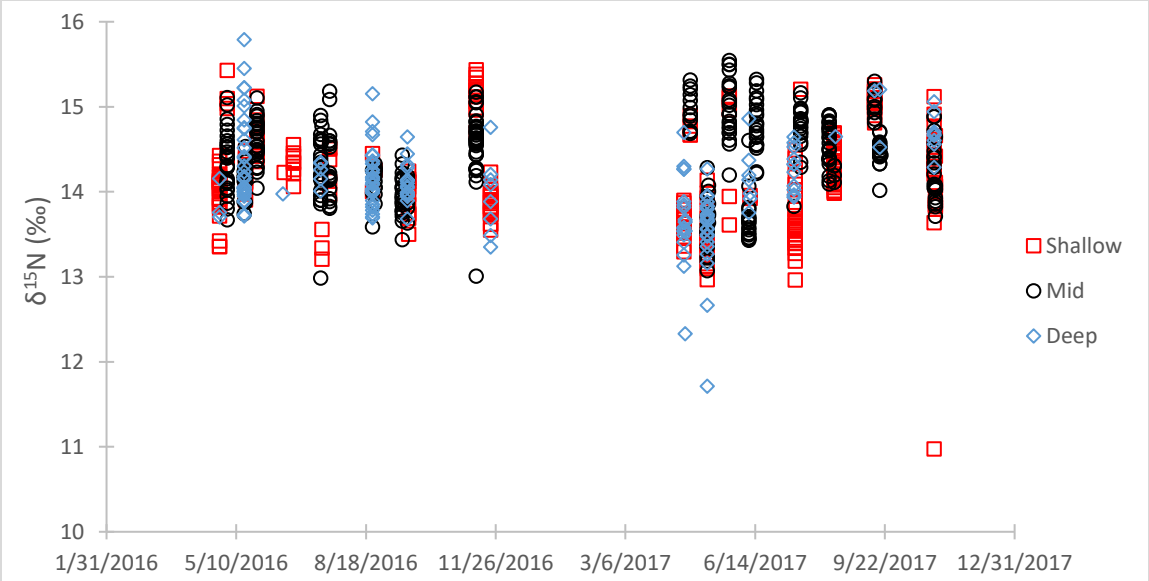


Figure 2.40*: $\delta^{15}N$ values of red snapper sampled in 2016 and 2017 based upon depth strata and sampling date.*

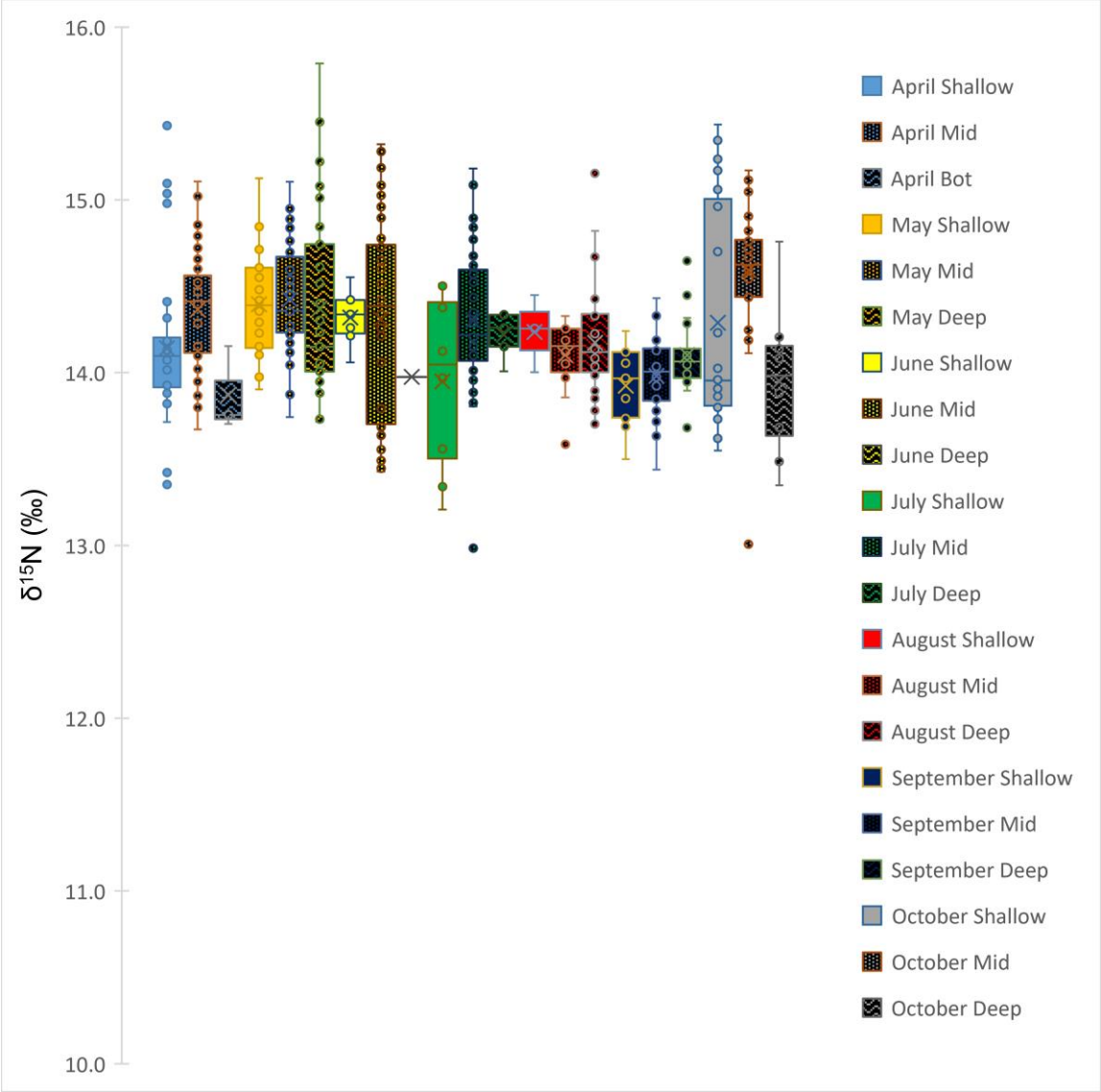


Figure 2.41: *$\delta^{15}N$ values of red snapper sampled in 2016 based upon depth strata and sampling month.*

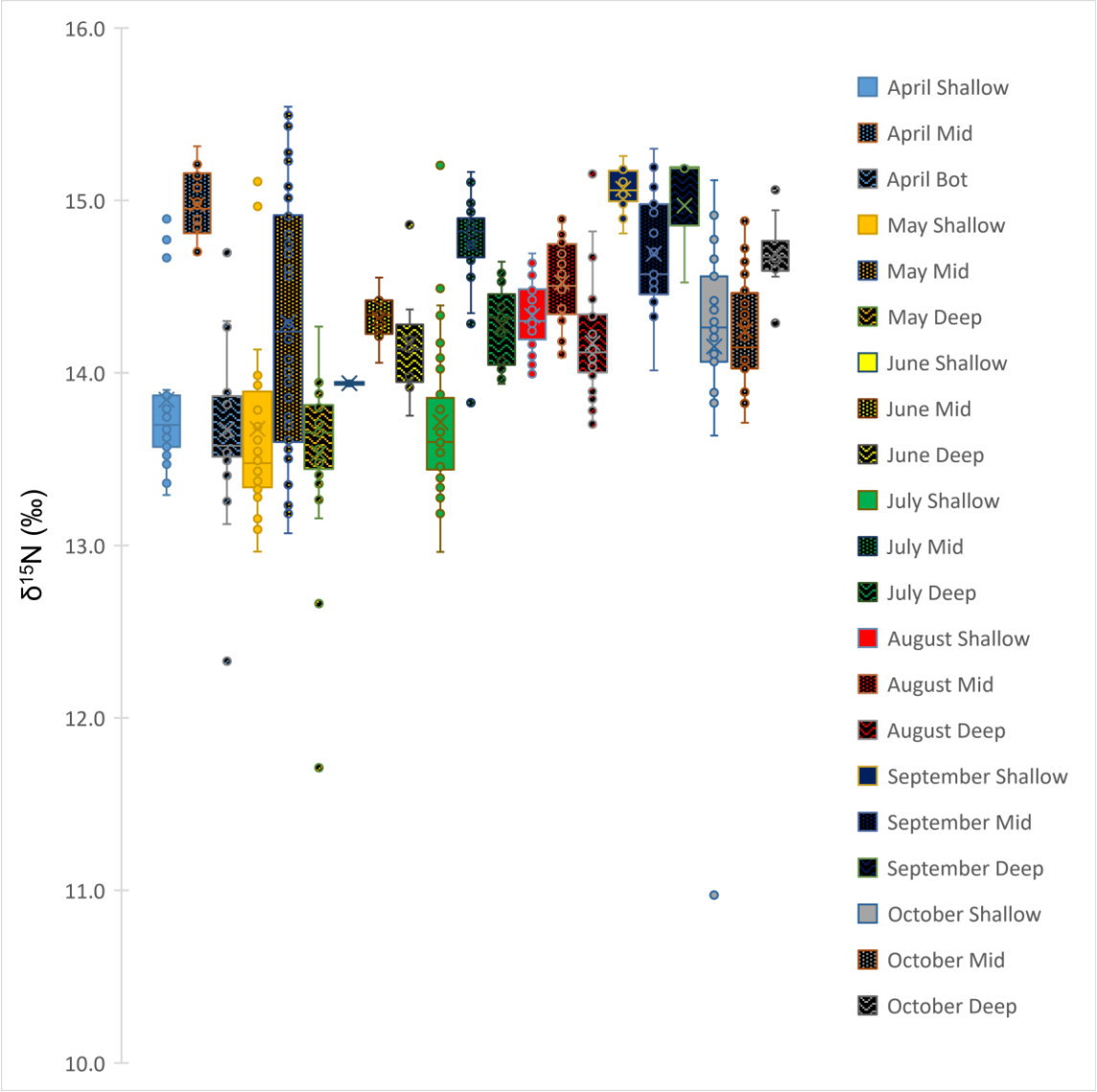


Figure 2.42*: $\delta^{15}N$ values of red snapper sampled in 2017 based upon depth strata and sampling month.*

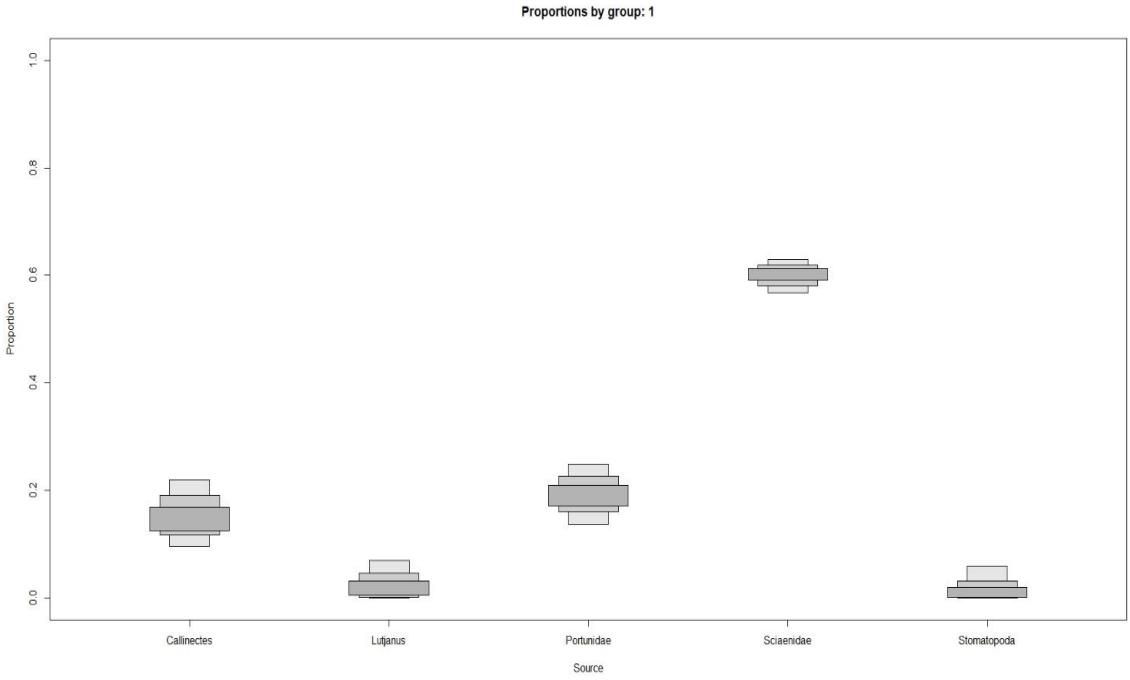


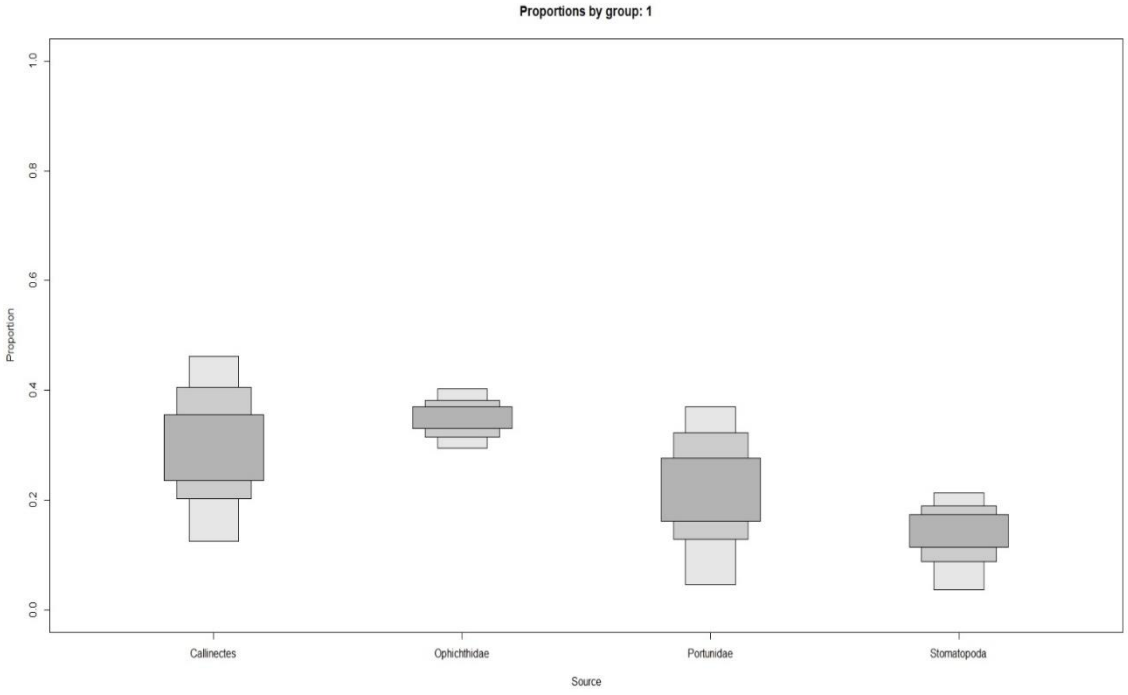


Figure 2.43*: SIAR model results for the 2016 (Top) and 2017 (Bottom) shallow depth strata.*

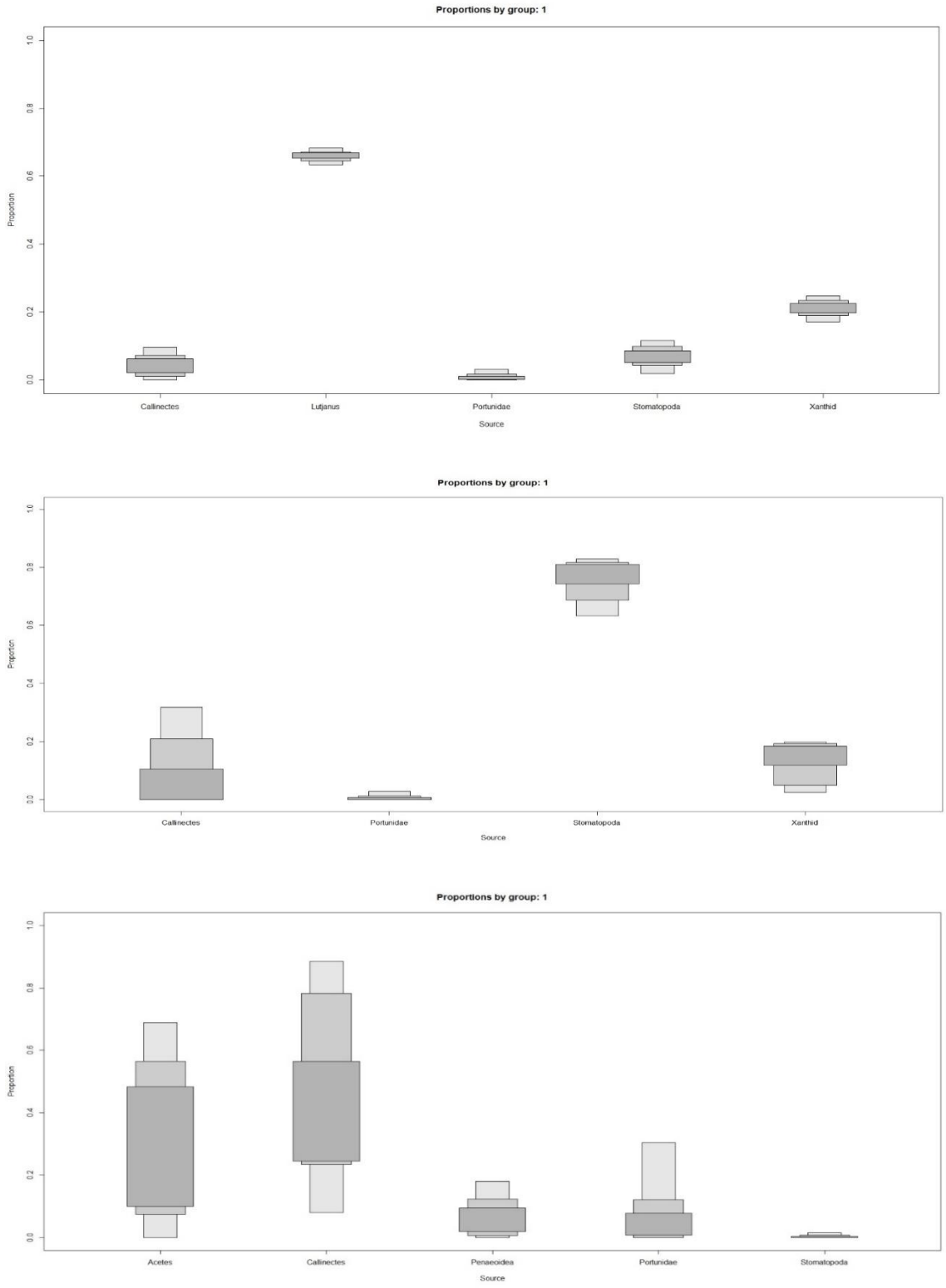


Figure 2.44*: SIAR model results for mid depth strata with the 2016 with the Lutjanus prey (Top), the 2016 without the Lutjanus prey (Mid) and 2017 (Bottom).*

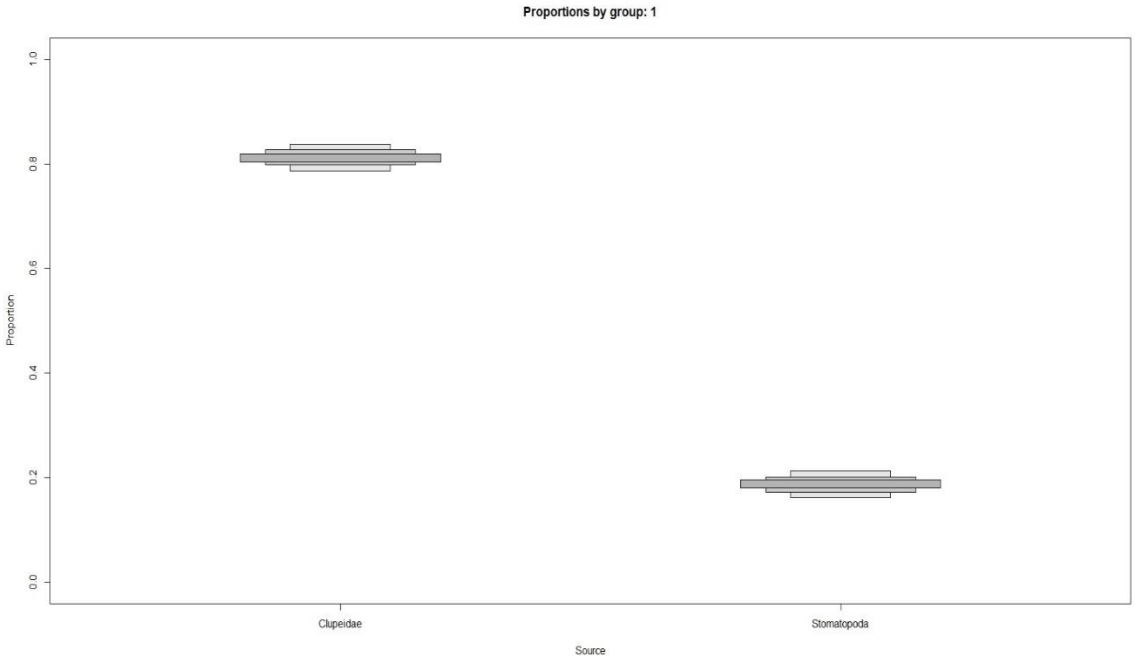


Figure 2.45*: SIAR model results for the 2016 deep depth strata. Only one prey type qualified for the 2017 deep depth strata.*

# REFERENCES


Akin. Senol and K.O. Winemiller. 2008. Body size and trophic position in a termperate estuarine food web. *Acta Oecologia* 33: 144-153.

Bailey, H. Killabrew IV, James H. Cowan Jr., and Robert Shipp. 2001. Experimental evaluastion of potential effects of habitat size and presence of conspecifics on habitat association by young-of-the-year Red Snapper. *Gulf of Mexico Science* 2: 119-131.

Baker, Ronald., Amanda Buckland, and Marcus Sheaves. 2014. Fish gut content analysis: robust measures of diet composition. *Fish and Fisheries* 15: 170-177.

Basu, Sayak., Shailesh Agrawal, Prasanta Sanyal, Porotish Mahato, Satyum Kumar, Anindya Sarkar. 2015. Carbon isotopic ratios of modern $C_3 – C_4$ plants from the Gangetic Plain, India and its implications to paleovegetational reconstruction. *Palaeoecology* 440: 22-32.

Bell, G. 2007. The evolution of trophic structure. *Heredity* 99(5): 494-505.

Bode, Antonio, Pablo Carrera and Santiago Lens. 2003. The pelagic foodweb in the upwelling ecosystem of Galicia (NW Spain) during spring: natural abundance of stable carbon and nitrogen isotopes. *Journal of Marine Science* 60: 11-22.

Bodin, Nathalie., Francois Le Loc'h and Christian Hily. 2007. Effect of lipid removal on carbon and nitrogen stable isotope ratio in crustacean tissues. Journal of Experimental Marine Biology and Ecology 341: 168-175.

Boecklen, William J., Christopher T. Yarnes, Bethany A. Cook and Avis C. James. 2011. On the use of stable isotopes in trophic ecology. *Annual Review of Ecology, Evolution and Systematics* 42: 411-40.

Buckland, Amanda. et al. 2017. Standardizing fish stomach content analysis: The importance of prey condition. *Fisheries Research* 196: 126-140.

Cai, Yihua., Laodong Guo, Xuri Wang and George Aiken. 2015. Abundance, stable isotopic composition, and export fluxes of DOC, POC, and DIC from the Lower Mississippi River during 2006-2008. *Journal of Geophysical Research: Biogeosciences* 120: 2273-2288.

Cai, Yihua, Laodong Guo, Xuri Wang, Allison K Mojzis and Donald G. Redalje. 2012. "The source and distribution of dissolved and particulate organic matter in the Bay of St. Louis, northern Gulf of Mexico." Estuarine, Coastal and Shelf Science 96: 96-104.

Camacho, Rene A. and James L. Martin. 2013. Hydrodynamic modeling of first-order transport timescales in the St. Louis Bay Estuary, Mississippi. *Journal of Environmental Engineering* 139: 317-331.

Casciotti, Karen L., Matthew McIlvin and Carolyn Buchwald. 2010. Oxygen isotope exchange and fractionation during bacterial ammonia oxidation. *Liminology and Oceanography* 55: 753-762.

Chang, Cecily C.Y., Carol Kendall, Steven Silva, William A. Battaglin and Donald H. Campbell. 2002. Nitrate stable isotopes: tools for determining nitrate sources among different land uses in the Mississippi River Basin. *Canadian Journal of Fisheries and Aquaculture Science* 59: 1874-1885.

Chakraborty, Sumit and Steven E Lohrenz. 2015. Phytoplankton community structure in the river-influenced continental margin of the northern Gulf of Mexico. *Marine Ecology Progress Series* 521: 31-47.

Collins, M.A., S. DeGrave, C. Lordan, G.M. Burnell and P.G. Rodhouse. 1994. Diet of the squid *Loligo forbesi* (Cephalopoda: Loliginidae) in Irish waters. *Journal of Marine Science* 51: 337-344.

Daigle, Sara T., Fleeger, John W., Cowan, J.H, and Pascal, Pierre-Yves. 2013. What is the relative importance of phytoplankton and attached macroalgae and epiphytes to food webs on offshore oil platforms? *Marine and Coastal Fisheries* 5: 53-64.

Dance, Kaylan M., Jay Rooker, J. Brooke Shipley, Michael Dance, and R.J. Wells. 2018. Feeding ecology of fishes associated with artificial reefs in the northwest Gulf of Mexico. *PLoS One* 13: 1-25.

Diercks, Arne R. and Vernon L. Asper 1997. In situ settling speeds of marine snow aggregates below the mixed layer: Black Sea and Gulf of Mexico. *Deep Sea Research I* 44: 385-398.

Dillon, Kevin S., Mark S. Peterson, and Christopher A. May. 2015. Functional equivalence of constructed and natural intertidal eastern oyster reef habitats in a northern Gulf of Mexico estuary. *Marine Ecology Progress Series* 528: 187-203.

Dittel, Ana I., Charles Epifanio and Marilyn Fogel. 2006. Trophic relationships of juvenile blue crabs (*Callinectes sapidus*) in estuarine habitats. *Hydrobiologia* 568: 379-390.

Dorado, Samuel., Jay Rooker, Bjorn Wissel and Antonietta Quigg. 2012. Isotope baseline shifts in pelagic food webs of the Gulf of Mexico. *Marine Ecology Progress Series* 464: 37-49.

Eadie, Brian J and Lela M. Jeffrey. 1973. $\delta^{13}C$ analyses of oceanic particulate organic matter. *Marine Chemistry* 1: 199-209

Fleming, Christopher. 2018. Spatial variation in basal resources and trophic position of selected fishes of the North-Central Gulf of Mexico. University of Southern Mississippi: Master's Thesis #361.

Fogel, Marilyn L., Carmen Aquilar, Russel Cuhel, David J. Hollander, Joan D. Willey and Hans W. Paerl. 1999. Biological and isotopic changes in coastal waters induced by Hurricane Gordon. *Liminology and Oceanography* 44(6): 1359-1369

Fry, B. 1983. Fish and shrimp migrations in the northern Gulf of Mexico analyzed using stable C, N, and S isotope ratios. *Fishery Bulletin* 81: 789-801.

Fry, Brain. (Ed.) 2006. Stable Isotope Ecology. New York, NY: Springer

Fry, Brian and Connie Arnold. 1982. Rapid $^{13}C/^{12}C$ turnover during growth of brown shrimp (*Penaeus aztecus*). *Oecologia* 54: 200-204.

Fry, Brian., Donald M. Baltz, Mark C. Benfield, John W. Fleeger, Arian Gace, Heather L. Haas and Zoraida J. Quinones-Rivera. 2003. Stable isotope indicators of movement and residence for brown shrimp (*Farfantepenaeus aztecus*) in coastal Louisiana Marshscapes. *Estuaries* 26: 82-97

Fry, Brian and Sam C. Wainright. 1991. Diatom sources of $^{13}C$ – rich carbon in marine food webs. *Marine Ecology Progress Series* 76: 149-157.

Gallaway, Benny J., Stephen T. Szedlmayer and William J. Gazey. 2009. A life history review for Red Snapper in the Gulf of Mexico with an evaluation of the importance of offshore petroleum platforms and other artificial reefs. *Reviews in Fisheries Science* 17: 48-67.

Gierach, Michelle M., Jorge Vazquez-Cuervo, Tong Lee and Vardis M Tsontos. 2013. AQUARIUS and SMOS detect effects of an extreme Mississippi River flooding event in the Gulf of Mexico. *Geophysical Research Letters* 40: 5188-5193.

Gulf of Mexico Fishery Management Council. 2019. Final Draft Amendment 50C to the Fishery Management Plan for the Reef Fish Resources of the Gulf of Mexico. *Mississippi Management for Recreational Red Snapper*.

Hobson, Keith A and Len I Wassenaar. 1999. International Association for Ecology Stable Isotope Ecology: An Introduction. *Oecologia* 120. 312-313.

Holl, Carolyn M., Tracy A. Villareal, Christopher D. Payne, Tonya D. Clayton, Cassandra Hart, and Joseph P. Montoya. 2007. Tricodesmium in the western Gulf of Mexico: $^{15}$N2-fixation and natural abundance stable isotope evidence. *Liminology and Oceanography* 52(5): 2249-2259.

Holthuis, L.B. 1980. Species Catalogue Vol. 1: Shrimps and prawns of the world, an annotated catalogue of species of intrest to fisheries. *FAO Fisheries Synopsis* 125(1): 271-272.

Jennings, S., S.P.R. Greenstreet, L. Hill, G.J. Piet, J.K. Pinnegar, and K.J. Warr. 2002. Long-term trend in the trophic structure of the North Sea fish community: evidence from stable-isotope analysis, size-spectra and community metrics. *Marine Biology* 141: 1085-1097.

Kaldy, James E., Luis A. Cifuentes and David Brock. 2005. Using stable isotope analysis to assess carbon dynamics in a shallow subtropical estuary. *Estuaries* 28: 86-95.

Karner, M.B., E.F. DeLong and D.M Karl. 2001. Archaeal dominance in the mesopelagic zone of the Pacific Ocean. *Nature* 409: 507– 10.

Kendall, Carol., Steven R. Silva, and Valerie J. Kelly. 2001. Carbon and nitrogen isotopic compositions of particulate organic matter in four large river systems across the United States. *Hydrological Processes* 15: 1301-1346.

Kerherve, Philippe., Masao Minagawa, Serge Heussner, and Andre Monaco. 2000. Stable isotopes in settling organic matter of the northwestern Mediterranean Sea: biogeochemical implications. *Oceanologica Acta* 24: 77-85.

Lehtovirta-Morley, Laura E. 2018. Ammonia oxidation: ecology, physiology and biochemistry and why they must all come together. *FEMS Microbiology Letters* 365: 1-9

Leichter, James J., Adina Paytan, Scott Wankel, Katharine Hanson, Steven Miller, Mark A Altabet. 2007. Nitrogen and oxygen isotopic signatures of subsurface nitrate seward of the Florida Keys reef tract. *Liminology and Oceanography* 52: 1258-1267.

Letelier, Ricardo M. and David M Karl. 1998. *Trichodesmium* spp. physiology and nutrient fluxes in the North Pacific subtropical gyre. *Aquatic Microbial Ecology* 15: 265-276.

Leu, Ming-Yih., I-Hui Chen and Lee-Shing Fang. 2003. Natural spawning and rearing of mangrove red snapper, *Lutjanus argentimaculatus*, in captivity. *The Israeli Journal of Aquaculture* 55: 22-30.

Lindeman, K. C., W. J. Richards, J. Lyczkowski-Shultz, D. M. Drass, C. B. Paris, J. M. Leis, M. Lara, and B. H. Comyns. 2005. "Lutjanidae: snappers." Early stages of Atlantic fishes. CRC Press, Boca Raton, FL: 1549-1586.

Logan, John M., Timothy Jardine, Timothy Miller, Stuart E. Bunn, Richard A. Cunjak and Molly E Lutcavage. 2008. Lipid corrections in carbon and nitrogen stable isotope analyses: comparison of chemical extraction and modelling methods. *Journal of Animal Ecology* 77: 838-846.

Longo, C., et al. 2015. Role of trophic models and indicators in current marine fisheries management. *Marine Ecology Progress Series* 538: 257-272.

McClain-Counts, Jennifer P., Amanda W.J. Demopoulos and Steve W. Ross. 2017. Trophic structure of mesopelagic fishes in the Gulf of Mexico revealed by gut content and stable isotope analyses. *Marine Ecology* 38: 1-23.

McCawley, J.R., James H. Cowan Jr., and Robert L. Shipp. 2003. Red snapper *(Lutjanus campechanus*) diet in the north-central Gulf of Mexico on Alabama artificial reefs. *Proceedings of the Gulf and Caribbean Fisheries Institute* 54: 372-385.

McMahon, Kelton W., Li Ling Hamady and Simon R Thorrold. 2013. A review of ecogeochemistry approaches to estimating movements of marine animals. *Liminology and Oceanography* 58(2): 697-714.

Minagawa, Maso and Eitaro Wada. 1984. Stepwise enrichment of $^{15}N$ along food chains: Further evidence and the relation between $^{15}N$ and animal age. *Geochemica et Cosmochimica* Acta 48: 1135-1140.

Patterson, William F. 2007. A Review of Movement in Gulf of Mexico Red Snapper: Implications for Population Structure. *American Fisheries Society Symposium* 60: 221-235

Paterson, William F., James H. Cowan Jr., Charles A. Wilson, and Robert L. Shipp. 2001. Age and growth of red snapper, *Lutjanus campechanus*, from an artificial reef area off Alabama in the northern Gulf of Mexico. *Fisheries Bulletin* 99(4): 617-628

Peterson, Bruce J. 1999. Stable isotopes as tracers of organic matter input and transfer in benthic food webs: A review. *Acta Oecologica* 20: 479-487.

Peterson, Bruce J. and Brian Fry. 1987. Stable Isotopes in Ecosystem Studies. *Annual Review of Ecological Systems* 18: 293-320.

Piko, A.A and S.T. Szedlmayer. 2007. Effects of habitat complexity and predator exclusion on the abundance of juvenile red snapper. *Journal of Fish Biology* 70: 758-769.

Post, David M. 2002 Using stable isotopes to estimate trophic position: models, methods and assumptions. *Ecology* 83: 703-718.

Post, David M., Craig A. Layman, D. Albrey Arrington, Gaku Takimoto, John Quattrochi and Carman G. Montana. 2007. Getting to the fat of the matter: models, methods and assumptions for dealing with lipids in stable isotope analysis. *Oecologia* 152: 179-189.

Radabaugh, Kara R., David J. Hollander and Ernst B. Peebles. 2013. Seasonal $\delta^{13}C$ and $\delta^{15}N$ isoscapes of fish populations along a continental shelf trophic gradient. *Continental Shelf Research* 68: 112-122.

Santoro, Alyson E. and Karen L. Casciotti. 2011. Enrichment and characterization of ammonia-oxidizing archaea from the open ocea: phylogeny, physiology and stable isotope fractionation. *ISME Journal* 5: 1796-1808.

Schwartzkopf, Brittany D., Todd A. Langland and James H. Cowan. 2017. Habitat Selection Important for Red Snapper Feeding Ecology in the Northwestern Gulf of Mexico. *Marine and Coastal Fisheries* 9: 373-387.

Sessions, Alex L. 2006. Isotope-ratio detection for gas chromatography. *Journal of Separation Science* 29: 1946-1961.

Sigman, D.M, K.L Karsh and K.L. Casciotti. 2009. Ocean process tracers: Nitrogen isotopes in the ocean. Encyclopedia of Ocean Sciences 2nd Edition: edited by by J.H Steele, Academic Press: Oxford. 40-54.

Simonsen, Kirsten A., James H. Cowan and Kevin M. Boswell. 2014. Habitat differences in the feeding ecology of Red Snapper (Lutjanus campechanus, Poey 1860): a comparison between artificial and natural reefs in the northern Gulf of Mexico. *Environmental Biology of Fishes* 98: 811-824.

Skinner, Megan M., Amy A. Martin and Barry C. Moore. 2016. Is lipid correction necessary in the stable isotope analysis of fish tissues? *Rapid Communications in Mass Spectrometry* 30: 1-9

Soares, Lucy S., Elizabeti Muto, Juliana Lopez, Gabriela Clauzet, and Ivan Valiela. 2014. Seasonal variability of $\delta^{13}C$ and $\delta^{15}N$ of fish and squid in the Cabo Frio upwelling system of the southwestern Atlantic. Marine Ecology Progress Series 512: 9-21.

Szedlmayer, Stephen and J.D. Lee. 2004. Diet shifts of juvenile red snapper (*Lutjanus campechanus*) with changes in habitat and fish size. *Fishery Bulletin – National Oceanic and Atmospheric Administration* 102(2): 366-375

Tarnecki, Joseph H. and William F. Patterson. 2015. Changes in Red Snapper Diet and Trophic Ecology Following the Deepwater Horizon Oil Spill. *Marine and Coastal Fisheries* 7: 135-147

Tinus, Craig. 2012. Prey preference of lingcod (*Ophiodon elongatus*), a top marine predator: implications for ecosystem-based management. *Fisheries Bulletin* 110: 193-204.

Waite, A.M., B.A Muhling, C.M Holl, L.E. Beckley, J.P. Montoya, J. Strzelecki, P.A. Thompson, and S. Pesant. 2007. Food web structure in two counter-roatating eddies based on $\delta^{13}C$ and $\delta^{15}N$ isotopic analysis. *Deep-Sea Research* 54: 1055-1075.

Wells, R. J David, James H. Cowan and Brian Fry. 2008. Feeding ecology of Red Snapper Lutjanus campechanus in the northern Gulf of Mexico. *Marine Ecology Progress Series* 361: 213-225.

Wells, R. J D and J. R. Rooker. 2009. Feeding ecology of pelagic fish larvae and juveniles in slope waters of the Gulf of Mexico. *Journal of Fish Biology* 75: 2719-1732.

Wells, R., Jay R. Rooker, Antonietta Quigg, and Bjorn Wissel. 2017. Influence of mesoscale oceanographic features on pelagic food webs in the Gulf of Mexico. *Marine Biology* 164: 92-102

Wilson, Charles A. and Nieland, David L. 2001. Age and growth of Red Snapper *Lutjanus campechanus*, from the northern Gulf of Mexico off Louisiana. *Fishery Bulletin* 99. 653-664.

Wissel, Bjorn, and Brian Fry. 2005. Tracing Mississippi River influences in estuarine food webs of coastal Louisiana. *Oecologia* 144: 659-672.

Zehr, Jonathan P. and Bess B. Ward. 2002. Nitrogen cycling in the ocean: new perspectives on processes and paradigms. *Applied and Environmental Microbiology* 68: 1015-1024

Zhao, Yan and Antonietta Quigg. 2014. Nutrient limitation in northern Gulf of Mexico (NGOM): Phytoplankton communities and photosynthesis respond to nutrient pulse. *PLoS One* 9: 1-12.